國 立 交 通 大 學

材料科學與工程學系

博 士 論 文

奈米金棒合成與其在活體細胞研究的應用

Fabrication of gold nanowires and their
applications in live cell research

研 究 生：郭瓊雯

指導教授：韋光華 教授

中華民國九十七年四月

奈米金棒的合成與其在活體細胞研究的應用

摘要

本論文主要討論如何合成及製造一維新穎奈米物質，並探討一維奈米物質的特殊性質，進而將其運用在活體細胞的研究。本論文主要的目標有三：一、發展新型一維奈米物質之製造技術，使其具有高深寬比、特殊功能性、大面積且規則性排列之特性。二、研究一維奈米物質的特殊功能性及其在活體細胞研究之應用。三、探討一維奈米物質可能的應用領域，如藥物傳遞方面。

由於陽極氧化鋁具多孔性及易製備之特性，長久以來陽極氧化鋁一直被當成合成奈米物質的模板。新近的研究顯示，利用陽極氧化鋁，可製成大面積且孔洞具周期性之奈米模板。陽極氧化鋁不僅可單獨成為模板，亦可長在基材表面，藉以在基材表面合成一維奈米物質。此外，商品化的陽極氧化鋁薄膜，也常被用來合成一維奈米物質，利用電化學方式，奈米金屬棒可在陽極氧化鋁奈米模板內被合成。變換不同的電鍍液，多截不同金屬的奈米棒可被合成出來，藉由表面修飾，可將奈米金屬棒修飾成具有功能之材料。

利用上述所合成具有功能性之奈米金棒，我們研究不同深寬比之奈米金棒在纖維母細胞與子宮頸癌細胞中的毒性。在奈米金棒溶液中，細胞增殖及細胞死亡的反應可使用 MTT 試劑測得。改變金棒表面之化學性質，我們可得知何種表面修飾毒性較低，可用在活細胞系統中。本論文研究發現，寬度為 200 奈米、長度為數微米具有功能性之奈米金棒，可以在兩種細胞株體內自由進出。其毒性量測結果與奈米金棒上之化學官能基有關，在低奈米金棒濃度下，血清吸附的奈米金棒對細胞毒性最小(細胞存活率大於 90％)。然而被 11- mercaptoundecanoic acid 分子修飾的奈米金棒，其毒性很大(細胞存活率約在 60％)，不同長度的奈米金棒的毒性有相同的反應趨勢。此外，我們也觀察到在細胞中，較短奈米金棒的吸收效率，比長的奈米金棒還多。因此，在考慮有效吸收之奈米金棒後，我們認為，在細胞體內長奈米金棒的毒性比短奈米金棒還要高。

本論文還探討奈米金棒作為生物探針的可能性，利用帶有正電荷離子之表面修飾(aminothiol)，DNA 及探針分子可被奈米金棒帶進活體細胞內。利用顯微鏡觀察，我們可獲得奈米金棒週遭的環境，因此我們認為奈米金棒可當成生物探針，自由進出活體細胞中，且因單獨奈米金棒不會聚集於細胞體內，非常適合用來研究奈米物質進入細胞之路徑機制等相關性質。

奈米金棒的藥物傳遞性質亦是本論文的探討重點之一，利用正電荷離子修飾

(aminothiol)的奈米金棒，可藉由靜電力吸附 DNA 分子，並將 DNA 分子運送至纖維母細胞與子宮頸癌細胞中，進行轉移感染實驗。我們研究的結果顯示，使用 200 奈米寬、5 微米長的奈米金棒，單一奈米金棒上可攜帶約 1pg 的藥物進行基因傳遞，相對於市面上所販售的轉染試劑，我們發現奈米金棒不但相對安全，在活體細胞系統中也有較高的轉染效率。因此，我們認為，如能利用多截且為不同金屬之奈米棒，我們可將不同的官能基修飾在不同截的金屬表面，使其同時可以攜帶藥物及作為生物探針使用，此種多功之奈米棒，對於研究藥物如何進入到活細胞體內的機制，有很好的運用潛力。

Abstract

In this thesis, the fabrication of one-dimensional functional nanomaterials has been established and the applications of one-dimensional functional nanomaterials for the study of living cells have also been investigated. The main goals for this study are i) to develop new techniques for synthesizing and fabricating one-dimensional nanomaterials with very high aspect ratio, unique functionalities, and preferably in an ordered fashion over a large area on various substrates; ii) to utilize the one-dimensional nanomaterials as the probe for the living cells; iii) to explore the possibility of using the one dimensional nanomaterials as the drug carriers.

To synthesize one-dimensional nanomaterials with very high aspect ratio, the anodic aluminum oxides (AAOs) were used as the templates owing to their simple fabrication processes and porous nature. Recent developments in the fabrication techniques of AAOs not only made it possible to fabricate large-area well-ordered AAO membranes, but also allowed such membranes to be grown on silicon and glass substrates. In the past few years, a two-step AAO fabrication technique for producing well-ordered AAOs has been developed. Using both commercial and home-made AAO membranes, nanowires with various composition and aspect ratios have been prepared by electrochemical deposition process. These nanowires were further modified with different functional groups on the surfaces. The cytotoxicity of various surface functionalized gold nanowires with different aspect ratios has

been investigated by MTT assays for two cell lines, fibroblast and HeLa. It was found that

the functionalized gold nanowires with 200 nm diameter and length up to a few micrometers

could be readily internalized by both types of cells regardless of the surface functionalization.

However, the cytotoxicity of the gold nanowires was measured to depend on their surface

modification. The serum coated gold nanowires were the least toxic surface coating because

of the presence of various proteins on the surfaces of gold nanowires. In contrast, more than

50% of cells were damaged in the presence of the mercapto acid modified gold nanowires

even at very low concentration (10^3 nanowire/ml). The nanowires with different aspect ratio

exhibited the same cytotoxicity within experimental error. However, the uptake efficiency

for the shorter nanowires was found to be higher than the longer ones. Therefore, we

concluded that the internalized nanowires with higher aspect ratio were more toxic to the

cells than the nanowires with lower aspect ratio. The positively charged aminothiol modified

gold nanowires have been employed to deliver both plasmid DNA and probe molecules into

cells without compromising the viability of cells. The local environment of the individual

nanowires inside the cells has been obtained by monitoring the fluorescence signal from the

probe molecules on the nanowires.

To explore the possibility of using nanowires as the drug carriers, the aminothiol

modified gold nanowires have been used as vectors for the delivery of plasmid DNA into

two different types of mammalian cells: 3T3 and HeLa. It was measured that the positively

charged gold nanowires with a diameter of 200 nm and a length around 5 μm were capable

of carrying 1 pg of plasmid DNA per nanowire into cells. Compared with other transfection

reagents, the gold nanowires exhibited the highest transfection efficiency while almost no

cytotoxicity was observed. In addition, it has been shown that individual nanowires can be

visualized with sub-micrometer resolution, which may allow the use of functionalized

multi-segment nanowires as the local probes for the investigation of the microenvironment

inside the cells.

誌 謝

Content

Figure list

Chapter 6 Nanowire as Living Cell Probes

Chapter 7 Nanowire for Gene Delivery

Chapter 1 Introduction

With the rapid advancement in nanotechnology, various techniques have been developed to synthesize nanoparticles with novel optical, magnetic, electrical, mechanical and catalytic properties [1]. By controlling the size, shape and composition of the nanoparticles, their properties can be tailored to fit a specific requirement, which allows great flexibility in designing new experiments or applications. Recently, there has been increasing research attentions focused on the development of nanomaterials for solving complicated biological problems. For example, nanoparticles, such as quantum dots or metallic nanoparticles, have been shown to exhibit superior performance to the conventional techniques in biosensing [2-5] and biolabeling [6-9]. However, the applications of nanoparticles in the study of living cells are less explored due to the issues of biocompatibility and cytotoxicity [10-17].

Noble metals, such as gold, have been used in the biological studies for a long time because of their stability and low toxicity. Lately, there are renewed research efforts in developing metallic nanoparticle-based techniques for labeling [18-20], drug delivery [21-24] and gene regulation [25]. A common approach used in these applications is to chemically modify the surface of the nanoparticles such that the nanoparticles can recognize a specific molecule or receptor on the cell surfaces or the nanoparticles can form complexes with drugs or genetic materials to enter the cells. However, in a more complicated experiment, it may require the nanoparticles to possess several functionalities so that several tasks can be performed by a

single particle. For example, two peptides have been attached to the same gold nanoparticles to allow both receptor-mediated endocytosis and endosomal escape [26]. Multi-segment nanowires or nanorods are particularly useful for such type of applications due to their symmetry. In a recent study, two types of molecules have been incorporated onto the gold-nickel nanowires where the gold end was used to bind to a plasmid DNA through electrostatic interaction while the nickel surface was engineered to carry a specific polypeptide for site recognition [22]. However, most of the studies on nanorods or nanowires have been limited to the nanometer length. The micrometer long nanowires were less explored. Micrometer long multi-segment nanowires have been used as barcodes for biological multiplexing, which could be easily visualized by an optical microscope [27]. Recently, it has been shown that the micrometer long nickel nanowires could be internalized by cells allowing the manipulation of living cells through magnetic field [28, 29]. However, it is not known whether the micrometer long nanowires can be internalized by the cells without damaging the cells, which is an important issue for the development of nanowire-based living cell probing system. If the nanowires can be internalized by the cells, it would allow us to observe directly the intracellular microenvironment around the individual nanowires through an optical microscope. We are interested in developing nanowires based living cell probing system. Our idea is to modify the surface of nanowires to carry the plasmid DNA or probe molecules into cells where the nanowires and the probe molecules can be monitored by a

microscope. Since molecules could be attached to the surface of the nanowires through electrostatic interaction, it is necessary to control the surface charge density, which can be achieved by various surface modification schemes. To utilize surface modified nanowires for the living cell study, it is very important to first investigate the cytotoxicity of these nanomaterials. As long as the surface modified nanowires could be internalized by the cells without damaging the cells, these nanowires could be used to explore the local environment inside the living cells. However, in some occasion the surface modified nanowires were found to settle on the bottom of the cell culture dishes. Therefore, it is essential to compare the internalization process of nanowires for the adherent cell and the non-adherent cells. In this research, we have studied the cytotoxicity and the internalization process of the functionalized gold with different surface charges for two different cell lines, NIH 3T3 fibroblast cells from normal tissue, which is an adherent cell line and HeLa S3 cells from neoplastic tissue, which can grow in suspension.
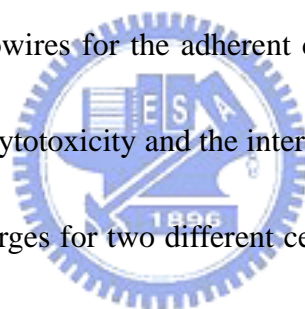
Learning that the micrometer long nickel nanowires could be internalized by cells, it is interesting to investigate whether the micrometer long nanowires are capable of delivering DNA molecules or drugs into the cells without damaging the cells, which is an important issue for the development of nanowire based live cell probing system. To investigate the possibility of using nanowires for DNA delivery, it is necessary to engineer the surface of the nanowires in such way that the DNA molecules can bind to the nanowires in a reversible

manner, which can protect the DNA molecules from the digestion of enzymes in the

extracellular environment while the DNA molecules can be released inside the cells for

effective transfection. Since the DNA molecules are negatively charged, a common practice is

to engineer the surface of the nanowires with positive charges. Therefore, the DNA molecules

can bind to the surface of the nanowires through the electrostatic interaction. Because of the

low cytotoxicity and easy surface modification process of gold nanowires, we have

investigated the interactions between the nanowires and the cells through the studies of the

DNA transfection efficiency using single segment surface modified gold nanowires.

Reference

1.   *Handbook of Nanostructured Materials and Nanotechnology*, (H.S. Nalwa, Editor),

    Academic Press, New York.

2.   J. W. Nam, C. S. Thaxton and C. A. Mirkin, *Science* 2003, **301**, 1884.

3.   Y. Xiao, F. Patolsky, E. Katz, J. F. Hainfeld and I. Willner *Science* 2003, **299**, 1877 .

4.   X. Zhao, L. R. Hilliard, S. H. Mechery, Y. Wang, R. P. Bagwe, S. Jin and W. Tan,

    Proc. Natl. Acad. Sci. USA 2004, **101**, 15027.

5.   E. Hutter and J. H. Fendler, *Adv. Mater.* 2004, **16**, 1685.

6.   X. Michalet, F. F. Pinaud, L. A. Bentolila, J. M. Tsay, S. Doose, J. J. Li, G.

    Sundaresan, A. M. Wu, S. S. Gambhir and S. Weiss, *Science* 2005, **307**, 538.

7.   I. L. Medintz, H. T. Uyeda, E. R. Goldman and H. Mattoussi, *Nat. Mater.* **2005, 4**,

    435.

8.   X. Gao, L. Yang, J. A. Petros, F. F. Marshall, J. W. Simons and S. Nie, *Curr. Opin.*

    Biotechnol. 2005, **16**, 63.

9.   C. Sonnichsen, B. M. Reinhard, J. Liphardt and A. P. Alivisatos, *Nat. Biotechnol.*

    2005, **23**, 741.

10.   A. M. Derfus, W. C. W. Chan and S. N. Bhatia, *Nano Lett.* 2004, **4**, 11.

11.   A. Hoshino, K. Fujioka, T. Oku, M. Suga, Y. F. Sasaki, T. Ohta, M. Yasuhara, K.

    Suzuki and K. Yamamoto, *Nano Lett.* **2004, 4**, 2163.

12. C. Kirchner, T. Liedl, S. Kudera, T. Pellegrino, A. M. Javier, H. E. Gaub, S. Stolzle and W. J. Parak, *Nano Lett.* 2005, **5**, 331.

13. B. D. Chithrani, A. A. Ghazani and W. C. W. Chan, *Nano Lett.* **2006,** 6, 662.

14. C. M. Goodman, C. D. McCusker, T. Yilmaz and V. M. Rotello, *Bioconjugate Chem.* 2004, **15**, 897.

15. E. E. Connor, J. Mwamuka, A. Gole, C. J. Murphy and M. D. Wyatt, *Small* **2005, 1**, 325.

16. H. Takahashi, Y. Niidome, T. Niidome, K. Kaneko, H. Kawasaki and S. Yamada, *Langmuir* 2006, **22**, 2.

17. G. Han, C. T. Martin and V. M. Rotello, *Chem. Biol. Drug Des.* 2006, **67**, 78.

18. C. C. Lin, Y. C. Yeh, C. Y. Yang, C. L. Chen, G. F. Chen, C. C. Chen and Y. C. Wu, *J. Am. Chem. Soc.* 2002, **124**, 3508.

19. J. Wang, *Small* 2005, **1**, 1036.

20. E. Katz and I. Willner, *Angew. Chem. Int. Ed.* 2004, **43**, 6042.

21. H. Shen, J. Tan and W. M. Saltzman, *Nat. Mater.* **2004, 3**, 569.

22. A. K. Salem, P. C. Searson and K. W. Leong, *Nat. Mater.* **2003, 2**, 668.

23. K. K. Sandhu, C. M. McIntosh, J. M. Joseph, S. W. Smith and V. M. Rotello, *Bioconjugate Chem.* 2002, **13**, 3.

24. M. Thomas and A. M. Klibanov, *Proc. Natl. Acad. Sci. USA*, 2003, **100**, 9138.

25. N. L. Rosi, D. A. Giljohann, C. S. Thaxton, A. K. R. Lytton-Jean, M. S. Han and C. A. Mirkin, *Science*, 2006, **312**, 1027.

26. A. G. Tkachenko, H. Xie, D. Coleman, W. Golmm, J. Ryan, M. F. Anderson, S. Franzen and D. L. Feldheim, *J. Am. Chem. Soc.* 2003, **125**, 4700.

27. C. D. Keating and M. J. Natan,   *Adv. Mater.* 2003, **15**, 451.

28. A. Hultgren, M. Tanase, C. S. Chen, G. J. Meyer and D. H. Reich, *J. Appl. Phys.* 2003, **93**, 7554.

29. M. Tanase E.J. Felton, D.S. Gray, A. Hultgren, C.S. Chen and D.H. Reich, *Lab Chip* 2005, **5**, 598.

Chapter 2 Fabrication of AAO Template

Porous anodic alumina has been studied for about 50 year. Recent advances in the fabrication technique made it possible to create uniform size of array of parallel pores, which were formed by pore nucleation owing to the electric field distribution at the pore tip. Porous anodic alumina has been frequently used as the template for the synthesis of various materials such as nanoparticles, nanowires and nanorods. These one dimensional nanomaterials could be potentially utilized in electric, optical devices and biological system.

2.1 Ordered AAO template

Recent developments in the ordered nanopores were achieved by Masuda and coworkers, who have first reported the control growth of the ordered array in the anodic alumina template in 1995 [1]. Such templates exhibited a long range ordering up to millimeter scale. In the original scheme for preparing ordered AAOs , it required imprinting aluminum surface with ordered templates before anodization so that the anodization of aluminum can follow the imprinted patterns. However, self-assembled well-ordered AAOs can be obtained by adding an additional anodization step. To fabricate ordered AAO templates, a two-step molding process was used. In the first stage, the aluminum was anodized in oxalic acid solution under appropriate anodizing voltage condition by a longer anodization period. The result can produce porous alumina structures, which was then removed by saturated $HgCl_2$ leaving

ordered nanostructures on the substrate. The ordered nanopores array could be obtained by the

second anodization process [2]. In another approach, a SiC master with hexagonally ordered

array was pressed against the aluminum sheet producing ordered patterns on the substrate

where the order nanopore array could be obtained by the anodization of the aluminum. Such

procedure can produce a large area, defect-free nanopores arrays [3]. One application of the

ordered AAO templates was to synthesize size-controlled carbon nanotubes using CVD

process on the surface of the porous alumina by depositing cobalt catalyst on the bottom of

the AAO template [4].

The ordered hexagonal pore arrays of anodic alumina are formed by the self-organization

process using oxalic acid or sulfuric acid as the electrolyte [5]. When the electric filed

increased at the bottom of the alumina pores, the pore growth may start. It was found that the

repulsive forces between neighboring pores during the oxidation process resulted in the

formation of ordered hexagonal structures in alumina. There are several parameters that

governed the pore size and pore distance including the applied voltages, the electrolyte

concentration, and the bath temperature. It was found by Li et al. [6, 7] that the domain size of

the nanopores depended on the temperature in a linear fashion. These porous anodic alumina

membranes have been used as the templates for the electrodeposition to produce long

nanowires with lengths of over a few hundred nanometers and aspect ratio as high as 300 [8].

When the pulsed electrodeposition was used to deposit metals, high density magnetic

memories could be obtained [9].

2.2 Fabrication of AAO template

In this study, the anodic aluminum oxide (AAO) templates were fabricated using a two-step oxidization method. First, a sheet of aluminum (99.9999% pure, Alfa) was etched in 1.0 M NaOH at room temperature for 5 min to remove the native oxide, and washed thoroughly with distilled water. The sample was then electropolished in a mixed solution of $HClO_4$ and CH_3CH_2OH ($HClO_4$:CH_3CH_2OH = 1:4) for 50 s and quickly rinsed with distilled water. To fabricate arrays of nanoholes, the aluminum sheet has to undergo anodization process. The anodization was conducted under constant cell potential in three types of aqueous solution, sulfuric, oxalic and phosphoric acids, which were used as electrolytes. Afterward, the Al foil was anodized at 20- 60 V in 1.2 M sulfuric or 0.3 M oxalic aqueous solution for 18 h at 10℃,this resulted in Al film approximately 70 μm thick. Subsequently, the first anodization step the Al film was stripped in a mixing solution of 0.4 M phosphoric and 0.2 M chromic acid for 5 to 15min at 60℃, leaving behind an aluminum surface textured with a hexagonal scalloped pattern.

To create ordering hexagonal pore structure, an Al thin film was first anodized at 20－60 V in 0.3 M oxalic aqueous solution for 3 to12 h . The pore-widening was then fulfilled in 5 wt % phosphoric acid at 50 °C. Finally the porous alumina membrane was rinsed thoroughly

with distilled water and dried by pure nitrogen blowing. The AAO template prepared under 40

V constant potential presents the optimum ordering. The pore diameter and spacing are

proportional to the forming voltage, which is due to the alternative migration velocity of

reactive ions under electric field according to the growth-dissolution model. Further pore

adjustment depends on the time of pore-widening in phosphoric acid. The characterization of

the AAO template was measured by field emission scanning electron microscope (FE-SEM,

LEO-1530).

2.3 Results and discussion

In this study we have fabricated the ordered porous alumina membranes via a two-step

anodization process. A schematic representation of the whole procedure is illustrated in figure

1. In the first step, the Al substrate was anodized for a long period of time (A). This step

resulted in the formation of channel arrays with a high aspect on random position.

Subsequently, this membrane was completely removed by phosphocromic acid solution

leaving a hexagonal scalloped pattern on the surfaces [1, 10-12](B). In the second anodization

process, ordered pore structures could be obtained, which will be used as template(C). The

SEM image of the top surface of the membrane formed using 30V is shown in figure 2A

whereas the image of the bottom surface obtained by applying 50V is depicted in figure 2B.

In the first anodization stage, the initial pore structure was quite random, which was

removed by phosphoric acid solution. However, in the bottom of the pore, hexagonal

scalloped patterns were formed, which was the result of electric field gradient. These patterns

were used to guide the pore growth in the second anodization process. At the end of the

second anodization process, uniform pore structure was observed, which would be used as the

templates. The SEM images of these ordered nanopores arrays fabricated under the applied

voltages of 30, 40, 50 and 60 V are shown in figure 3 to 6 respectively. It was measured that

pore and wall diameter was nearly proportional to the anodization voltage, which was in good

agreement with the literature.

In this study the best ordered structures were obtained under the applied voltage of 40V

as shown in figure 4 [1, 5]. The domains size of the hexagonally ordered pores were found to

be in the micrometer region, which was consistent with a previous measurement where the

neighboring domains with different orientation of the pore lattice were divided by a grain

boundary [5]. When the applied voltage was changed to 30V, a much smaller size of uniform

domain were observed as shown in the figure 3 where the pore distances were measured to be

around 83 nm. When the voltage was increased to 50V or 60V, the size of ordered domains

were roughly the same. The pore distances of 139 nm and 167 nm were measured respectively

as shown in figure 5 and 6. It was noticed that large volume expansion may lead to the

structural defects on the substrate and irregular pore growth. The large volume expansion was

associated high anodizing voltage and growth rates as a result of the reduction in the

interaction between the neighboring holes. To investigate the ordering of the pore arrangement, a Fourier transformation (figure 7A) was apply to the SEM image of the well-ordered pored obtained at the applied voltage of 40 V where the pore distance was about 110 nm as displayed in figure 7B. The cross-sectional images of the high aspect-ratio channel in the anodic porous alumina were shown in figure 8 A and B. It can be clearly seen that each channel grew straight perpendicular to surface.

2.4 Conclusions

We have obtained the AAO membranes with average pore diameters of $80-160$ nm in a two step anodization process. The pore densities of the AAO membranes were in the range of $10^{11}-10^{8}$ cm^{-2} depending on the applied voltage. The pore size and distribution were measured by the SEM images. It was shown that the best ordering structure was formed at an applied voltage of 40 V where the pore size was measured to be 110 nm. In this study, we have demonstrated that it is possible to obtain highly-oriented porous structure with very uniform and nearly parallel pores.

Reference

1. H. Masuda and K. Fukuda, *Science* 1995, **268**, 1466.

2. H. Masuda, F. Hasegwa and S. Ono, *J. Electrochem. Soc.* 1997, **144**, L127.

3. H. Masuda, H. Yamada, M. Satoh, H. Asoh, M. Nakao and T. Tamamura, *Appl. Phys. Lett.* 1997, 71, 2770.

4. T. Yanagishita, M. Sasaki, K. Nishio and H. Masuda, *Adv. Mater.* 2004, **16**, 429.

5. O. Jessensky, F. Muller and U. Gosele, *Appl. Phys. Lett.* 1998, **72**, 1173.

6. F. Y. Li, L. Zhang and R. M. Metzger, *Chem. Mater.* 1998, **10**, 2470.

7. L. Zhang, H. S. Cho, F. Li, R. M. Metzger and W. D. Doyle, *J. Mate. Sci. Lett.* 1998, **17**, 291.

8. M. S. Sander and L. S. Tan, *Adv. Funct. Mater.* 2003, **13**, 393.

9. K. Nielsch, F. Muller, A. P. Li and U. Gosele, *Adv. Mater.* 2000, **12**, 582.

10. T. T. Xu, F. T. Fisher, L. C. Brinson and R. S. Ruoff, *Nano Lett.* 2003, **3**, 1135.

11. H. Masuda and M. Satoh, *Jap. J. Appl. Phys. 2* 1996, **35**, L126.

12. T. Xu, G. Zangari and R. M. Metzger, *Nano Lett.* 2002, 2, 37.
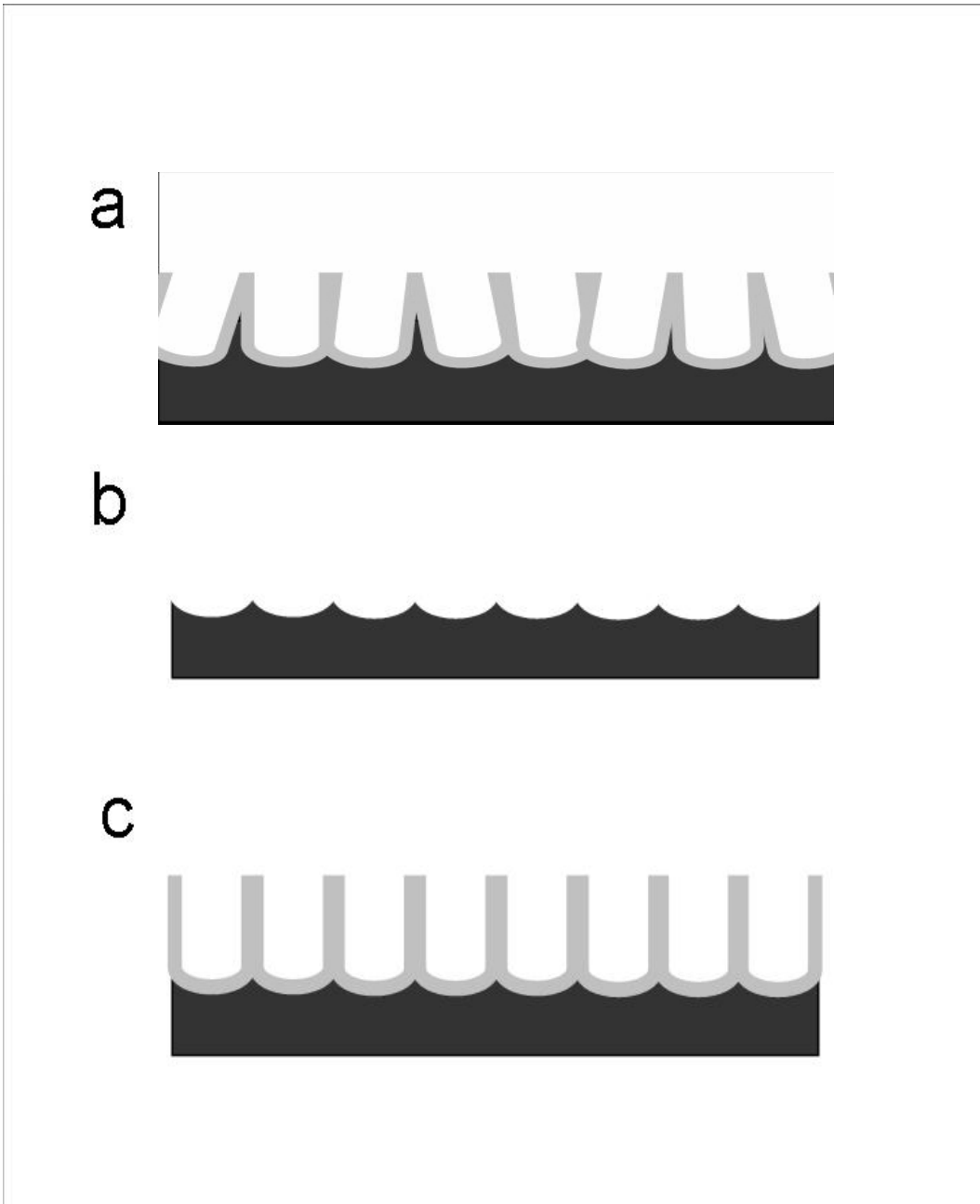
Figure1. Schematic for fabricating ordered porous alumina nanochannels. (A) Random porous aluminum oxide is formed in the first anodic oxidation process. (B) The porous alumina is then removed leaving ordered nanopattern on the surfaces. (C) The ordered porous nanochannels can be obtained after the second anodic oxidation process.

(A)
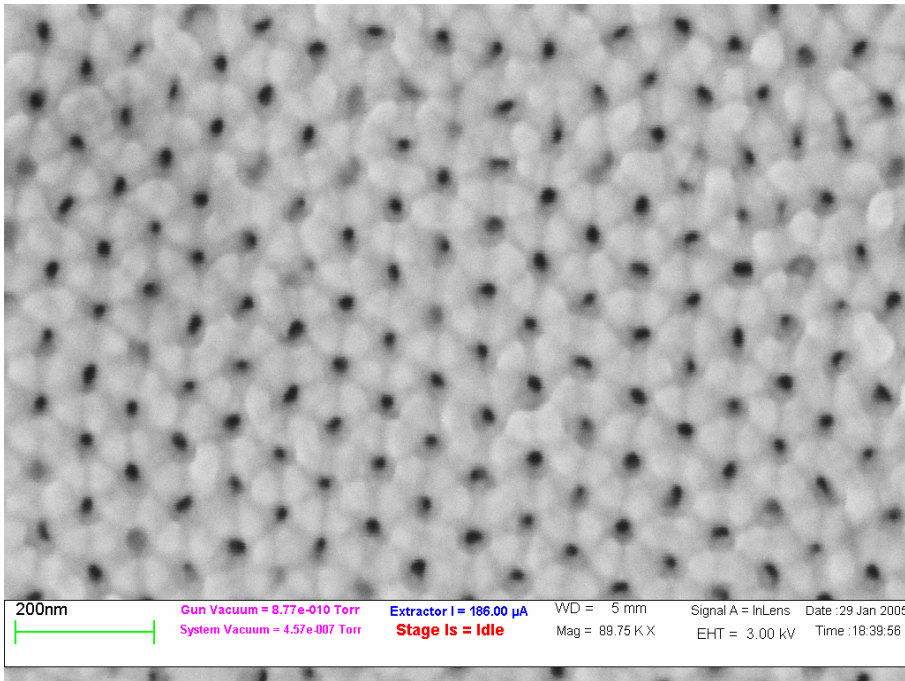
(B)
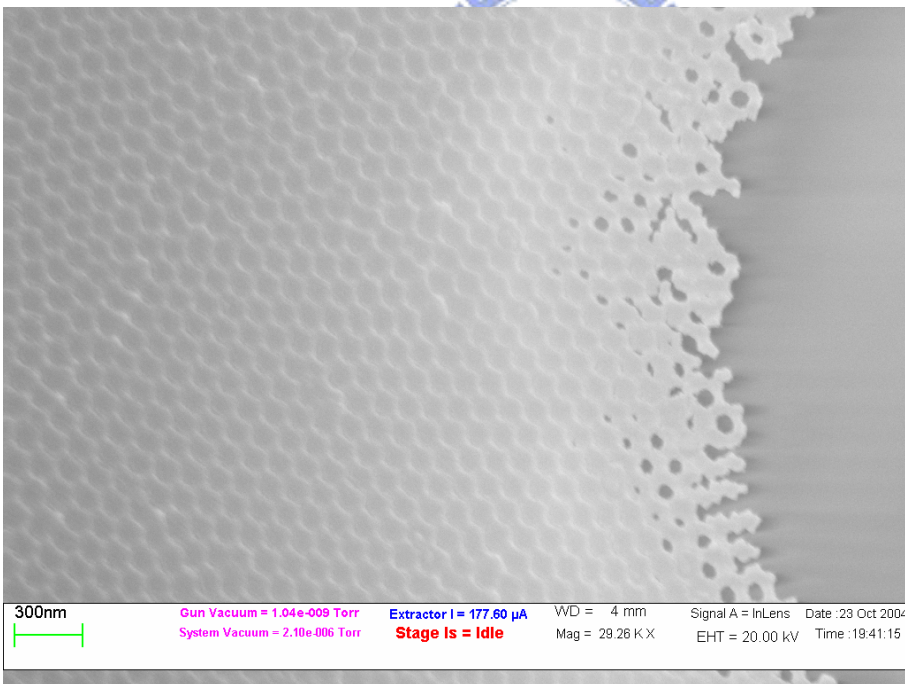
Figure 2. The SEM images of the (A) top and (B) bottom of the anodic alumina.

(A)
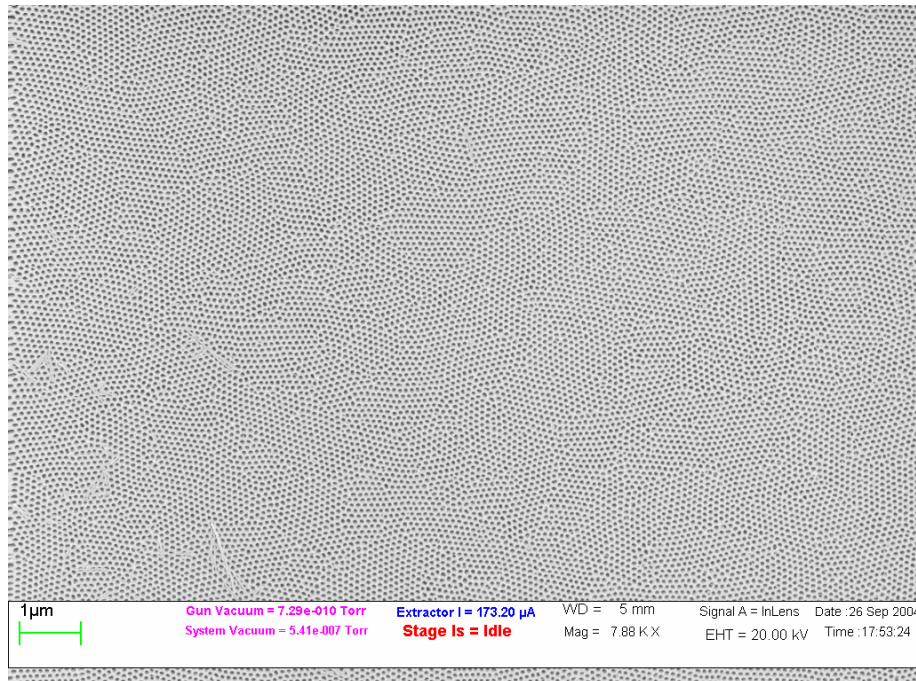
(B)
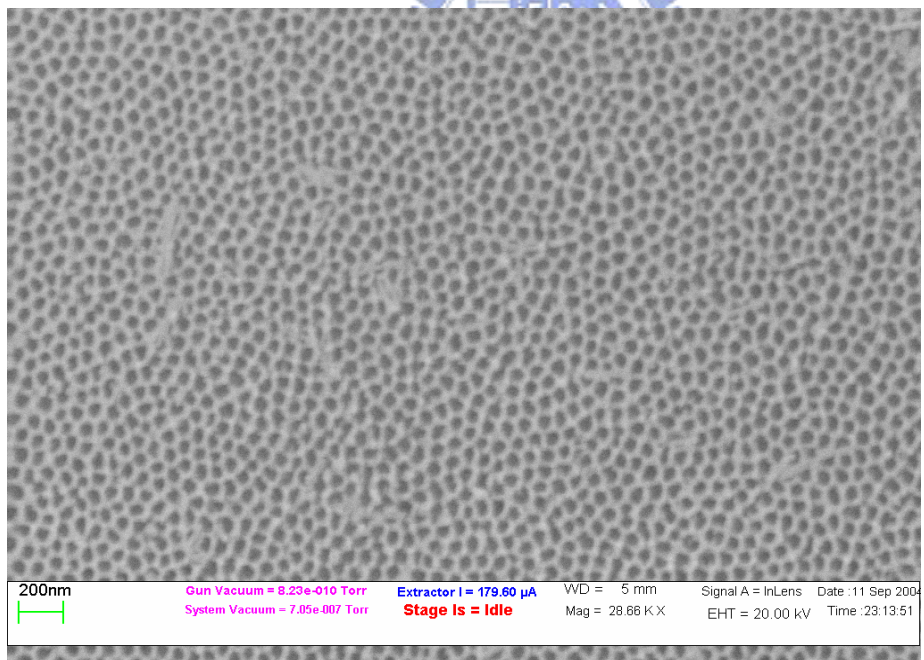
Figure 3. The SEM images of uniform porous alumina fabricated using 0.3 M oxalic acid

solution anodized at 30V for 5 hours at 5℃. (A) Low magnification. (B) High magnification.

(A)

(B)
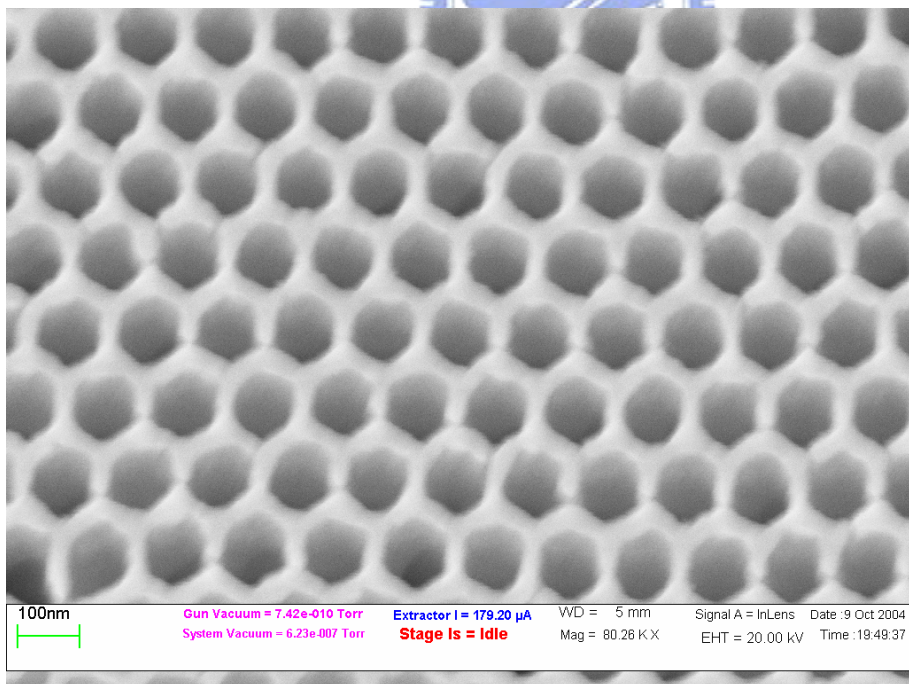
Figure 4. The SEM images of the ordered alumina using 0.3M oxalic acid solution anodized

at 40V for 12 hours at 5℃: (A) Low magnification. (B) High magnification.

(A)
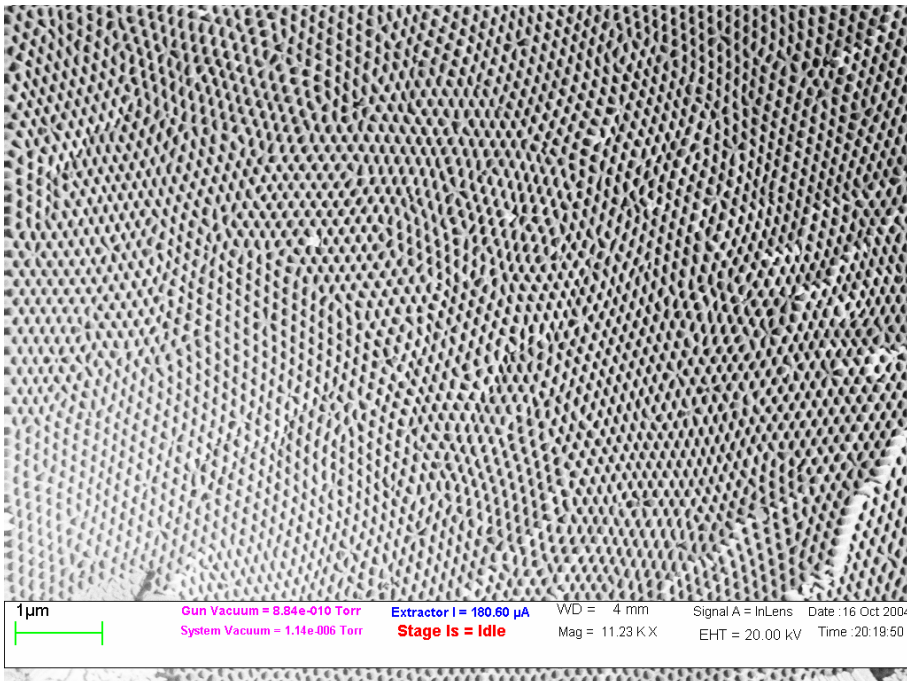
(B)
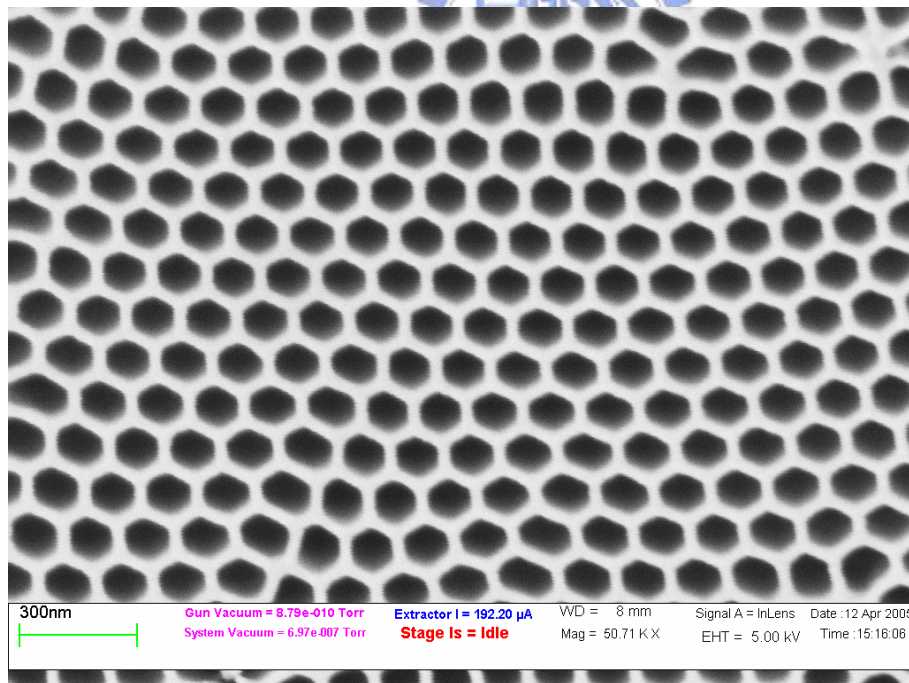
Figure 5. The SEM images of the ordered alumina fabricated using 0.3M oxalic acid solution

anodized at 50V for 12hr at $10°C$: (A) Low magnification (B) High magnification.

(A)
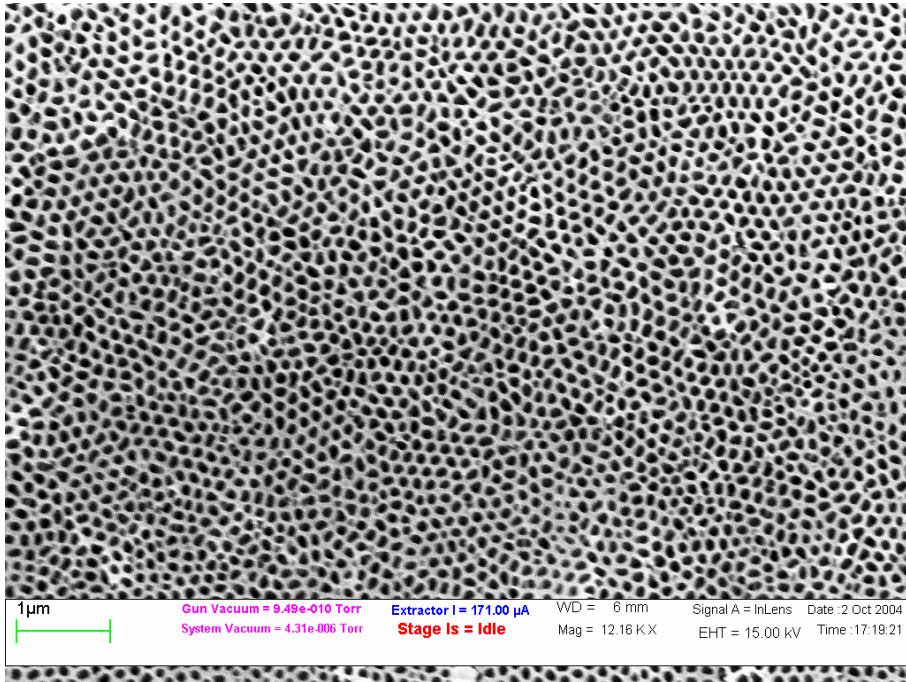
(B)
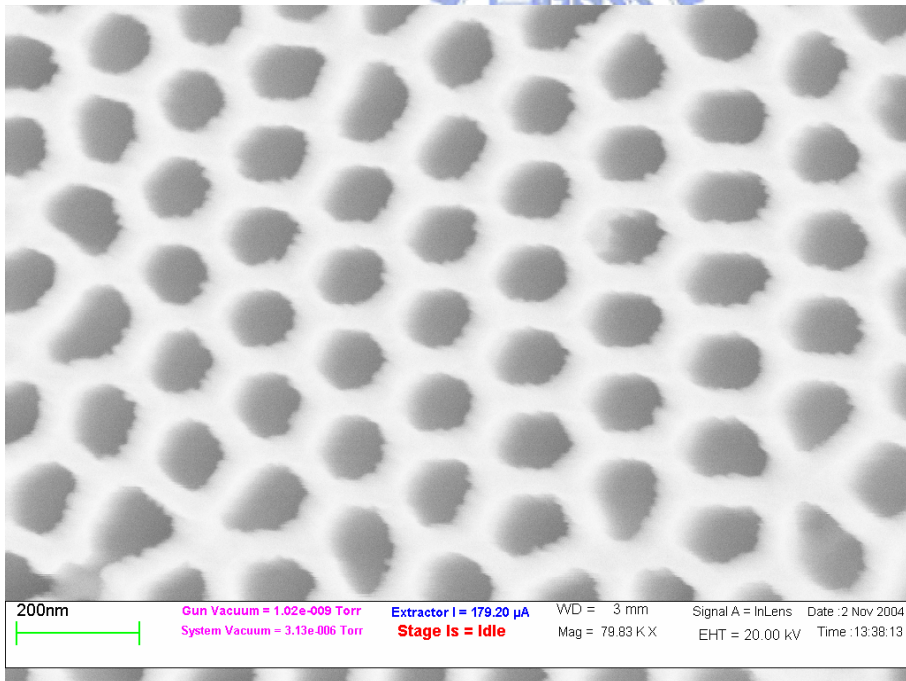
Figure 6. The SEM images of ordered alumina fabricated using 0.3M oxalic acid anodized at

60V for 9 hours at 3℃: (A) Low magnification. (B) High magnification.

(A)
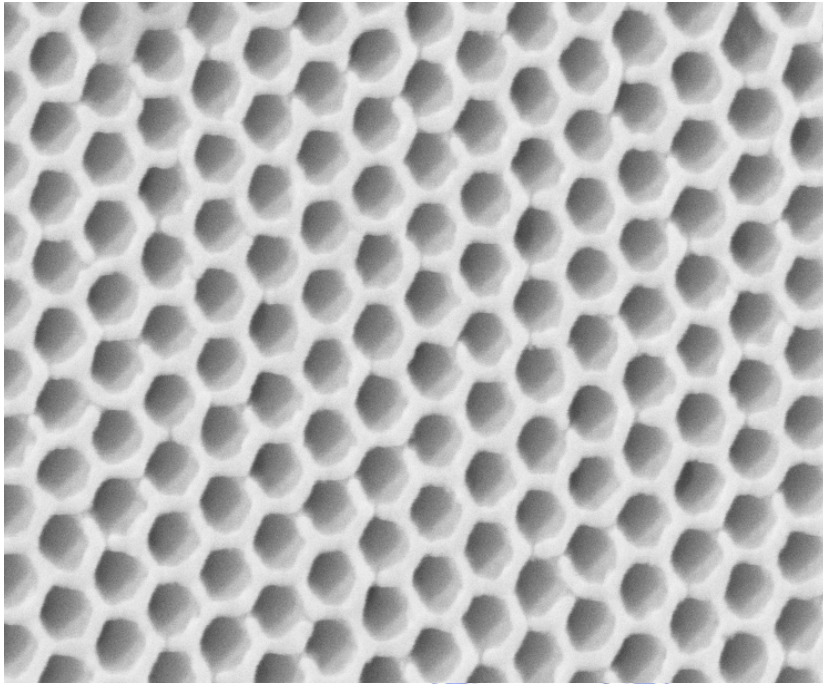
(B)
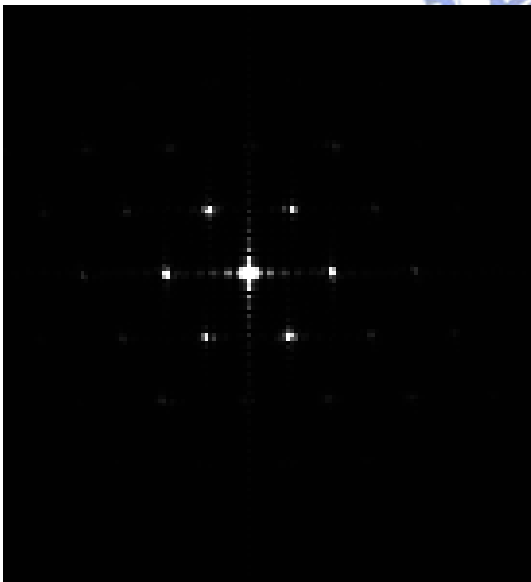
Figure 7. (A) The SEM image of ordered alumina fabricated using 5wt % phosphate acid

anodized at 40V. (B) The FFT image of the SEM image

.

(A)
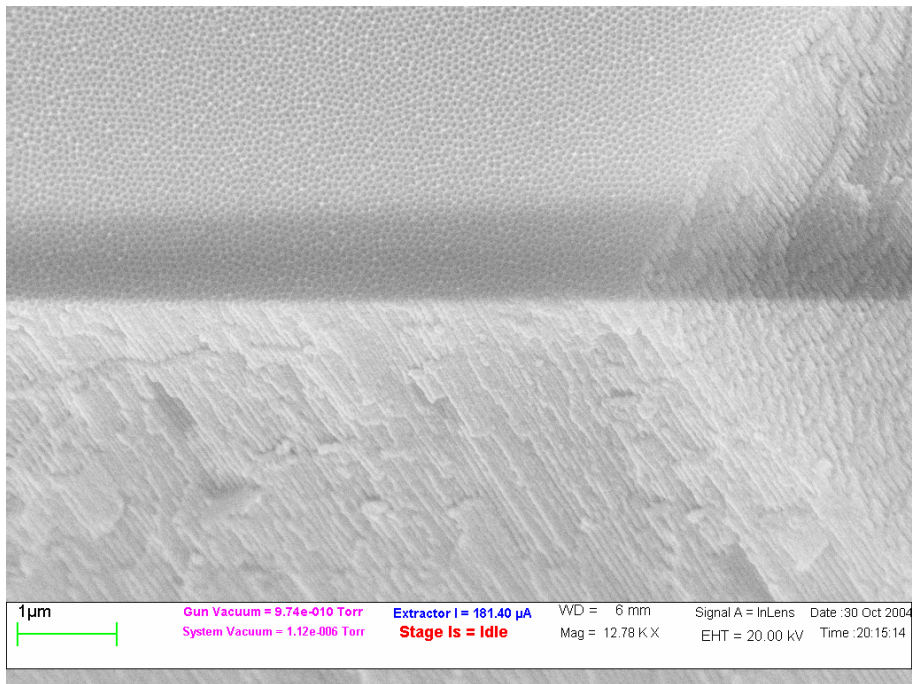
(B)
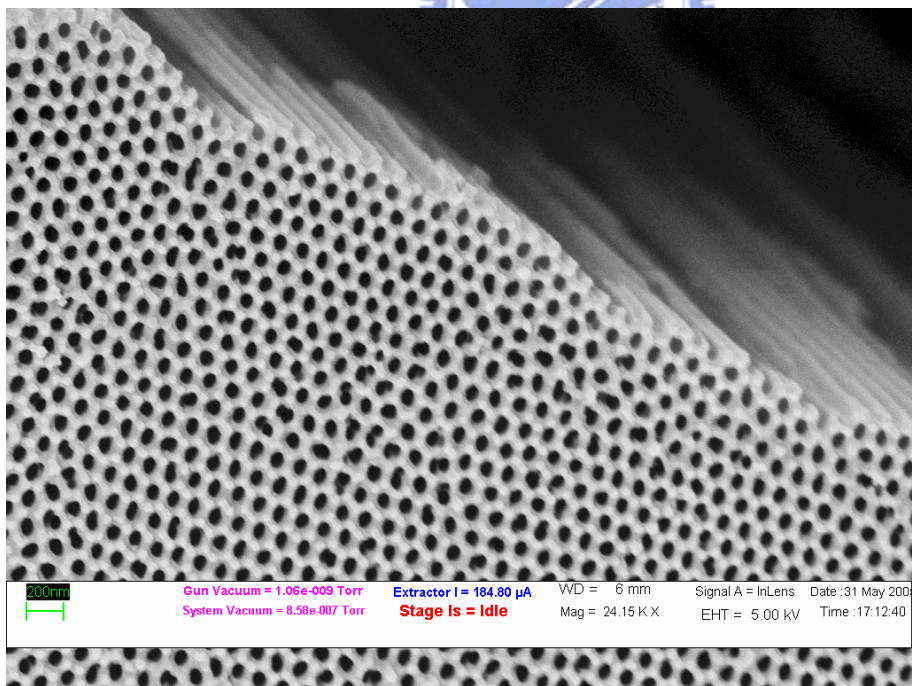
Figure 8. The cross sectional images of anodic alumina films fabricated at (A) 30V (B) 40V.

Chapter 3 Synthesis of Nanowires

3.1 Introduction

AAO templates have been widely used for the fabrication of various one dimensional

nanomaterials such as polymer [*1, 2*], semiconductors [*3, 4*], metals [*5*] using electrochemical

deposition. For example, using sequential electrodeposition it has been shown by Keating et

al.[*6*] that it was possible to fabricate multi-component nanowires. Because of the variations

in composition along the length, it has been suggested that different surface chemistry could

be used to modify individual segment of the nanowires. These functionalized nanowires have

been demonstrated capable of conducting chemical and bio-sensing. In another study, Ozin et

al. have shown that by taking the advantage of the catalytic reaction of the nickel, it was

possible to observe the rotation of the nanowires in the presence of the hydrogen peroxide due

to the catalytic decomposition of hydrogen peroxide on the nickel segment [*7*].

In addition to the anodization of aluminum foil to produce free standing AAO membrane,

it was shown that periodic pore array (PPA) can be grown on the silicon wafer by anodization

of the aluminum film. For example, Rabin et al. have demonstrated that PPA on the silicon

wafer can be used to fabricate large area arrays of high aspect ratio nanowires on the silicon

wafers where the nanowires could be electrically connected to characterize the transport

properties of the nanowires [*8*]. The porous film on the silicon wafer could also be used as the

deposition mask by etching away the barrier layer as suggested by Crouse et al. [9]. It has

been shown that silver nanodot arrays with diameter of 100nm could be obtained by

evaporation of silver and subsequent removal of alumina film [10]. Cojocaru et al. have

reported the lateral oxidation of the thin aluminum film on silicon substrate by artificially

controlling the orientation of the electric filed. It has been shown that the diameter of the

lateral pore could be as small as 3 to 4 nm arrays. Such process can be used to fabricate

self-order, highly regular in plane arrays of nanopores for micromechanical system (MEMS)

application [11].

One-dimensional nanomaterials have also been shown to be an important building block

materials in the self-assembly process. To demonstrate the possibility to control the assembly

process into the flat two-dimensional or curved three-dimensional structures, the polymer

(oxidized polypyrrole) – gold nanorods have been deposited into AAO templates [12, 13].

Depending on the chemical functionalization, it was shown that both close 3D bundles and

open 2D networks of the nanowire assembly have been obtained. It was also shown by Gu et

al. [14] that the surface tension could be used to control the self-assembly process. Magnetic

and capillary interactions can also be used to control the 3D self-assembly of the nanowire if

the nanowires were consisted of alternating sections of ferromagnetic (nickel) and

diamagnetic materials (gold). The nickel segment was magnetized spontaneously to assemble

into stable "bundles" in the absence of an external field. Such assembly process did not

require specific surface chemistries [15].

3.2 Experimental

3.2.1 Preparation of nanowires

To fabricate the AAO template for the nanowires, we first utilized the two step anodization

process of the aluminum foil. However, the anodization process was often time consuming

and low yield for production of nanowires. Therefore, we have switched to the commercial

AAO membranes purchased form Whatman as the template for the nanowires. To produce

nanowires by electrodeposition, alumina oxide membranes with 200 nm pore diameter

(Andisc, Whatman) were used as the templates. To perform electrodeposition, one side of

membrane was sputter-coated with a 200 nm thick silver film for conducting purpose. This

template was placed in contact with a copper plate and restrained with a glass joint and sealed

with an o-ring. The counter electrode was a 2 mm diameter platinum wire. The template was

rinsed with DI water for 10 minutes and immersed in the desired the electrolytic solution.

Commercial plating solutions were used to produce gold (Technic Gold 25E), Ag (Technic

Cy-less Silver 2 RTU,) and Ni (Techni Nickel RTU) nanowires.

3.2.2 Pulse electrodeposition

In this experiment, the pulse electrodeposition was used to produce metallic nanowires.

In a typical electroplating period, a negative current at – 10V was applied 8 ms and followed by a short pulse of positive current at 3 V for 2 ms. Before the next negative current arrived, the system was sustained at 0V for 990 ms [16]. Metallic nanowires with different lengths could be produced by adjusting the electrodeposition time. For example, the pulse sequence was repeated for 30 minutes to fabricate 3μm long Ag nanowires. However, the deposition time for the 5 μm gold nanowire was 90 minutes. The length of the nanowires can be controlled by monitoring the total charge passing through the electrochemical cells and the deposition time. The plating solution can be changed during the electroplating process to produce multisegment nanowires.

After the electrodeposition process, the silver film was removed in a 3 M nitric acid and the metal nanowires were released by dissolving alumina membranes in a 3 M NaOH aqueous solution. Template dissolution produces a monodispersed suspension of individual wires, which can then be modified with desired functional group. The nanowires were then washed by DI water and centrifuging at 5000 rpm for 10 minutes several times. Since the length of the nanowires was in the micrometer region, the concentration of the nanowires was determined by counting the number of nanowires using a hemacytometer on an inverted microscope (Olympus, IX 71).

3.3 Results and discussion

When AAO template was used for electroplating, the metal ions can be reduced into the nanochannels where the metal could grow from the bottom of channel to form nanowires. Shown in figure 1A is the AAO template with silver nanowire. These AAO templates (figure 1B) with 40 to 50 nm pore diameter were fabricated by anodization of the aluminum substrate in 0.3 M oxalic acid aqueous solution. The average pore size was measured to be 43nm. Since the production of such template was time consuming, the commercial AAO membrane was used this experiment for the fabrication of nanowires. Shown in figure 2A is the SEM image of a commercial AAO membrane with irregular pore arrangement where the pore size was about 200nm. When different electroplating solutions were used, it was possible to produce nanowires with multi-components. Shown in figure 2B is the SEM image of the gold-nickel nanowires on the AAO membrane before the removal of the silver backing.   To remove the silver backing, the AAO membrane was dissolved in 6 M HNO_3 solution for 10 minutes. The alumina membrane was then rinsed with DI water and placed in NaOH solution, and sonicated for 10 minutes to release the nanowires from the AAO membrane. This process was repeated several times. Figure 2C illustrates the cross-sectional SEM image of 2.5 μm long nickel nanowires in the nanochannels.

After the AAO templates with high purity nickel nanowires were annealed at 350 ℃ for 2 h, the nickel metal nanowires could be released by dissolving alumina membranes. The wires were then rinsed with ethanol solution and spin coated on the ITO substrate. When the

ethanol solution was evaporated, magnetic nickel nanowires bundles could be obtained.

Shown in figure 3 is the back scattered SEM image of the bundles of nickel nanowires. These

nanowires were approximately 6 to 7 μm in length. Since AAO templates are stable at high

temperatures, it has been suggested that the annealing process for the magnetic nanowire

could produce GMR effect [17].

To fabricate 200 to 300 nm long gold nanorods, the gold plating solution was used and

the electrodeposition time was about 20 minutes. After removing the silver backing by nitric

acid, the isolated gold nanorods were obtained as shown in figure 4. The same approach can

be used to obtain multi-component nanowires composed of silver and nickel segment. Shown

in figure 5 is the back scattered SEM image of Ag-Ni nanowire where the silver portion was

about 2 μm long and nickel portion was about 4 μm. Gold –nickel nanowires could also be

obtained by the same process as shown in fig 6 [14]. In the SEM image, the gold portion

seems to be brighter than the nickel portion due to the difference in the electron scattering

cross section of gold and nickel. It should be noticed that care must be taken to avoid the

fracture of the high aspect ratio nanowires.

Figure 7 shows a high density assembly of nanowire composed of silver and gold with 2

~ 3 μm in length. The gold portions of the two-component structure were used to protect

silver domain during the silver backing removal process. In case of the production of the

Ag-Au-Ag-Au nanowires, it is very important to control the growth process as shown in

figure 8. Since the extinction coefficient of the silver and gold are different in the UV region and the electron scattering cross section is also different for these two metals, they exhibit different reflectivity in both optical image and electron image as shown in figure 9 and 10 [*18*].

3.4 Conclusions

Using porous alumina as template for electroplating, we have developed a protocol to synthesize encoded multi-component nanorods, which could be used to label biomolecules and deliver genetic materials. By controlling the timing of electroplating at constant current density, metallic nanowires with desired length have been fabricated. Using different electroplating solution and different amount of electroplating time, multi-component nanowires or "striped" nanowires have been obtained. Multi-segment wires such as gold, silver and nickel with differential length have been fabricated via the sequential electrochemical deposition into the commercial AAO templates.

Reference

1. O. Jessensky, F. Muller and U. Gosele, *Appl. Phys. Lett.* 1998, **72**, 1173.

2. H. Xu, R. Hong, X. Y. Wang, R. Arvizo, C. C. You, B. Samanta, D. Patra, M. T. Tuominen and V. M. Rotello, *Adv. Mater.* 2007, **19**, 1383.

3. D. J. Pena, J. K. N. Mbindyo, A. J. Carado, T. E. Mallouk, C. D. Keating, B. Razavi and T. S. Mayer, *J. Phys. Chem. B* 2002, **106**, 7458.

4. I. B. Divliansky, A. Shishido, I. C. Khoo, T. S. Mayer, D. Pena, S. Nishimura, C. D. Keating, T. E. Mallouk, *Appl. Phys. Lett.* 2001, **79**, 3392.

5. D. T. Mitchell, S. B. Lee, L. Trofin, N. C. Li, T. K. Nevanen, H. Soderlund and C. R. Martin, *J. Am. Chem. Soc.* 2002, **124**, 11864.

6. C. D. Keating and M. J. Natan, *Adv. Mater.* 2003, **15**, 451.

7. S. Fournier-Bidoz, A. C. Arsenault, I. Manners and G. A. Ozin, *Chem. Commun.* 2005, 441.

8. O. Rabin, P. R. Herz, Y. M. Lin, A. I. Akinwande, S. B. Cronin and M. S. Dresselhaus, *Adv. Fun. Mater.* 2003, **13**, 631.

9. D. Crouse, Y. H. Lo, A. E. Miller and M. Crouse, *Appl. Phys. Lett.* 2000, **76**, 49.

10. H. Masuda, K. Yasui, Y. Sakamoto, M. Nakao, T. Tamamura and K. Nishio, *Jap. J. Appl. Phys. 2* 2001, **40**, L1267.

11. C. S. Cojocaru, J. M. Padovani, T. Wade, C. Mandoli, G. Jaskierowicz, J. E. Wegrowe,

A. F. I. Morral and D. Pribat, *Nano Lett.* 2005, **5**, 675.

12. C. A. Mirkin, S. Park, J. H. Lim and S. W. Chung, *Abstr. Pap. Am. Chem. S.* 2004, **227**, U259.

13. S. Park, J. H. Lim, S. W. Chung and C. A. Mirkin, *Science* 2004, **303**, 348.

14. Z. Y. Gu, Y. M. Chen and D. H. Gracias, *Langmuir* 2004, **20**, 11308.

15. J. C. Love, A. R. Urbach, M. G. Prentiss and G. M. Whitesides, *J. Am. Chem. Soc.* 2003, **125**, 12696.

16. K. Nielsch, F. Muller, A. P. Li and U. Gosele, *Adv. Mater.* 2000, **12**, 582.

17. P. R. Evans and G. Yi, W. Schwarzacher, *Appl. Phys. Lett.* 2000, **76**, 481.

18. S. H. Liu, J. B. H. Tok and Z. N. Bao, *Nano Lett.* 2005, **5**, 1071.

(A)
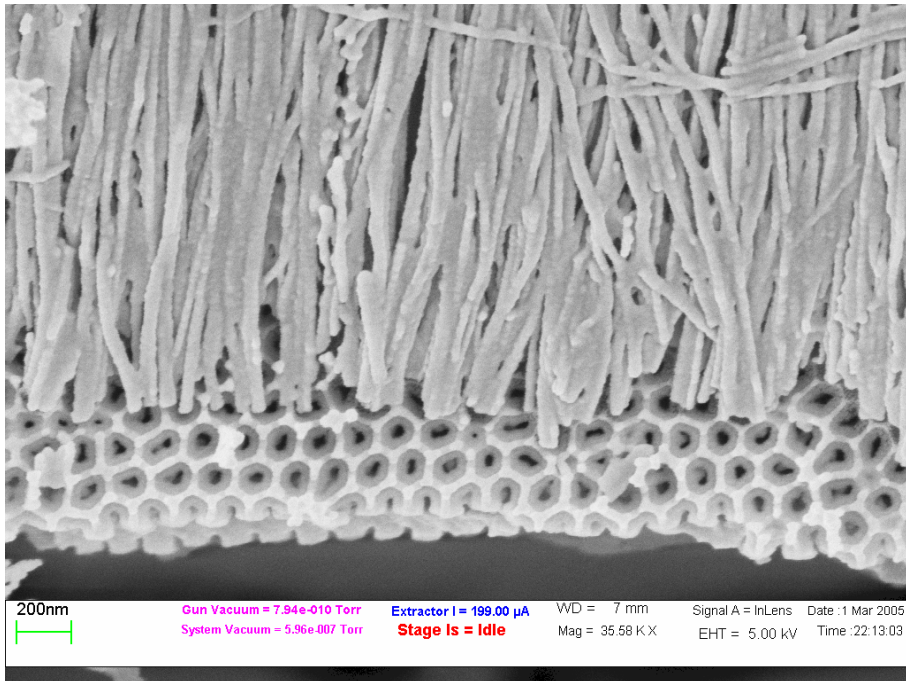
(B)
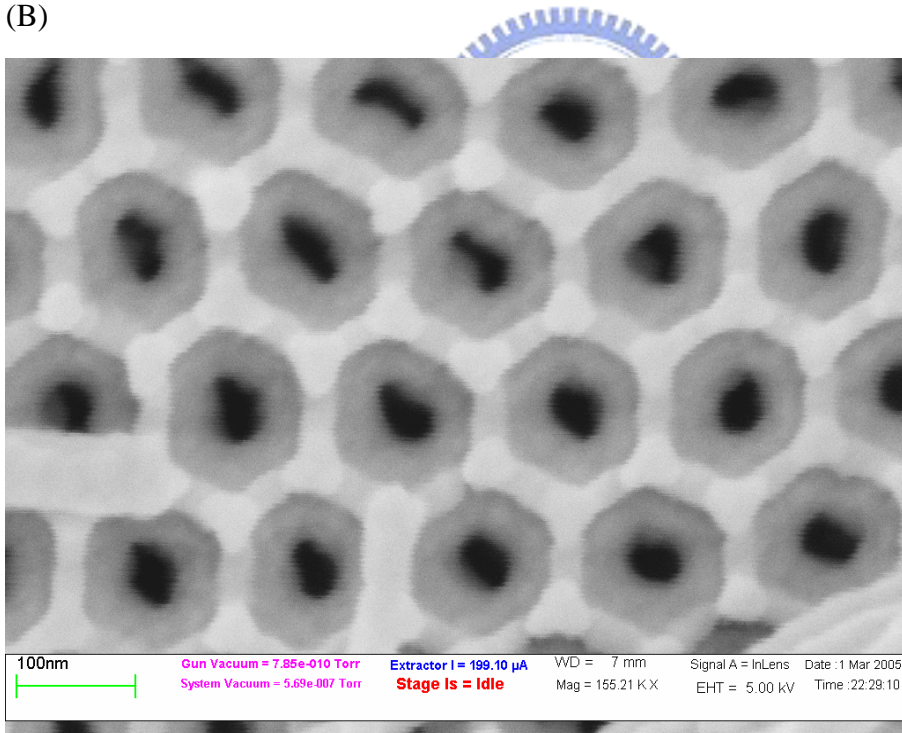
Figure 1. The SEM images of (A) 40 nm silver nanowires on the AAO template (B) uniform pore arrays fabricated using 0.3M oxalic acid solution anodized at $4°C$ (the average pore diameter is 42.5 nm).

(A)
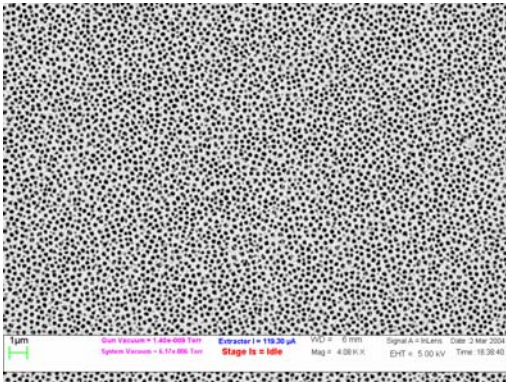
(B)
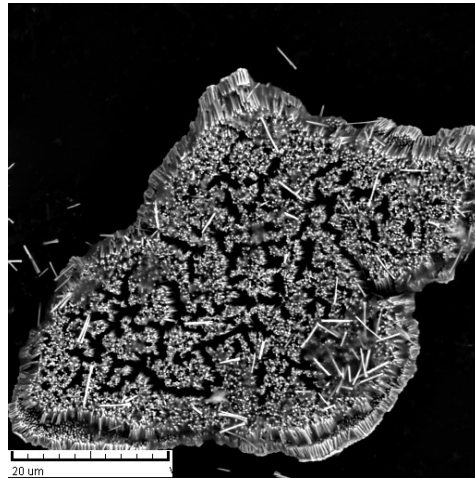
(C)
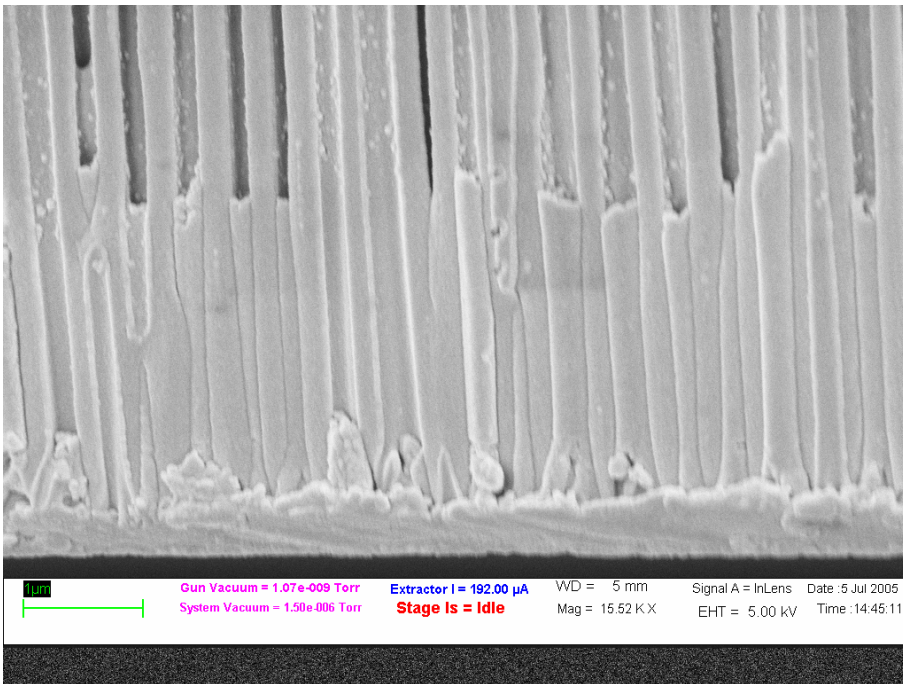
Figure 2 The SEM images of (A) AAO template (B) Au-Ni nanowires arrays on the AAO

template. (C) Cross-sectional view of Ni nanowires in AAO template.
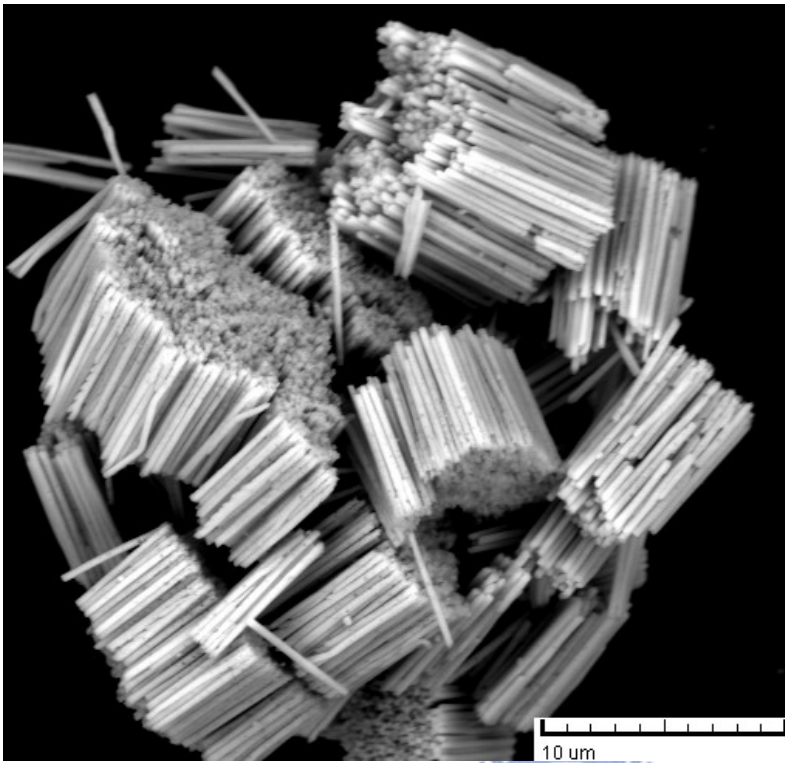
Figure 3. The backscattered SEM image of the 3D bundles of the Ni nanowires.

(A)

1/19/2007	HV	det	mode	mag	WD	3 μm
7:01:13 PM	18.00 kV	BSED	A+B	15 564 x	4.9 mm	
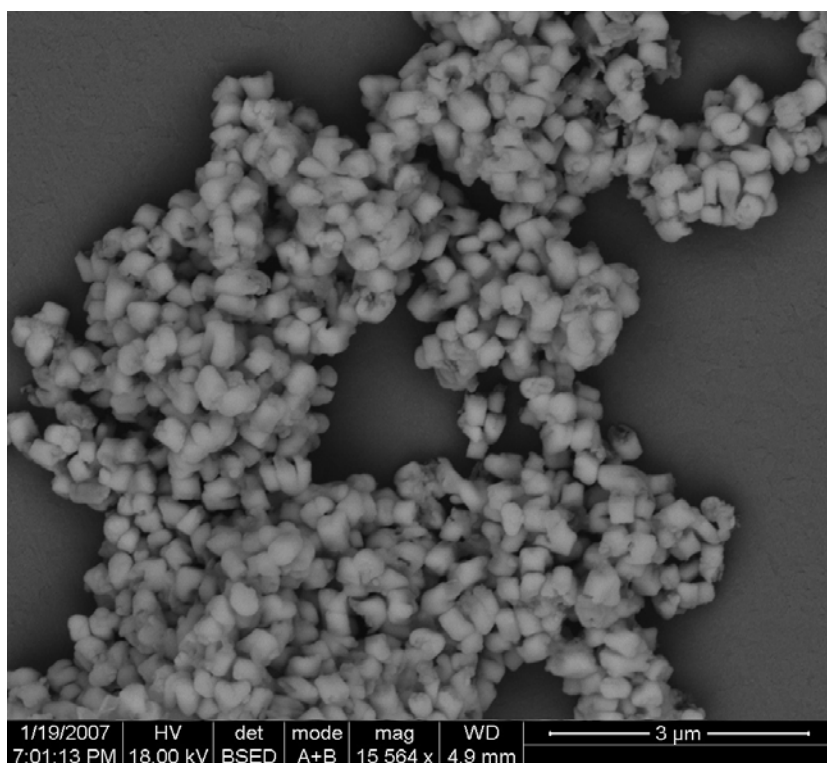
(B)
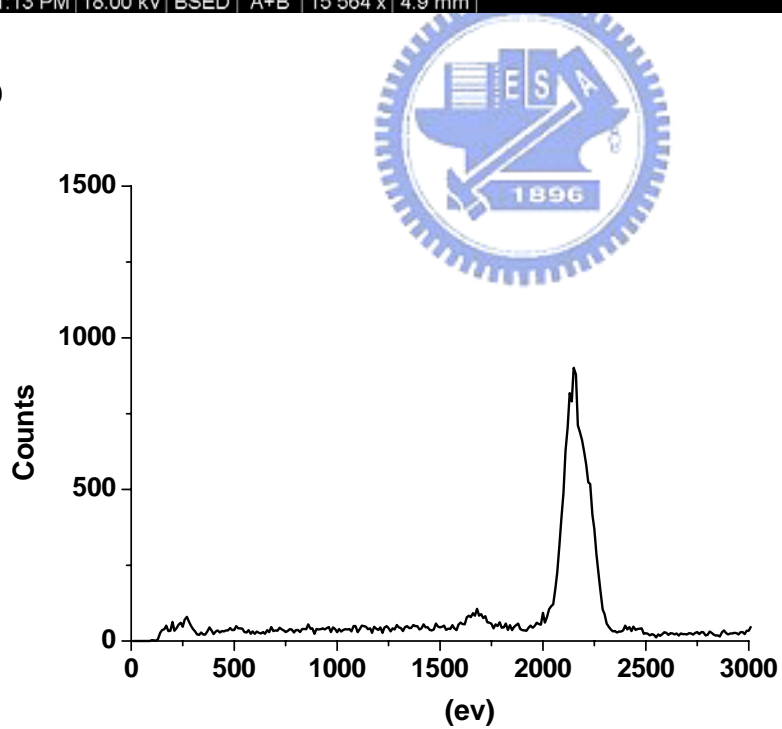
Figure 4. (A) The backscattered SEM image of the gold nanorods. (B) The EDX spectrum of

the gold nanorods.

(A)
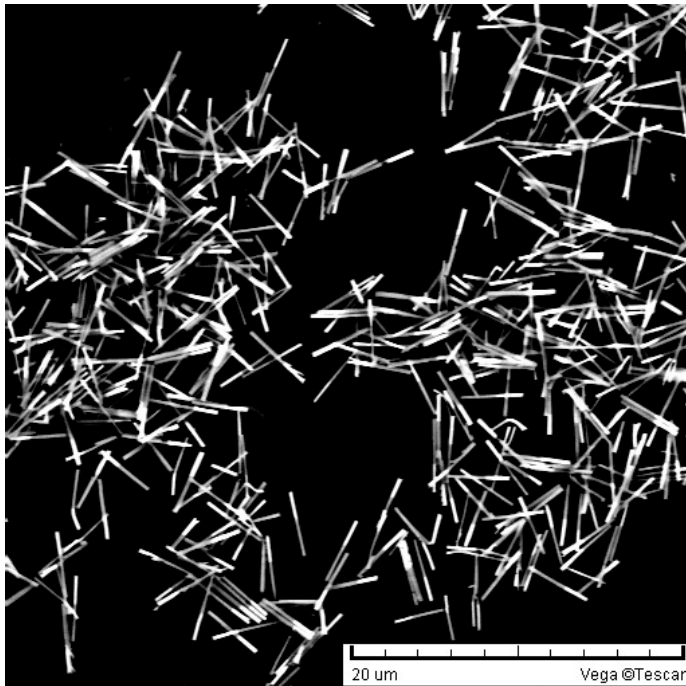
(B)
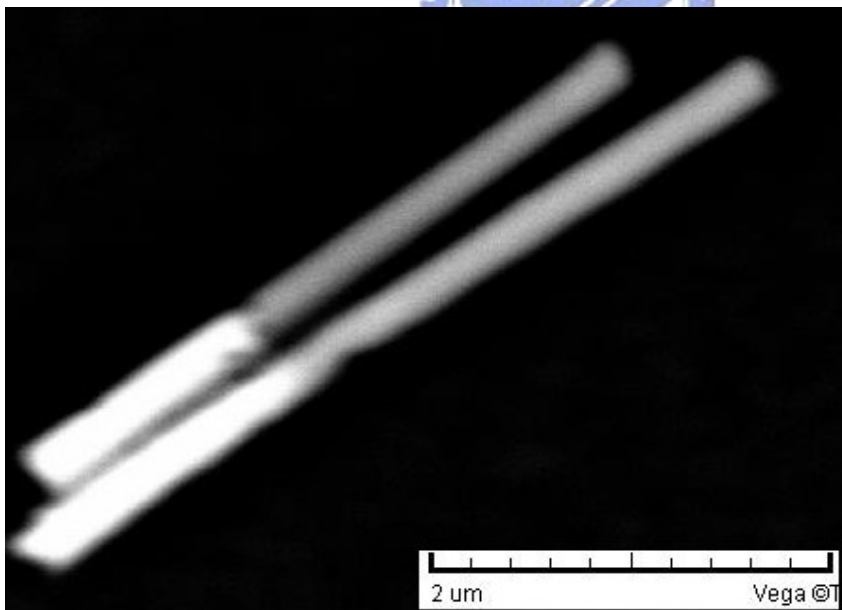
Figure 5. The backscattered SEM images of Ag-Ni nanowires. The darker part is made of

silver and brighter part is made of nickel. (A) Low magnification (B) High magnification.
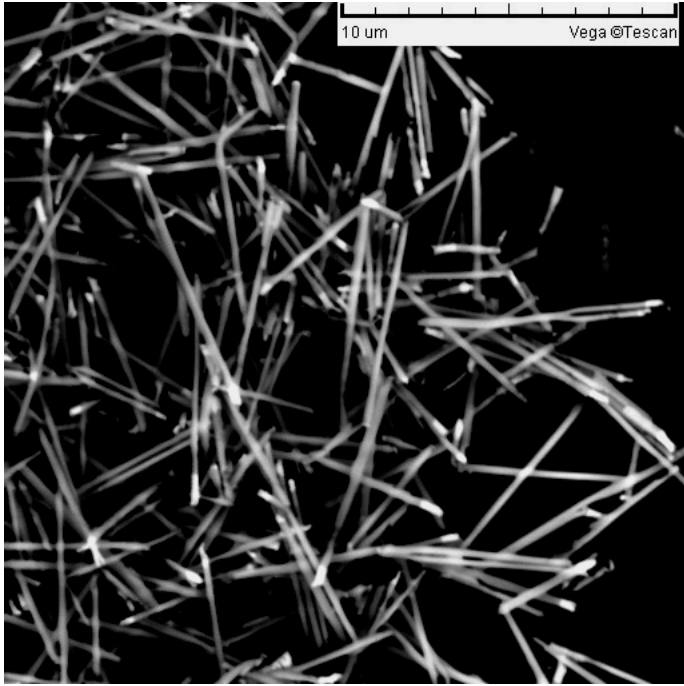
Figure 6.The backscattered SEM image of Au-Ni nanowires.
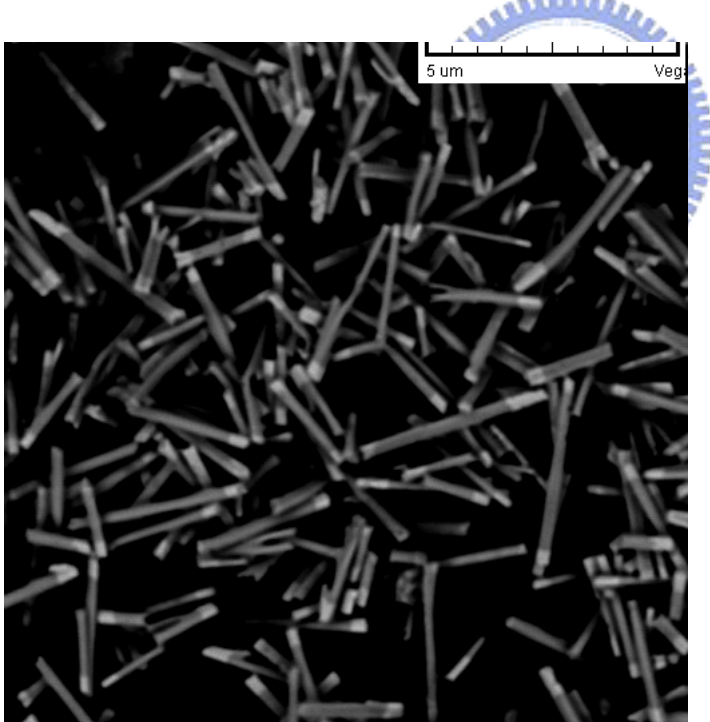
Figure 7. The backscattered electron image of the stripped Au-Ag nanowires.
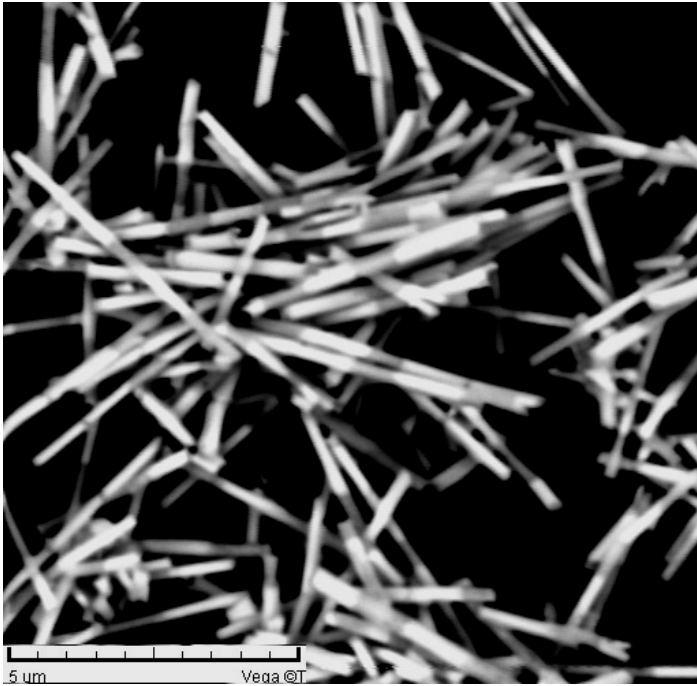
Figure 8 .The backscattered SEM image of the stripped nanowires. The stripped pattern is

Ag-Au-Ag-Au.
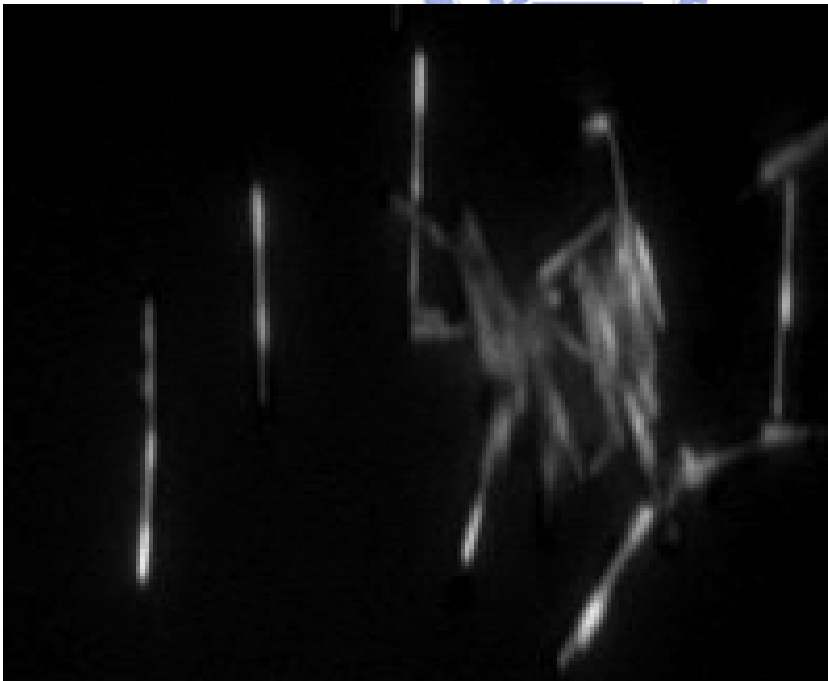
Figure.9. The optical image of Au-Ag-Au-Ag nanowires.

Figure10. The optical image of a Au-Ag-Au nanowire. Objective: 100× oil immersion lens.

Chapter 4 Functionalization and Characterization of Nanowires

4.1 Introduction

To utilize the nanoparticles in the biological system, it often requires surface modification of the nanoparticles for the biocompatibility consideration. Since the surface modification techniques are well-established for gold, gold nanoparticles are frequently used for biomolecular surface recognition. Monodispersed gold nanoparticles have been routinely produced through various techniques. The most common approach for the synthesis of monodispersed gold colloidal particles was to reduce the metal salts in the presence of surfactants. The size, shape, and interparticle separation of these uniform size colloidal particles could be controlled by the capping ligands, which often involve thiol, amino, cyanide, and carboxylic acid group. Colloidal gold nanoparticles provide a large surface area for surface recognition of biomacromeolecules. Several groups have investigated the biomolecular surface recognition using gold nanoparticles. For example, Rotello and coworker [1-4] have fabricated core-shell gold nanoparticles where the gold monolayer protected clusters were displaced via the Murray place-exchange method to create the mixing monolayer protected cluster (MMPCs). This process can provide a reactive group at the surface for biomolecular surface recognition. Han et al. have demonstrated that the trimethylammonium end-group on the MMPC surface could bind to 37mer duplex DNA through electrostatic interaction [5]. This MMPC successfully inhibited the DNA transcription

by T7 RNA polymerase. The MMPC was also used to bind DNA for gene delivery into cells. The nanoparticles with various amounts of the amino functional group were incubated with DNA plasmid encoding β−galactosidase into human embryonic kidney cells. The optimal transfection observed was about ~68 %.

Charged or hydrophilic groups are often incorporated into the nanoparticle surface to provide solubility in water and functionality for interaction with biomolecules. Hydrophilic groups, such as oligo(ethylene glycol)(OEG) and Poly(ethylene glycol) (PEG) are commonly used on the gold surface. Surface adsorption of proteins can denature the proteins and in some cases, limit the interactions of the ligand with the target on the cell surface due to steric hindrance [4]. OEG and PEG are known to resist the non-specific interaction with biomolecules, which in turn improves the biocompatibility of nanoparticles. Rotello and coworkers have investigated the attachment of branched 2KD polyethylenimine(PEI) to gold nanoparticles, which could double the efficiency of gene delivery.

As for the surface modification of nanorods or nanowires, it has been demonstrated that it was possible to selectively modify the multi-segment nanorods and nanowires. For example, Meyer et al. have employed selective surface modification scheme to the two component nickel-gold nanowires to achieve bi-functionality [6]. In this case, the nanowire were reacted with 11-aminoundecanoic acid and 1,9-nonanedithol. It was shown that the carboxylic acid could bind to the nickel segment while the thiol group was used to modify the gold segment

surface. The result of the dual functionalization could be observed by the fluorescence microscopy [1, 7]. Since multi-segment nanowires could exhibit dual functionalities, they can provide methods for simultaneous detection and separation of multiple species in solution. For example, Mirkin et al. have demonstrated that Au-Ni-Au nanowire could be used for target binding and separation of biomolecules process. To achieve this goal, the gold portions of the nanorods were passivated with 11-mercaptoundecyl-tri (ethylene glycol)(PEG–SH) and fluorescein-tagged poly-His (His > 6) was then bound to the Ni portions of the substrate as evidenced by confocal fluorescence microscopy [8, 9].

In this study we have focused on the surface modification of gold nanowires for gene deliver. By simple surface modification scheme, we are trying to find out the less toxic surface modification for the gold nanowires.
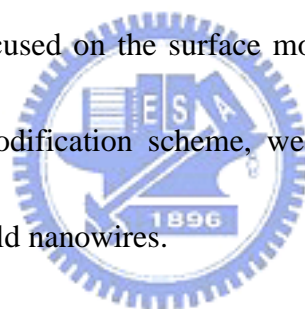
4.2 Experimental

The nanowire surfaces were coated by a monolayer of thiols with amino, alkyl or carboxyl end group. To modify the surface of nanowires, the suspended gold nanowires (1 x 10^8 nanowire/ml) solutions were mixed with an ethanol solution of 1 mM of 11-amino-1-undecanethiol (Dojindo), 1 mM of octadecanethiol (Aldrich), or 1 mM of 11-mercaptoundecanoic acid (Aldrich). After 24 hours of incubation, the nanowires were cleaned by the doubly distilled water and the excess thiols were removed by dialysis for 24 hours using a 3.5kD cut off dialysis membrane with the doubly distilled water. For

comparison, the serum coated nanowires was also investigated where the serum coated

nanowires were obtained by incubating the nanowires in the PBS solution containing serum

for 24 hours. All surface modified nanowires can be suspended in aqueous solutions by strong

vortexing. However, longer nanowires exhibited higher sedimentation rate. The

zeta-potentials of the surface modified nanowires around neutral pH value were measured by

a Zeta Potential Analyzer ZetaPALS (Brookhaven Instruments Corp.) at a field of 8-16V/cm.

4.3 Results and discussion

Gold nanowires used in this experiment were fabricated by electrochemical deposition

utilizing commercial alumina membranes (200 nm) as templates. The detail fabrication

procedures and experimental parameters are described in chapter 3. In order to investigate the

influence of aspect ratio (length to diameter) on the cytotoxicity, nanowires with four different

aspect ratios were prepared. The size distributions and the SEM images of the four different

size of gold nanowires are shown in figure 1. The lengths of gold nanowires were 0.58 ±0.07,

1.8 ±0.6, 4.5 ±0.9, 8.6 ±1.4 μm as measured by the SEM images and the corresponding

aspect ratios were 2.9, 9, 23 and 43, respectively. To study the cytotoxicity of the surface

modification, the surfaces of nanowires were functionalized by a monolayer of thiols with

amino, alkyl or carboxyl end group or coated with serum, which was known to adsorb on the

gold nanoparticles [10]. In a previous report [11], the zeta potentials for the self-assembled

monolayer on the nanoparticle surface with amino, alkyl and carboxyl end group were about

+10, -30 and -50 mV, respectively, at pH 7.   In this experiment, the zeta potential for the

unmodified gold nanowires was measured to be -82 mV in the doubly distilled water whose

pH value stabilized in air at pH 6 (due to the dissolution of CO_2). And the zeta-potential of the

nanowires modified with amino, alkyl, carboxyl and serum were measured to be +11.4±1.4,

-7.2±0.6, -25.5±1.3, -39.6±0.1 mV, respectively, at pH 6. It was clear that the amino modified

nanowires exhibited positive zeta potential while the negative charged surface was observed

for the mercapto acid modified nanowires. The nanowires functionalized with alkanethiols

were slightly negatively charged, which may due to the adsorption of anions on the surfaces.
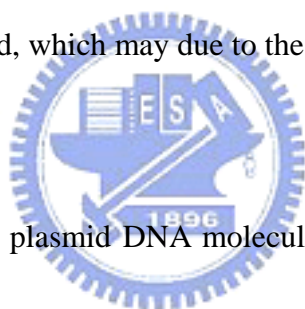
A typical strategy to bind plasmid DNA molecules or probe molecules on the metallic

nanoparticle is to employ the electrostatic interaction. Since the plasmid DNA molecules are

negatively charged, the positively charged amino-modified gold nanowires were used to bind

the plasmid DNA molecules. The zeta potential for the nanowires/plasmid DNA complex was

about -9.3±0.5mV in the doubly distilled water at pH 6. However, when the growth media

were used, the zeta-potentials of the amino, alkyl, carboxyl and serum modified nanowires

changed to -7.6±1.4, -6.9±1.2, -17.4±1.0, -16.6±1.6 mV at pH 7.8. In the growth media, some

of the surface modified gold nanowires settled on the bottom of the cell culture dishes.

However, no aggregation of these nanowires was found at the nanowire concentration up to

10^6 nanowire/ml.

4.4 Conclusions

In summary, we have synthesized gold nanowires with various aspect ratios. Four different surface modification schemes including serum, alkanethiols, mercapto acids and aminoalkylthiols were used to functionalize the surface of the gold nanowires. It was found that all surface modifications expect aminothiols produced negatively charged gold nanowires. Therefore, the amino presenting gold nanowires were used bind the negatively charged plasmid DNA molecules. From the zeta potential measurement, it was concluded that the DNA molecules could bind to the amino presenting gold nanowires.
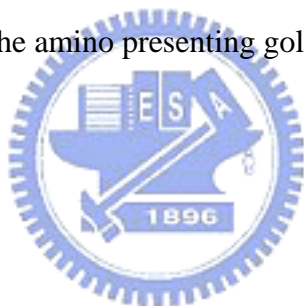
Reference

1.   P. S. Ghosh, A. Verma and V. M. Rotello, *Chem. Commun.* 2007, 2796.

2.   C. M. Goodman, K. K. Sandhu, J. M. Simard, S. W. Smith and V. M. Rotello, *Abstr. Pap. Am. Chem. S.* 2002, **224**, U131.

3.   A. Verma and V. M. Rotello, *Chem. Commun.* 2005, 303.

4.   C. C. You, A. Chompoosor and V. M. Rotello, *Nano Today* 2007, **2**, 34.

5.   G. Han, N. S. Chari, A. Verma, R. Hong, C. T. Martin and V. M. Rotello, *Bioconjugate Chem.* 2005, **16**, 1356.

6.   L. A. Bauer, D. H. Reich and G. J. Meyer, *Langmuir* 2003, **19**, 7043.

7.   L. A. Bauer, N. S. Birenbaum and G. J. Meyer, *J. Mater. Chem.* 2004, **14**, 517.

8.   K. B. Lee, S. Park and C. A. Mirkin, *Angew. Chem. Int. Edit.* 2004, **43**, 3048.

9.   S. J. Hurst, E. K. Payne, L. D. Qin and C. A. Mirkin, *Angew. Chem. Int. Edit.* 2006, **45**, 2672.

10.   B. D. Chithrani, A. A. Ghazani and W. C. W. Chan, *Nano Lett.* 2006, **6**, 662.

11.   J. J. Shyue and M. R. De Guire, *Langmuir* 2004, **20**, 8693.
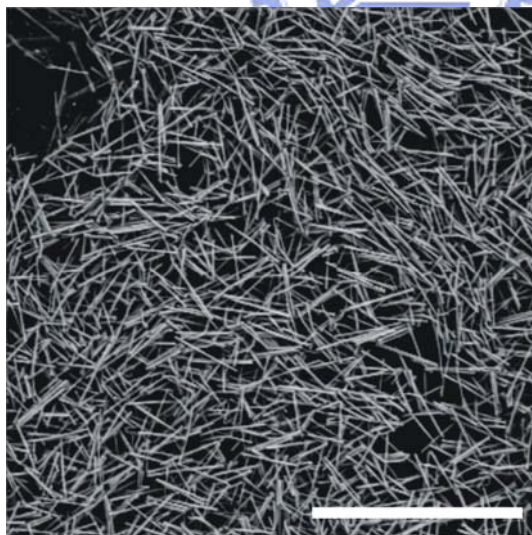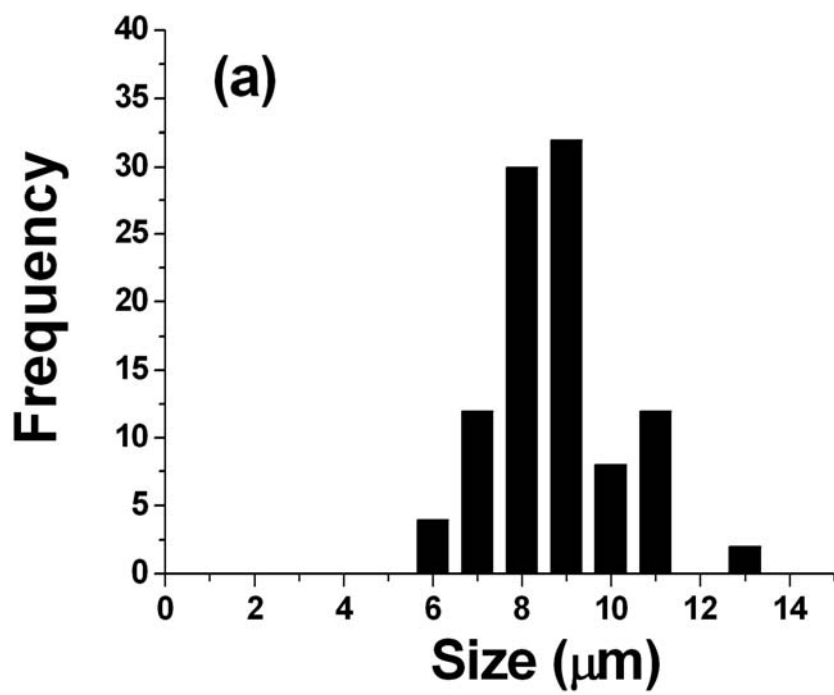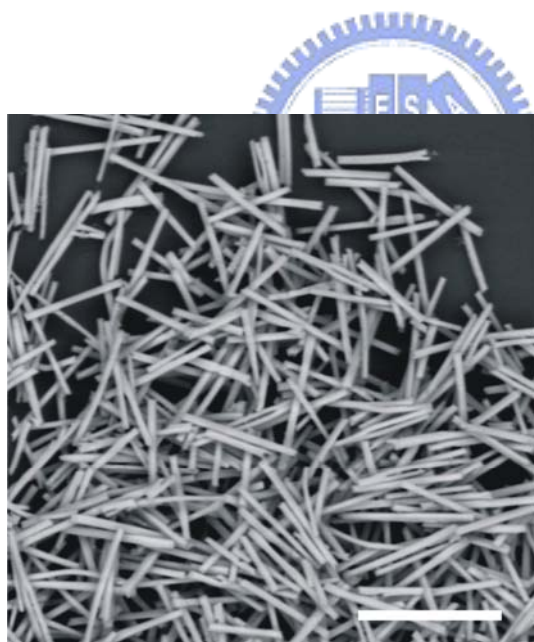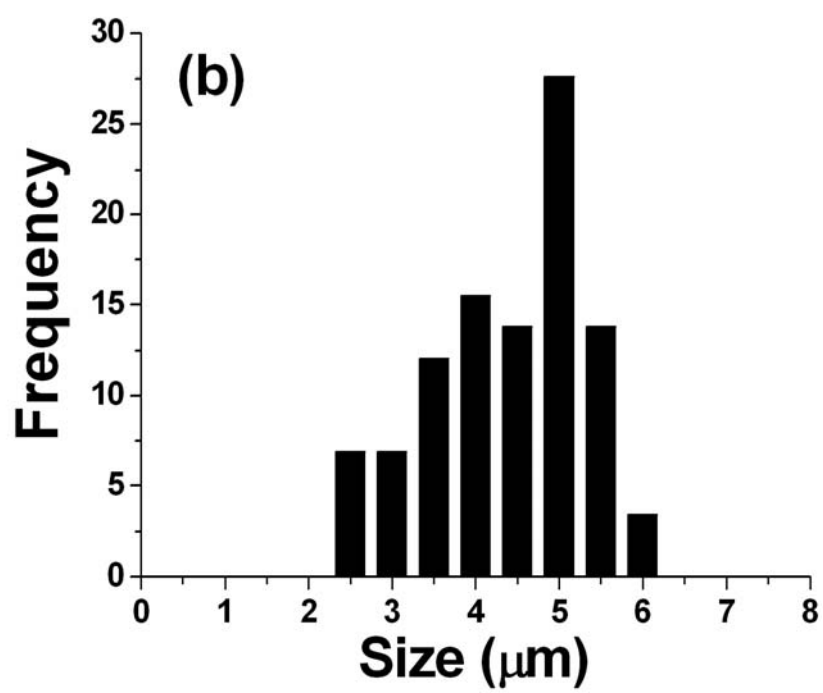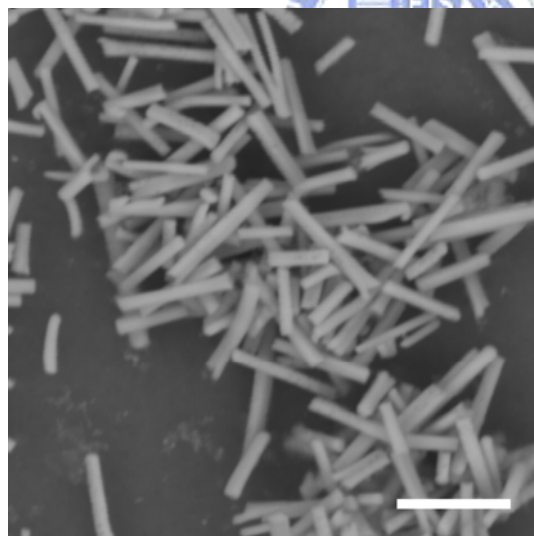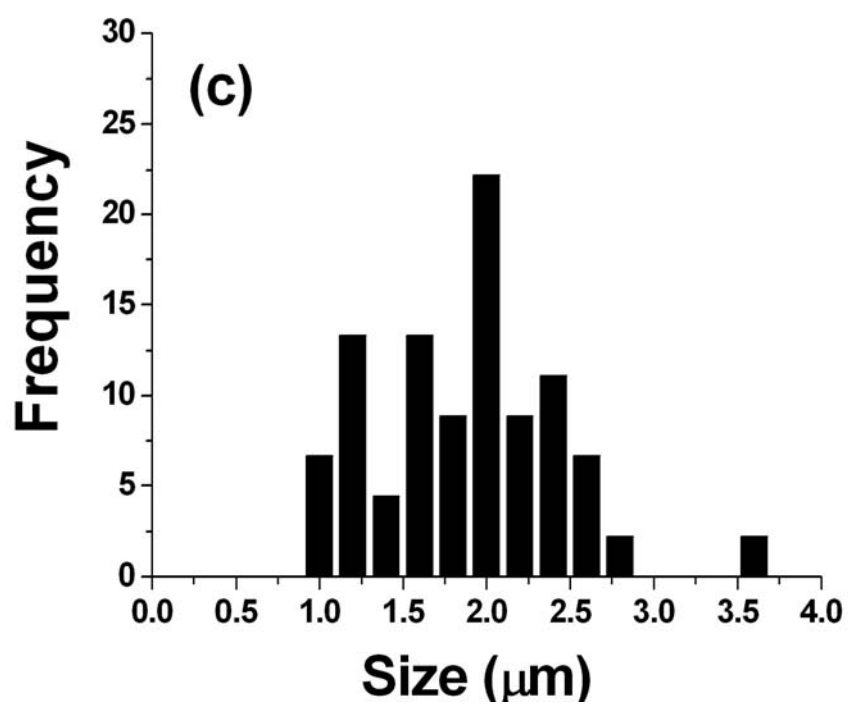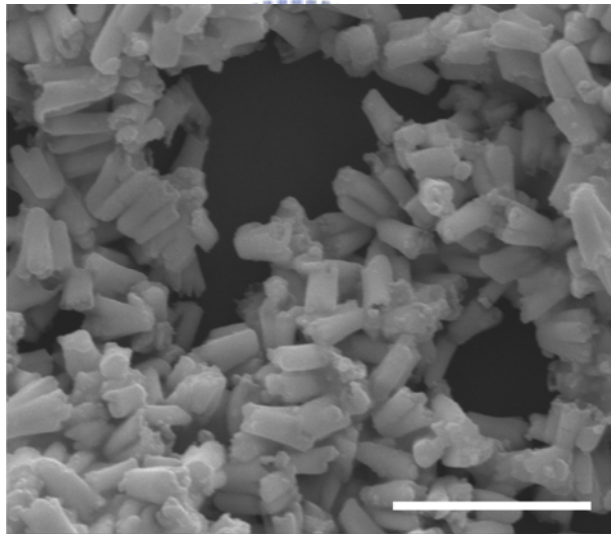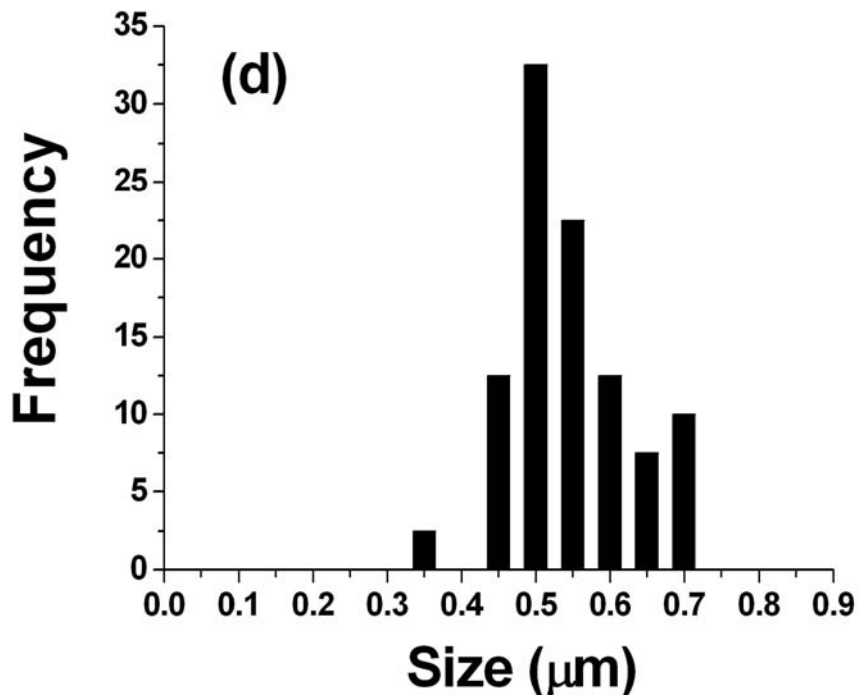
Figure 1. The SEM images of the four different size of gold nanowires .The size distributions

of (a) 8.6 μm gold nanowires. Inset: SEM image. Bar: 20 μm. (b) 4.5 μm gold nanowires.

Inset: SEM image. Bar: 5 μm.(c) 1.8 μm gold nanowires. Inset: SEM image. Bar: 2 μm. (d)

0.56 μm gold nanowires. Inset: SEM image. Bar: 1 μm.

Chapter 5 Cytotoxicity of Nanowires

5.1 Introduction

Nanomaterials, which exhibited unique physicochemical properties due to their size, chemical composition, surface structure, solubility, and shape, have been increasingly utilized in the biomedical applications for the purpose of diagnosis, imaging, and drug delivery. However, there has been very little investigation on the issue of the toxicity and health effects of the nanoparticle, especially for in vivo application. Therefore, there has been increasing interests in evaluating the toxicity of nanomaterials such as magnetic nanoparticle, semiconducting nanoparticle (quantum dots), gold or silver nanoparticle. Several groups have investigated the influence of the surface coatings of nanoparticle to the cell behavior and morphology. In many cases, additional coating for the nanoparticles is needed to optimize their utility in the cellular studies. For instance, magnetic nanoparticles without polymer coating were often suffered from the aggregation problem in the water or tissue fluid, which may limit in vitro magnetic based isolation and detection. In the following section, we will survey recent studies on the biocompatibility of different types of nanoparticles.

5.1.1 Magnetic nanoparticles

In a previous study, it was know that surface coating affects the particle size and physical properties, and corresponding effects on toxicological properties. For example, Yin et al. reported that the uncoated nickel ferrite particles had a hydrophilic surface that was not a significant factor in cytotoxicity [*1*]. However, when they were modified on the surface, cytotoxicity was clearly observed. Nickel ferrite particle coated with one layer of oleic acid (hydrophobic $-CH_3$ functional group) were more toxic than those nanoparticles coated with two layers (hydrophobic –COOH

functional group). Therefore, it was conclude the hydrophobic surface was more toxic than the hydrophilic surface. At higher concentrations, both small and large nanoparticles exhibited similar cytotoxicity. Since the size of the nanoparticles could be related to their surface interaction area and surface energy, it was found larger nanoparticles (about 150nm) was a more toxic than smaller nanoparticles (10 nm). In a separate experiment, Pisantic and coworkers have shown that the interacellular delivery of anionic iron oxide nanoparticles reduced the ability of PC12 cells to effectively respond to nerve growth factor in a dose dependent manner. The used anionic MNPs, which changed cell phenotype and behavior, could be directly correlated with the level of nanoparticle exposure [*2*].

On the other hand, Cheng and coworkers have demonstrated that non-polymer dispersive superparamagnetic iron oxide nanoparticle could be used as a new class of MRI contrast agent [*3*]. These magnetic nanoparticles, which have excellent biocompatibility, could be used to perform in vivo imaging. Similarly, Gupta et al. have observed that the 40-50 nm nanoparticles with magnetite inner core and hydrophilic outer shell of pullulan were non-toxic and could induce change in the cytoskeleton [*4, 5*]. Zhang and co-workers observed that the synergistic effect of magnetic particles on the anticancer drug uptake of daunorubicin in drug sensitive and drug resistant cancer cells [*6*]. The enhancement effect of Fe_3O_4 nanoparticles was much stronger than that of Fe_2O_3 and Ni nanoparticles. Therefore, it was concluded that the surface chemical properties and size of magnetic nanoparticles may play an important role in the synergistic enhance effect of the drug uptake in cancer cells.

5.1.2 Semiconducting nanoparticles

In the past two decades, research on fluorescent semiconductor nanoparticles has evolved from electronic to biological materials. Recent research efforts by several groups have

52

demonstrated that quantum dot (QDs) can be used to label fix cells and cell membrane acceptors. However, for live cell studies, it is important to know that the cytotoxicity and the possible interference of QDs [*7, 8*]. Although QDs were not found to significantly influence the cell viability, morphology, and functionality, it was noticed that they may be harmful to the embryo development at higher concentration. Both core and core-shell QDs materials were reported to release free cadmium ion or Se^{2-} ion, whose impact on cells appeared on cell function or cell viability. It was learned that the surface coatings such as ZnS and BSA could significantly reduce, but not eliminate cytotoxicity.

Cytotoxicity of QDs with different surface modification has been thoroughly investigated. For example, Hoshino and coworker have reported the cytotoxicity of QDs coated with MUA (QD-COOH), cysteamine (QD-NH$_2$), and thioglycerol (QD-OH) [*9*]. The MUA (QD-COOH) coated QDs caused strict cytotoxicity at dose grater than 100 μg /ml as detected by a DNA-damaging assay. Recent studies have shown that QDs inclined to aggregate inside living cells and often limited in organelles such as endosomes, lysosomes, and vesicles. More recently, it has been shown that the surface molecules on nanoparticle could significantly affect the degree of cellular uptake of nanoparticles through endocytosis. It is very important issue to be able to distinguish the origin of the cellular toxicity, whether from the interaction of surface molecules of the nanopaticels with the cell membrane or from the intracellular uptake of nanoparticles. For example, Duan et al. have investigated the quantum dots associated with copolymers such as polyethylene glycol (PEG) grafted polyethyleneimine (PEI-*g*-PEG) [*10*].

5.1.3 Gold nanoparticles

Gold nanoparticles have unique optical properties, which are often used in analytical or

bioanalytical applications. Because of the simple surface modification scheme, functionalized gold nanoparticles are very often used for the cellular research. For example, spherical gold nanoparticles with a variety of surface modifications were found to be not naturally toxic on human cells. However, it was found that some precursors in the CTAB-capped gold nanoparticle solution might cause toxicity [*11, 12*]. Niidome et al. have clearly shown that the use of phosphatidylcholine molecules for the surface modification can reduce the cytotoxicity. In another experiment, PEG-modified gold nanorod was shown to reduce the nonspecific binding with blood component such as blood proteins and cells.

In the thesis, we have investigated the cytotoxicity and the internalization process of the functionalized gold nanowires with different surface charges for two different cell lines, NIH 3T3 fibroblast cells from normal tissue, which is an adherent cell line and HeLa S3 cells from neoplastic tissue, which can grow in suspension.
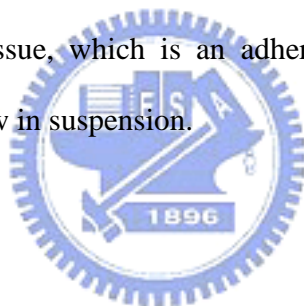
5.2 Experimental

5.2.1 Cell culture

Fibroblast NIH/3T3 and HeLaS3 (BCRC) were used in the cell culture experiment. Fibroblast cells were cultured in Dulbecco's Modified Eagle's Medium (DMEM) supplemented with 10% born calf serum. Minimum Essential Medium (MEM) supplemented with 10% fetal bovine serum (FBS,PAA Laboratories) was used for HeLa cells. PEN-STREP-AMPHO solution (Biological Industries) was added both culture media. The cells were incubated at 37 ℃ in a 5% CO_2 atmosphere.

5.2.2 Cytotoxicity of surface-modified nanowires

To determine the cytotoxicity in the presence of gold nanowires, the cells were first seeded in 96-well plates at a density of 1×10^5 cell/ml at 37^0C in 5% CO_2 atmosphere. After 24 hours of culture, the wells were refilled with the fresh medium and serial dilutions of nanowires with nanowire concentration ranging from 10^3 to 10^6 nanowire/ml. 90µl of the gold nanowires solutions at different concentrations were added to each well. Control experiments were carried out with cells treated with an equivalent volume of serum medium without any nanowires. Cells were then incubated for 24 hours at 37^0C. Cytotoxicity was measured using an MTT (3-(4,5-dimethylthiazol-2-yl)2,5- diphenyltetrazolium bromide) assay to measure the succinate dehydrogenase mitochondrial activity. PBS solutions containing 10µl of 5mg/ml MTT stain (*in vitro* toxicology kit, Sigma) were added into each well and incubated for 4 hours. After mixing, 90µl of MTT solubilization solution was added into each well. The stain was aspirated and the purple color crystal was dissolved with acidic isopropyl alcohol. After 15 minutes, the absorbance in each well was measured at 570 nm in a microplate reader (μQuant, Biotek Instrument). Background absorbance was measured in PBS solution without the presence of cells and nanowires. All experiments were repeated 3 to 9 times. The cell viability (%) related to the control wells containing the cell culture medium without nanowires was calculated by $[A]_{test}/[A]_{control}$ X 100 where $[A]_{test}$ was the absorbance of the test sample and $[A]_{control}$ was the absorbance of the control sample. We have also tested the cytotoxicity of the gold nanowires using media without serum. However, no significant difference was observed.

5.2.3 The uptake of nanowires

To further understand the internalization process of the nanowires, we have studied the uptake kinetics of aminothiol modified gold nanowires for both cell lines. In these experiments,

the suspensions of 10^6 gold nanowires were incubated with both cell lines in 96-well dishes with media. After 2, 4, 6, 8, 10 and 12 hours of incubation with the aminothiol modified gold nanowires, the cells in each well were rinsed with doubly distilled water several times to remove the excess nanowires in the media. And then the cells were detached from the dish by enzyme trypsin. The internalized nanowires were obtained by lysing the cells with alcohol and counted by a hemacytometer.

5.3 Result and discussion

5.3.1 The cytotoxicity of the nanowires

To investigate the cytotoxicity effect of these surface modifications, we performed a viability test using MTT assays on three different types of self-assembled monolayer (SAM) modified surfaces. The aminothiols were used to produce surfaces with positive charge, and the mercapto acids were used to generate negatively charged surfaces whereas the alkanethiols were used as a nonionic surface modification. For comparison, the nanowires coated with serum were also tested. The viability tests for fibroblast 3T3 and HeLa cells were summarized in figure 1(A) and (B). In a typical viability test, 4.5 μm long gold nanowires with various surface modifications were used. The density for both cells was about 10^5 cell/ml, and the density of the nanowires was varied from 10^3 to 10^6 nanowire/ml. After 24 hours incubation of the cells, it was found that the cytotoxicity increased as the density of the nanowires increased and all surfaces modified nanowires except the serum coated nanowires exhibited some degree of toxicity to both cell lines.

At a lower density ($< 10^4$ nanowire/ml), most of the cells were unaffected by the addition of the nanowire solution. However, the carboxyl presenting nanowire surfaces exhibited very strong cytotoxicity even at a very low nanowire density (10^3 nanowire/ml). At a higher nanowire density,

most of the cells were injured by the addition of nanowire solution except for the serum coated nanowires.   Large aggregation of nanowires was observed at a density of 10^7 nanowire/ml upon the introduction of nanowire solution to the cell culture, which made it difficult to evaluate the number of nanowires. At a nanowire density higher than 10^8 nanowire/ml, the bottom of the well was completely covered by the nanowires. The LD_{50} value of the serum coated gold nanowires for 3T3 cells was estimated to be 5 x 10^7 nanowire/ml (~150 g/ml), which was lower than the value measured for smaller gold nanoparticles (~750 g/ml) [13].The reason for the lower LD50 for the gold nanowires could be attributed to larger size nanowires used in this experiment.

In a previous study [14], it was reported that the cellular uptake of gold nanoparticles depended on both the size and the shape of the nanoparticles. With nanoparticle size smaller than 100 nm, it was found that the uptake efficiency of different size of nanoparticles peaked at 50 nm. And it was also concluded that the uptake efficiency decreased as the aspect ratio increased. If the cellular uptake depends on the size of the nanoparticles, the cytotoxicity will also vary with the size of nanoparticles. Therefore, we have investigated the cytotoxicity of different sizes of nanowires with aspect ration up to ~43. In this study, the concentration of mercapto acid modified gold nanowires was 10^5 nanowire/ml for all aspect ratios. The results of cytotoxicity for 3T3 and HeLa cells were depicted in figure 2 (A) and (B). Surprisingly, the cytotoxicity of the micrometer long nanowires exhibits little dependence on their aspect ratios for both cell lines. However, in a separated experiment, the cytotoxicity of 250 nm spherical gold nanoparticles (BBInternational) modified with mercapto acid was tested. The viability for both cell lines was measured to be larger than 80% with nanoparticle concentrations up to 10^7 nanoparticle/ml in figure 3(A) and (B). Considering that the mass concentration of 10^7 nanoparticle/ml 250 nm spherical gold nanoparticles is equivalent to that of 10 μm long nanowires with 200 nm diameter at a

concentration of 1.6 x 10^5 nanowire/ml, the nanowires are more toxic than the spherical nanoparticles, which is probably due to the geometry of the nanowires. However, the exact origin of the cytotoxicity of the nanowires requires further investigation.

5.3.2 The uptake of nanowires

To further understand the internalization process of the nanowires, we have studied the uptake kinetics of aminothiol modified gold nanowires for both cell lines. The internalized nanowires were obtained by lysing the cells with alcohol and counted by a hemacytometer. The results for the nanowires with various aspect ratios are plotted in figure 4(A) and (B). The uptake kinetics for all sizes of nanowires was very similar in both HeLa and 3T3 cells. Both types of cells exhibited maximum uptake after 8 hours of incubation with the nanowires and followed by a decrease in the uptake efficiency. The maximum internalization efficiency was higher than 50% for both cell lines. The reason for the decrease in the uptake was due to the cell death at high concentration of nanowires as indicated in the viability test (figure 1).   Another trend observed in this experiment was that the uptake efficiency for the longer nanowire was lower than the shorter one except the 0.58 μm long gold nanowires, which were too short to determine the number of nanowires accurately. This trend agreed with the previous measurement using smaller nanorods [15]. Since nanowires with different aspect ratios exhibited the same cytotoxicity and the uptake efficiency of the nanowires decreased as the aspect ratio increased. We concluded that the internalized nanowires with higher aspect ratio were more toxic to both cell lines. This conclusion agreed with the conclusion that the gold nanowires were more toxic than the spherical (250 nm) gold nanoparticles and also explained why the LD50 of the nanowires was lower than the nanorods with smaller aspect ratio.

5.4 Conclusion

In summary, we have investigated the cytotoxicity of the micrometer long gold nanowires with four different aspect ratios and four different surface modifications. It was found that the serum coated nanowires exhibited the least cytotoxicity with a LD_{50} value around 150 μg/ml, which was less than those measured for the smaller gold nanoparticles. All other surface functionalized nanowires possessed some degree of toxicity, which depended on the surface charge. Among them, the mercapto acid modified nanowires were the most toxic nanowires. For the same type of surface modification, HeLa cell, which can grow in suspension, were found to be more resistant to the addition of the nanowires solution. As for the nanowires with different aspect ratio, the cytotoxicity experiments indicated that nanowires with different aspect ratios exhibited the same degree of toxicity. However, the uptake efficiency for the shorter nanowires was measured to be higher than the longer nanowires. Therefore, we concluded that the internalized nanowires with higher aspect ratio were more toxic than the shorter one, which explained that the LD_{50} value for the nanowires was lower than that of the low aspect ratio nanorods. This conclusion also agreed with the cytotoxicity experiment for the spherical nanoparticle where the nanowires were found to be more toxic than the spherical nanoparticles.

Reference

1. H. Yin, H. P. Too, G. M. Chow and *Biomaterials* 2005, **26**, 5818.

2. T. R. Pisanic, J. D. Blackwell, V. I. Shubayev, R. R. Finones and S. Jin, *Biomaterials* 2007, **28**, 2572.

3. F. Y. Cheng, C. H. Su, Y. S. Yang, C. S. Yeh, C. Y. Tsai, C. L. Wu, M. T. Wu and D. B. Shieh, *Biomaterials* 2005, **26**, 729.

4. A. K. Gupta and M. Gupta, *Biomaterials* 2005, **26**, 1565.

5. A. K. Gupta, R. R. Naregalkar, V. D. Vaidya and M. Gupta, *Nanomedicine* 2007, **2**, 23.

6. R. Y. Zhang, X. M. Wang, C. H. Wu, M. Song, J. Y. Li, G. Lv, J. Zhou, C. Chen, Y. Y. Dai, F. Gao, D. G. Fu, X. O. Li, Z. Q. Guan and B. A. Chen, *Nanotechnology* 2006, **17**, 3622.

7. B. Dubertret, P. Skourides, D. J. Norris, V. Noireaux, A. H. Brivanlou and A. Libchaber, *Science* 2002, **298**, 1759.

8. X. Michalet, F. F. Pinaud, L. A. Bentolila, J. M. Tsay, S. Doose, J. J. Li, G. Sundaresan, A. M. Wu, S. S. Gambhir and S. Weiss, *Science* 2005, **307**, 538.

9. A. Hoshino, K. Fujioka, T. Oku, M. Suga, Y. F. Sasaki, T. Ohta, M. Yasuhara, K. Suzuki and K. Yamamoto, *Nano Lett.* 2004, **4**, 2163.

10. H. W. Duan, S. M. Nie, *Journal of the American Chemical Society* **129**, 2412 (Mar 7, 2007).

11. E. E. Connor, J. Mwamuka, A. Gole, C. J. Murphy and M. D. Wyatt, *Small* 2005,**1**, 325.

12. H. Takahashi, Y. Niidome, T. Niidome, K. Kaneko, H. Kawasaki and S. Yamada, *Langmuir* 2006, **22**, 2.

13. A. K. Salem, P. C. Searson and K. W. Leong, *Nat. Mater.* 2003, **2**, 668.

14. B. D. Chithrani, A. A. Ghazani and W. C. W. Chan, *Nano Lett.* 2006, **6**, 662.

15. L. A. Bauer, D. H. Reich and G. J. Meyer, *Langmuir* 2003, **19**, 7043.
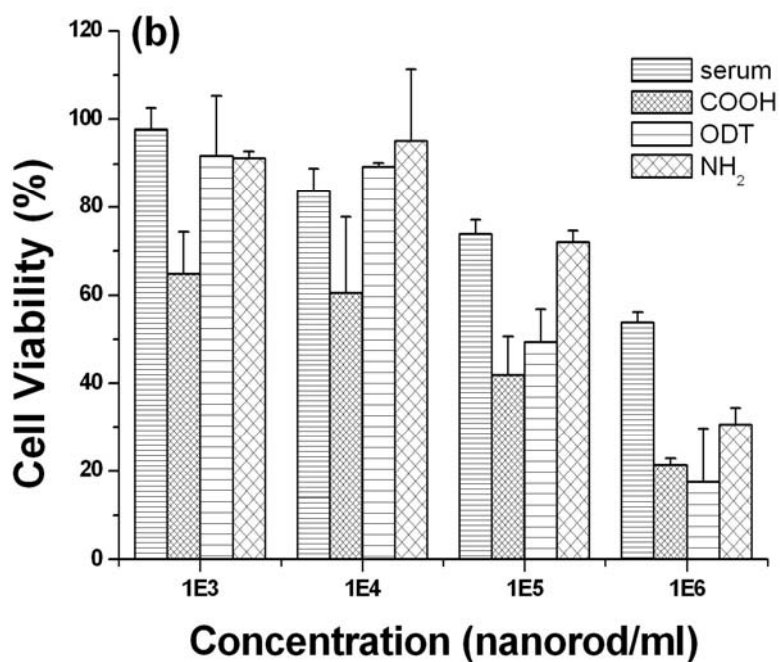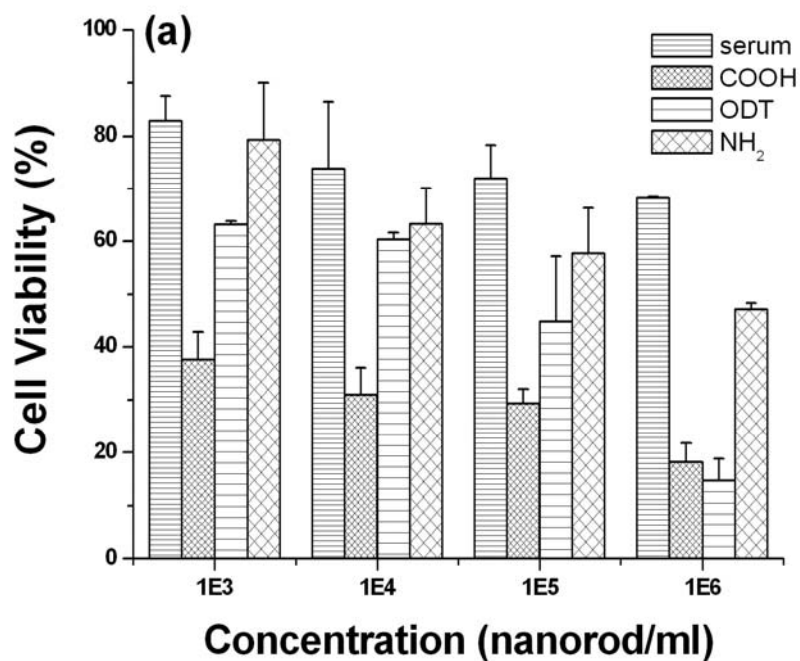
Figure 1. The cytotoxicity of gold nanowires with various surface modifications for (A) fibroblast cells and (B) HeLa cell.
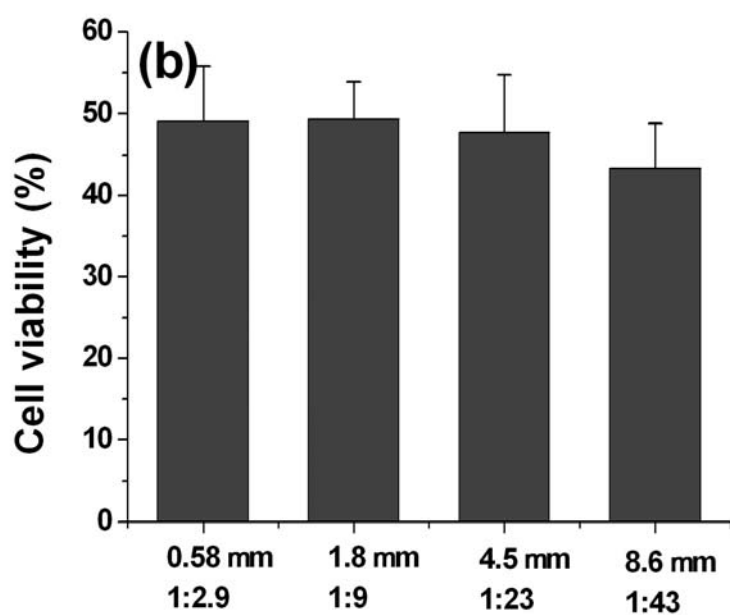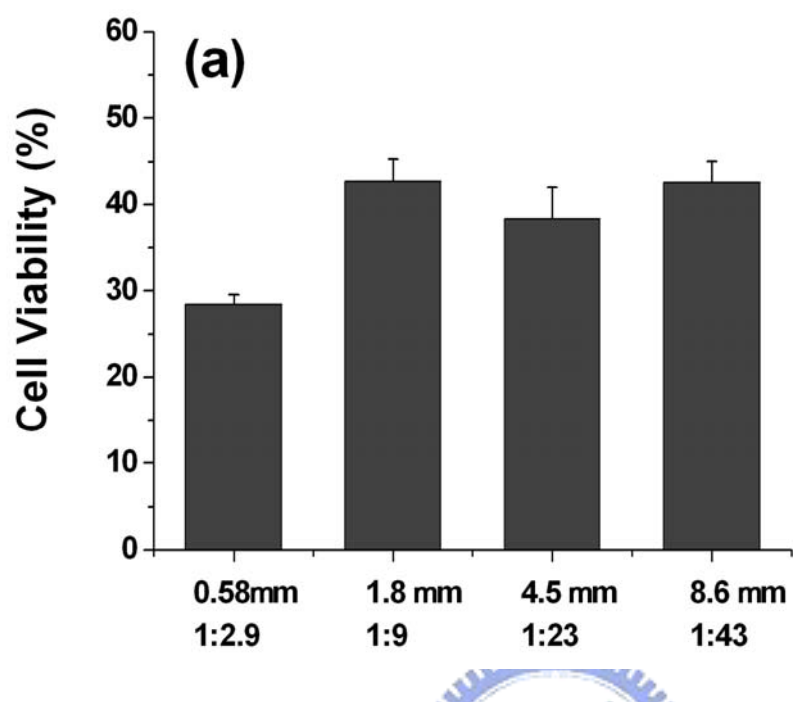
Figure 2. The cytotoxicity of different sizes of gold nanowires modified with mecapto acid for (A) fibroblast cells (B) HeLa cell.

(A)
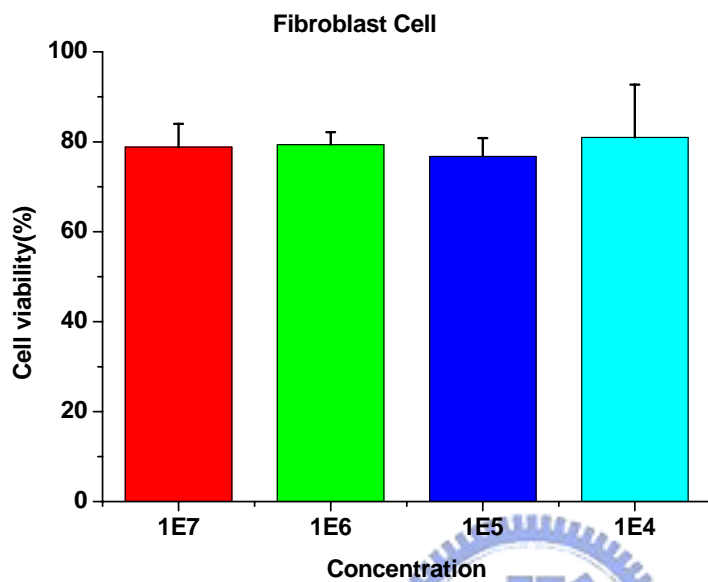
(B)
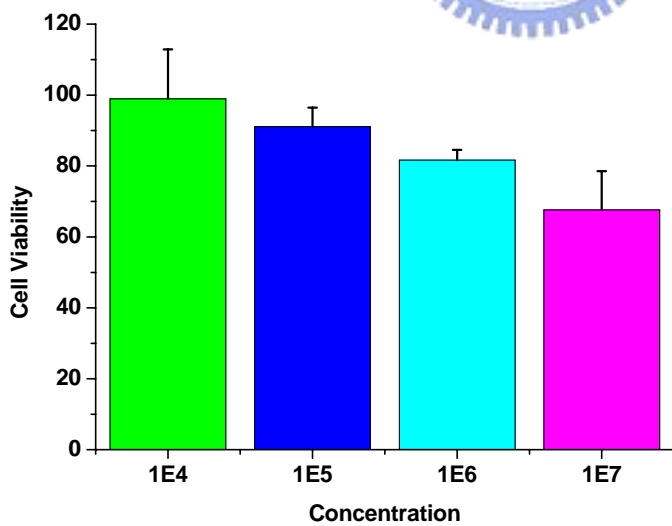
Figure 3. The cytotoxicity of 250nm gold nonoparticles at different concentrations for (A)

fibroblast cells (B) HeLa cell.
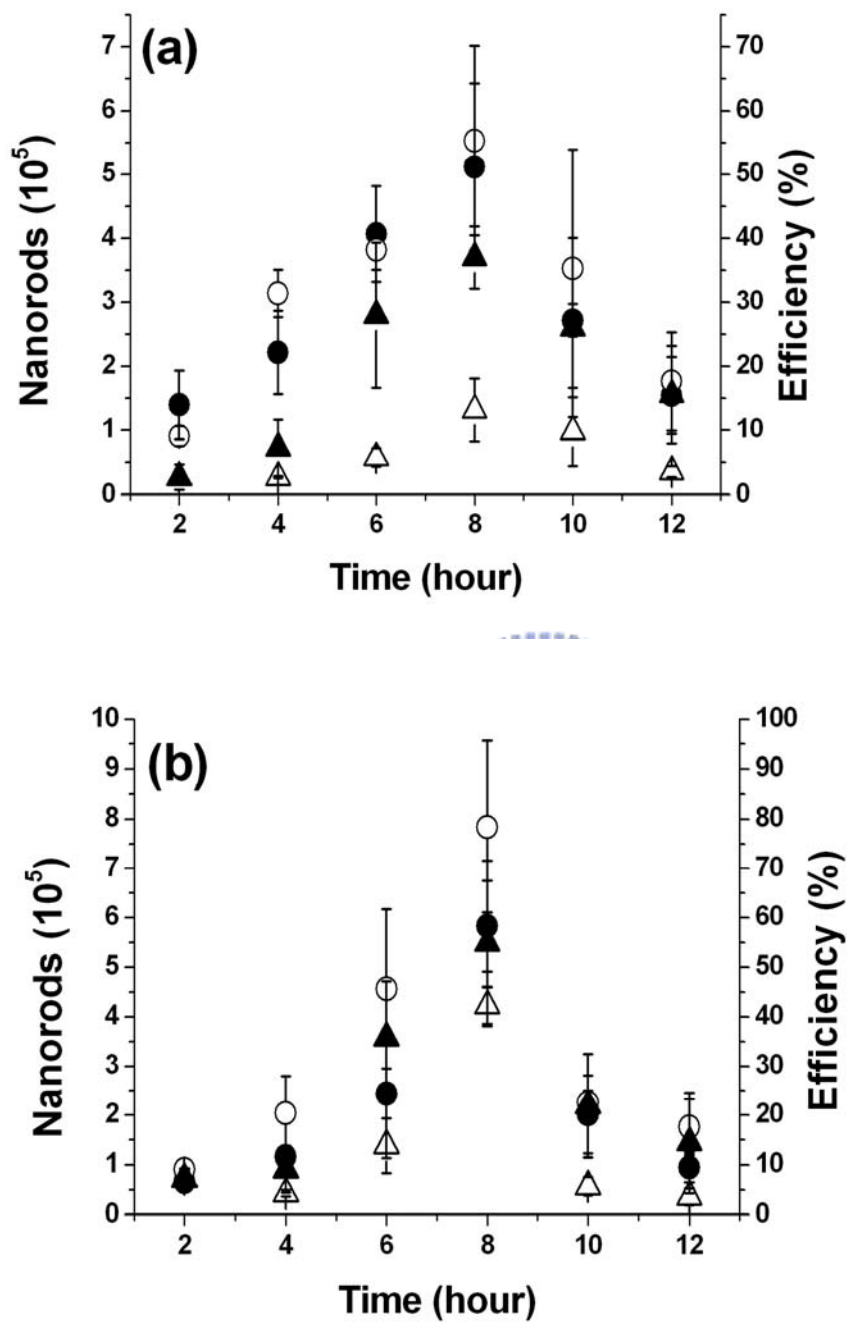
Figure 4. The uptake of aminothiol modified gold nanowires with four different lengths in (A) fibroblast cell and (B) HeLa cell. 0.5μm (solid circles), 1.8 μm (open circles), 4.8μm (solid triangles), 8.6 μm (open triangles).

Chapter 6 Nanowire as Living Cell Probes

6.1. Introduction

In the advent of nanotechnology, various nanomaterials with distinct properties have synthesized routinely. To take the advantages of the novel properties of these nanomaterials in the field of biological studies, it is very important to investigate the interaction between the nanomaterials and the biological objects such as cells. Recently, there have been increasing research activities in developing novel functionalized nanomaterials for biological applications, especially for the cellular study. These nanomaterials have been designed to enter the cells efficiently and to escape endosomal/lysosomal complexes while the local environment within the living cells can be revealed by these nanomaterials. For this purpose, the nanomaterials must remain stable in the intracellular environment and not disturb the cell's normal biochemical functioning.

Several types of nanomaterials such as magnetic, polymeric, metallic, semiconductor nanoparticles or nanowires have been introduced for the cellular study. For example, Goodman et al. have focused the capability of gold nanoparticles to incorporate secondary tags such as peptides to target specific cell types [1]. In their study, the gold nanoparticles have been functionalized with cationic and anionic side chains. The carboxylated modification on the gold nanoparticles was found to be nontoxic to the cells. In contrast, the cationic side chain bound to the gold nanoparticles exhibited moderately toxicity. It was found

that the toxicity of gold nanoparticles was related to their interactions with the cell membranes. In another study, Derfus et al. have explored the intracellular delivery of quantum dots (QD) for live cell labeling and organelle tracking [2].The QDs modified with polyethylene glycol (PEG) were mixed with different transfection reagents and then were delivered to the interior of the HeLa cells. The flow cytometry was used to quantify the amount of QD delivered to the cells. It was found that QDs often tended to accumulate in vesicles and distributed non-homogeneously in the cytoplasm [3]. Therefore, to investigate the subcellular localization, the QDs were modified with 23 mer nuclear localization sequence peptide and a 28 mer mitochondrial localization sequence peptide allowing tracking QDs to the nucleus and mitochondrial respectively.

As regarding to metallic nanoparticles, recent studies have shown that it was possible to use metallic nanoparticle for targeted nuclear delivery. For example, Tkachenko and coworkers investigated that the multifunctional gold nanoparticle –peptide complexes for nuclear targeting [4]. The 20nm diameter gold particle was modified with bovine serum albumin (BSA) bound with various cellular targeting peptides. These nanoparticles must have carried both receptor-mediated endocytosis (REM) and nuclear localization signal (NLS) peptides to enter HepG2 cells and perform nuclear localization. Non-spherical nanorods also have been demonstrated capable of conducting gene delivery. It was shown that the conjugation of DNA plasmid and targeting ligands can be achieved simultaneously in a

spatially defined manner. For example, Salem and coworkers have demonstrated that it was

possible to transfer gene using bifunctional Au/Ni nanorods [5]. In their approach, the

carboxylate end group was first attached to the Ni segment. Subsequently, the plasmids were

bound to the protonated amines on the surface of nickel segment by electrostatic interactions.

The transferrin was bound to the gold segment of the nanorods through thiolate linkage. These

dual-functionalized Au/Ni nanorods were used in a vitro transfection experiment using human

embryonic Kindney (HEK 293) mammalian cell line.

To optimize non-viral gene delivery systems, Akita and co-workers have developed a

novel technique for quantitative three-dimensional analysis of the intracellular trafficking of

the plasmid DNA [6]. They evaluated the fraction of the plasmid DNA in cytosol,

endosome/lysosome, and nucleus in the cell based on the z-series images sequentially

obtained by confocal laser scanning microscopy. Lacerda et al. have investigated the

interactions between mammalian cells and ammonium-functionalized single-walled carbon

nanotubes [7]. Using this approach, they could track the luminescence signal of SWNT-NH$_3^+$

by using confocal laser scanning microscopy. Recently, Lu et al. have developed fluorescein

isothiocyanate (FITC)-incorporated silica core-shell iron oxide nanoparticles as bifuntional

contrast agents [8]. These dye molecules could be easily integrated into a silica cell, and silica

is known to be biocompatible and resistant to biodegradation in the biological environment.

Moreover, these nanoparticle complexes exhibited both fluorescent and magnetic properties to

serve as good molecular imaging probe to monitor cell trafficking.

In this thesis, we have introduced functionalized gold nanowires as new probes that took the advantage of the nanowires-thiol group conjugation. Using various types of functionalization, it was possible to probe the local environment inside the cells by confocal microscopy.

6.2 Experimental

6.2.1 Preparation of cells for confocal analysis

HeLa cells (10^5/ml) were cultured in minimal essential media in 35 mm glass bottom dishes coating with poly-D-lysin. After 24 hours of incubation, the media was removed and the cells were washed by PBS solution. For visualization purpose, the plasmid DNA coated gold nanowires were mixed with 50nM YOTO-1 dye (Molecular Probe, Invitrogen) for 20 minutes in the media without serum. The mixture solution was added to cells culture and incubated for 24 hours. Subsequently, the cells were stained with Image iT LIVE plasma Membrane and Nuclear Labeling Kit (Molecular Probe, Invitrogen) for 20 minutes.

6.2.2 Transfection experiment

Fibroblast cell were seeded onto 35 mm glass bottom culture dishes at a density of $2\times$ 10^5. After 24 hours, the cells were washed and supplied with 0.5 ml fresh growth medium.

The plasmid used in this study was pAcGFP1-Actin (BD), which expresses green fluorescence protein (GFP). The surface modified gold nanowires (4×10^5) was mixed with 5.6 μg of Plasmid DNA for 20 minutes. The mixture solution was added into cell culture and incubated for 24hour. The behavior of fibroblast cells with plasmid coated nanowires was monitored under a laser scanning confocal microscope (Olympus, Fluroview 300).

6.2.3 Intracellular behavior monitored by the Lysosensor yellow/Blue dye

Generally, fibroblast cell were seeded at a density 10^5 in 1ml DMEM medium with 10% serum. Amino-functionalized gold nanowires were prepared as described previously. An appropriate amount of 2 μm long amino-modified gold nanowires (10^5) was mixed with 75 nM Lysosensor yellow/Blue dye DND-160 (Molecular Probe, Invitrogen) for 10 minutes. After the sample was centrifuged at 5000 rpm for 2 minutes, the supernatant was removed. The nanowire/dye complexes were then added to a 0.5 ml growth medium with fibroblast cell and incubated for 12 hours.

6.3 Results and discussion

It has been shown that the nanoparticles with diameter less than 100 nm can be internalized easily by cells through the endocytosis pathway [9]; therefore, smaller gold nanoparticles have been used as the carriers of the genetic materials through electrostatic or covalent

interaction for gene therapy, which has been demonstrated to be very effective and not very toxic (LD_{50} was about 750 μg/ml) [10-12] However, it is not known that the micrometer long metallic nanowires can be internalized by cells without damaging the cells, which is important if the nanowires are to be utilized for probing the local environment inside a living cell. To observe the internalization process of nanowires, 4.5 μm long gold nanowires (200 nm in diameter) coated with serum were added into a glass bottom culture dish containing HeLa cells, which were placed in a CO_2 incubator on an inverted microscope. The phase contrast images of the cells and the nanowires were recorded by a CCD camera every 10 minutes. Shown in figure 1 is the image of a gold nanowire sitting outside the cell. When the cell migrated around the glass surface, the nanowire was enclosed inside the cell as shown in figure 1(a) to (d). As the result of this enclosure, the nanowire was internalized by the cells which took about four hours to complete.
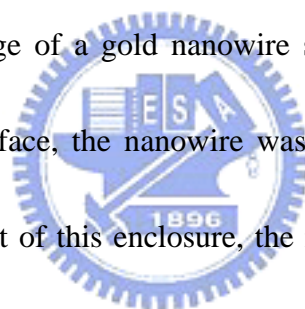
To investigate the capability of delivering DNA molecules into the cells by the nanowires, 5 μm long nanowires were first functionalized with aminothiols, which covered the nanowire surfaces with positive charges [13]. Then the negatively charged plasmid DNA molecules were attached to the nanowires through electrostatic interaction. For visualization purposes, the plasmid DNA on the nanowire surfaces were further labeled with YOYO-1, which emitted a strong green fluorescence when bound to a double strain DNA, and the cells were stained with Image iT LIVE Plasma Membrane and Nuclear Labeling Kit (Invitrogen). Shown in

figure 2 (A) the nanowire was clearly visualized. The nanowires were discovered intracellularly at the perinuclear region. This was thought to directly indicate that nanowire traffic intracellularly, the nanowire seems the ability to travel intracellularly around the cell cytoplasm form outside intact cell. Figure 2 (B) z-stack imaging data obtained from the 5μm functionalizd gold nanowires coated with plasmid and labeled with YOYO-1 dye. A series of the z- stack imaging indicated that the intracellular and perinuclear localization of the nanowire signal was at the same plane of focus as the nuclear stain. We have demonstrated that nanowire themselves are capable of internalizing and trafficking within cell for several hour. Moreover, at a dose of up to high concentrated ($> 10^6$/ml) of nanowires cell easily death was observed by confocal microscopy.
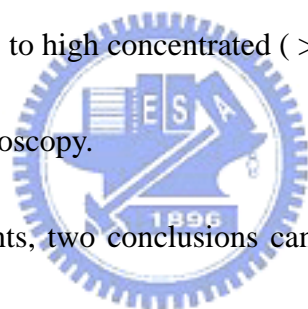
From these two measurements, two conclusions can be drawn: first, the micrometer long nanowires can be readily internalized by the cells despite of their relative large size. Secondly, from the sectioning images, it is evident that the surface of individual nanowires could be visualized with sub-μm resolution, which may allow the use of functionalized multi-segment nanowires to probe the microenvironment inside the cells.

To demonstrate that the surface functionalized nanowires can carry the plasmids into the cytoplasm, it is important to investigate the functionality of plasmids on the gold nanowires after entering the cell. To study the functionality of the plasmids, a green fluorescence protein (GFP) expressing plasmid (pAcGFP1-Actin, BD) was coated on the gold nanowires modified

by aminothiols and incubated with the fibroblast cells for 24 hours. Shown in figure 3 is a combined fluorescence and DIC image of gold nanowires with GFP expressing plasmids inside a fibroblast cell. It can be clearly seen that there were still several gold nanowires remained inside the fibroblast cell after 24 hours of incubation. The fact that the whole cell exhibited a strong green fluorescence signal indicated that the plasmids on the nanowires were still functional and capable of expressing GFP. This experiment confirmed that the micrometer long aminothiol modified gold nanowires can not only protect plasmid DNA molecules from degradation but also release plasmid NDA molecules inside the cells.

To investigate the behavior of the surface modified nanowires inside the cells, DIC images of the living cells were monitored in an incubator on an Olympus Fluoview 300 confocal microscope. Figure 4 (A) shows the image of the 5 μm long alkanethiol modified gold nanowires internalized by the HeLa cells after 24 hours of incubation. The density of the nanowires was about 5 x 10^4 nanowire/ml and the cell density was about 10^5 cell/ml. From the DIC image, it can be seen that the nanowires were internalized unevenly among cells. When a 2 μm long nanowire solution at a concentration of 5×10^5 nanowire/ml was used, several gold nanowires could be found inside most of the HeLa cells as seen in figure 4 (B). In some occasion, nanowires aggregation in a single cell was observed similar to the one shown in figure 4 (C). The exact origin of such behavior is not known at this time. At this concentration, more than 50% of the HeLa cells were not viable, which could be seen by the decrease in the

cell density. This observation also agreed with the results of the uptake measurement in chapter 5 figure 4 (B), which the shorter nanowires exhibited higher uptake efficiency. When a serum coated gold nanowire solution at 2×10^{6} nanowire/ml were added to the culture dish containing 3T3 cells, most cells were found to be attached on the surfaces. At this concentration, more than 70% the cells were still viable and on average each cell internalized about 10 nanowires as shown in figure 5 (A) and (B). This result also agreed with the uptake measurement for the 3T3 cells as shown in figure 4 (A) in chapter 5.

For gold nanoparticles with size smaller than 100 nm, it is believed that the nanoparticles entered the cells via the receptor mediated endocytosis pathway [14]. However, it is not clear which mechanism dominates the cellular uptake behavior of the micrometer long nanowires. In this experiment, we have monitored the internationalization process of nanowires through a confocal microscope. In most cases, we have found the nanowires entering the cell with one end pointing to the cell similar to the one shown in figure 1. It is reasonable that the smaller dimension of the nanowires has higher probability to be taken by the cells. Once one end of the nanowire was internalized by the cell, the rest of the nanowire would be surrounded by the cell membrane and finally the whole nanowire was taken by the cell. As long as the nanowires stayed inside the cell, they could explore the space inside the cytoplasm. In most of the time, we have found the nanowires maneuvered along the edge of the cell. More studies are needed

to understand the detail mechanism of the endocytosis pathway for the micrometer long

nanowires [15].

To demonstrate that it is possible to monitor the local environment of the nanowires, the

LysoSensor Yellow/Blue DND-160 (Invitrogen), was incubated with the 2 μm long

amino-modified gold nanowires for 10 minutes. The nanowire solution was then incubated

with 3T3 cells for 24 hours. It can be clearly seen that both LysoSensor and nanowires can be

visualized simultaneously on a confocal microscope. Shown in figure 6 are the confocal

images of the LysoSensor coated nanowires inside the 3T3 cells. Since LysoSensor

Yellow/Blue exhibited pH dependent dual emission spectra where the emission in 500-600

nm region (artificial red color in figure 6 (B) was observed in the acidic environment and

the fluorescence in 410-500 nm region (artificial green color in figure 6) was observed in the

less acidic environment, LysoSensor can be used to probe acidic organelles such as

endosomes or lysosomes. The colocalization of the nanowires and the green fluorescence

signals indicated that all the nanowires were located in less acidic compartments, presumably

endosomes, as a result of endocytosis process of the nanowires. By monitoring both the DIC

image of the nanowires and confocal image of the probe molecules as a function of time, the

evolution of the local environment around the nanowires can be explored. In general, this

approach can be extended to other types of probe molecules or biological assays.

6.4 Conclusion

In summary, we have demonstrated that the 5 μm long nanowires with surface modifications are capable of delivering plasmid DNA molecules, which has been visualized and recorded on an optical microscope. In addition, LysoSensor was attached to the nanowires revealing the local environment of the nanowires. By monitoring the color change of the Lysosensor on the nanowires, it was found the nanowires stayed in the less acidic environment indicting that nanowires never escaped from the endosome/lysosome complexes.

Reference

1.   C. M. Goodman, C. D. McCusker, T. Yilmaz and V. M. Rotello, *Bioconjugate Chem.* 2004, **15**, 897.

2.   A. M. Derfus, W. C. W. Chan and S. N. Bhatia, *Adv.   Mater.* 2004, **16**, 961.

3.   F. Q. Chen and D. Gerion, *Nano Lett.* 2004, **4**, 1827.

4.   A. G. Tkachenko, H. Xie, D. Coleman, W. Glomm, J. Ryan, M. F. Anderson, S. Franzen and D. L. Feldheim, *J. Am. Chem. Soc.* 2003, **125**, 4700.

5.   A. K. Salem, P. C. Searson and K. W. Leong, *Nat. Mater.* 2003, **2**, 668.

6.   H. Akita, R. Ito, I. A. Khalil, S. Futaki and H. Harashima, *Mol. Ther.* 2004, **9**, 443.

7.   L. Lacerda, G. Pastorin, D. Gathercole, J. Buddle, M. Prato, A. Bianco and K. Kostarelos, *Adv. Mater.* 2007, **19**, 1480.

8.   C. W. Lu, Y. Hung, J. K. Hsiao, M. Yao, T. H. Chung, Y. S. Lin, S. H. Wu, S. C. Hsu, H. M. Liu, C. Y. Mou, C. S. Yang, D. M. Huang and Y. C. Chen, *Nano Lett.* 2007, **7**, 149.

9.   B. D. Chithrani, A. A. Ghazani and W. C. W. Chan, *Nano Lett.* 2006, **6**, 662.

10.   N. L. Rosi, D. A. Giljohann, C. S. Thaxton, A. K. R. Lytton-Jean, M. S. Han and C. A. Mirkin, *Science* 2006, **312**, 1027..

11.   T. Niidome, K. Nakashima, H. Takahashi and Y. Niidome, *Chem. Commun.* 2004, 1978.

12. C. M. Goodman, K. K. Sandhu, J. M. Simard, S. W. Smith and V. M. Rotello, *Abstr Pap. Am. Chem. S.* 2002, **224**, U131.

13. D. Putnam, *Nat. Mater.* 2006, **5**, 439 .
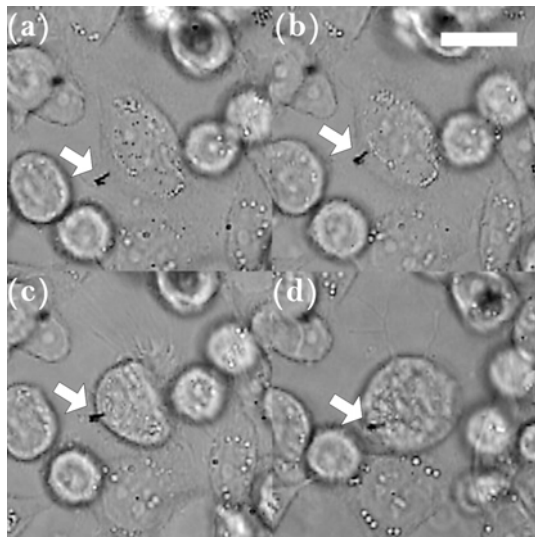
Figure 1.The phase contrast image of the serum coated with gold nanowires entering HeLa

cell. The bar is 20 μm.
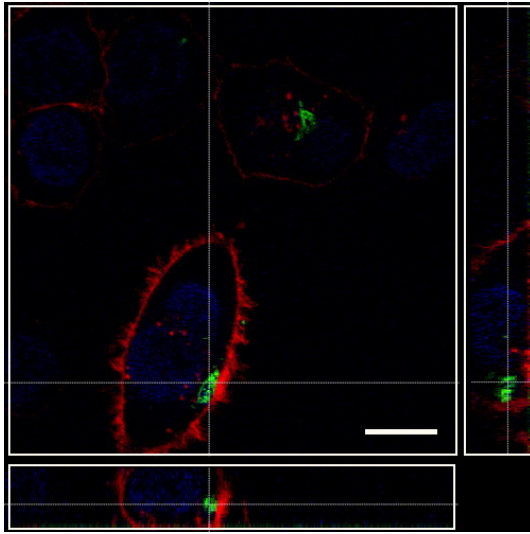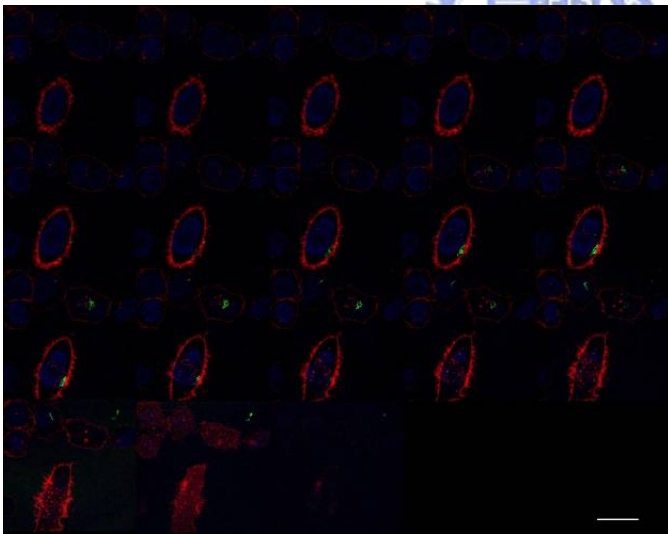
Figure 2. Multiple stained confocal image of HeLa cell. (A).stacked laser scanning confocal

image of nanowires in HeLa cell. (B) z-stack imaging obtained from the 5μm functionalizd

gold nanowires coated with plasmid and labeled with YOYO-1 dye.
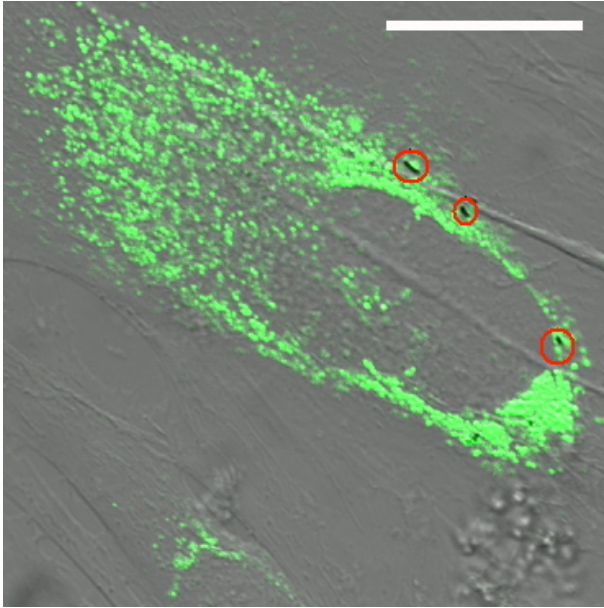
Figure 3. The combined DIC and fluorescence image of plasmid coated nanowires and fibroblast cell expressing green fluorescence proteins. Nanowires are indicated by the red circles. The bar is 20 μm.
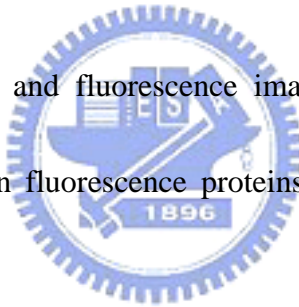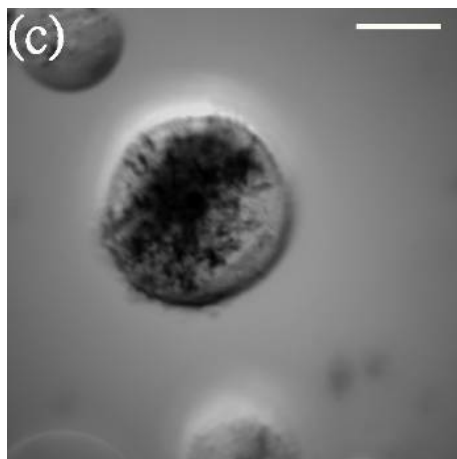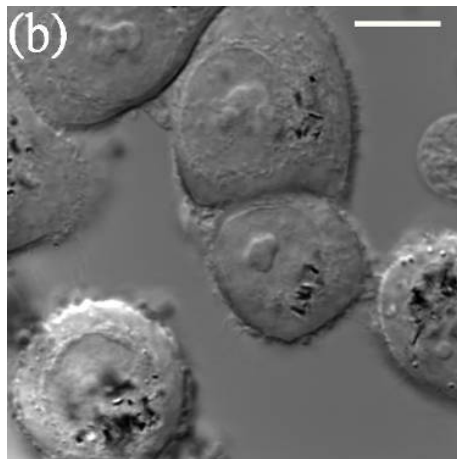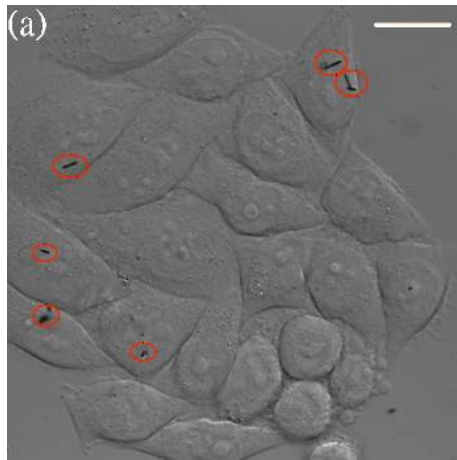
Figure 4.DIC images of the alkanethiol modified gold nanowires in the HeLa cells at different

nanowire concentrations. (A) 5×10^4 nanowire/ml. Bar:20μm (B) 5×10^5 nanowire/ml. Bar:10

μm (C) nanowires aggregation in a single HeLa cell. Bar:10 μm
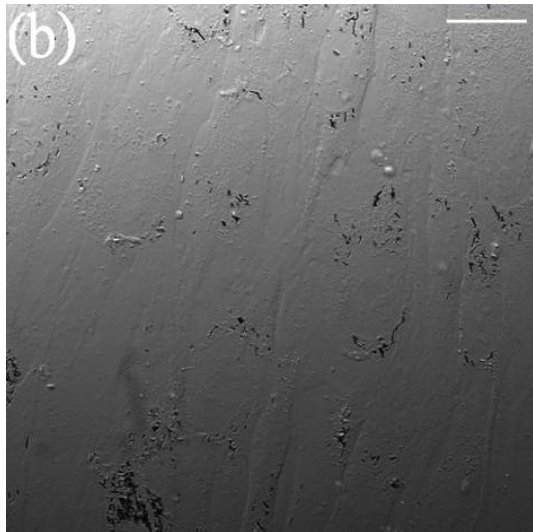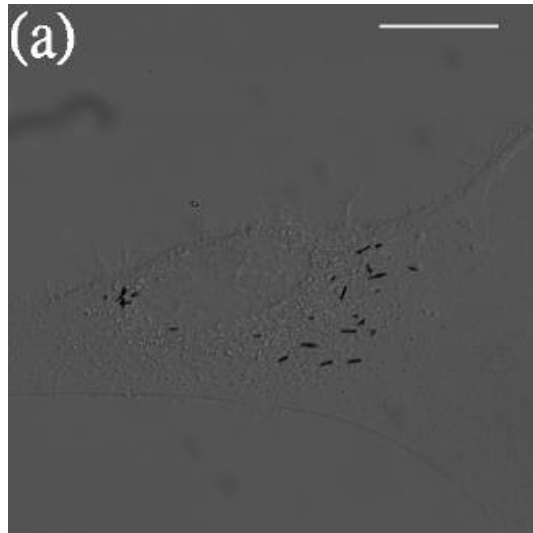
Figure 5. The DIC images of the serum coated gold nanowires in the fibroblast cells at 10^6

nanowire/ml nanowire concentrations. (A) the nanowires distribution in a single cell. (B) the

nanowires distribution among cells. The bar is 20 μm.
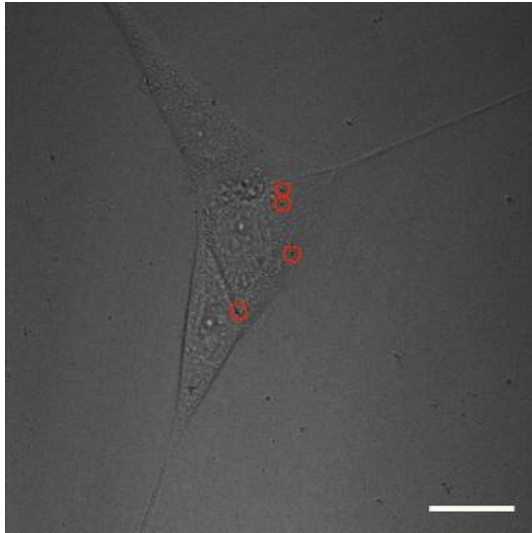
(B)
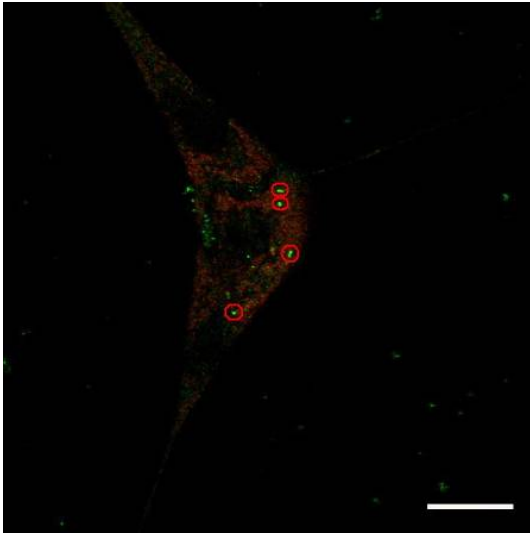
Figure 6. (A) The DIC image (B) combined confocal image of the gold nanowires inside Hela

cells. The bar is 20 μm.

Chapter 7 Nanowire for Gene Delivery

7.1 Introduction

Gene therapy is becoming an important strategy in the treatment of various diseases such as AIDS, cancer. The challenge of *in vivo* gene therapy is to develop safe and efficient gene delivery system. For the gene therapy to be used in the clinical applications, it requires the development of efficient DNA delivery vehicle that can be synthesized both easily and in large quantities. It has been demonstrated that the viral vectors can provide the most efficient gene transfer. Viral vectors were originally developed as an alternative to the transfection of the naked DNA in molecular genetic experiments. So far, there are several types of viral vectors have been developed for the gene transfection including retroviruses, lentiviruses, adenoviruses, and adeno-associated viruses. However, the immuno-response induced by the viral vector has raised a lot of concerns of using viral vector as the drug delivery system.

To reduce the immuno response, several non-viral vectors have been developed including calcium phosphate, cationic lipids, cationic polymer, dendrimers, and cyclodextrins. These non-viral vectors have been shown to exhibit lower transfection efficiency than the viral vectors. However, they are much safer than viral vectors. Recent researches on the non-viral vectors have been focused on the improvement of their transfection efficiency. Non-viral vector approach usually has involved the use of plasmid DNA or oligonucleotides, which are considered to be safer than the viral rectors. Because of the DNA molecules are negatively charged, the zeta potentials of naked DNA are ranging from -30 to -70 mV. Larger

DNA molecules exhibit larger negative surface charge density, which limits the uptake of DNA by cells. However, the details of the mechanism by which DNA molecules are internalized by the cells are not well understood [1].

7.2 Nanomaterials as non-viral transfection reagents

With recent advances in nanotechnology, researchers are now routinely synthesizing various nanomaterials with desire properties such as size, shape, charge density, surface modifications, optical and magnetic properties. Therefore, the use of nanomaterials has attracted a lot of research attentions in the fields of biomedical and bioengineering. In recent reports, polymer nanoparticles or nanowires have been introduced as the vehicles for the drug delivery to enhance the efficiency for entering the cells. For this purpose, the nanomaterials have been developed to incorporate with DNA molecules such that they can directly facilitate cellular interactions. The nanomaterial based drug delivery systems are being developed to overcome the barrier of size, stability, charge density, and biodistrution. Furthermore, the development of synthetic delivery systems to control gene expression efficiently is a powerful tool that will lead to novel therapeutic strategies for the treatment of a variety of inherited or acquired disorders.

However, the novel therapeutic strategies using these targets are dependent on the ability to manipulate the expression of target genes in the desired cell population.

The commonly approach involves the use of naked NDA with cationic lipids or poly-cationic polymers that work as containers the DNA for effective delivery. These containers can be engineered to provide different kinds of functionalities including protection against the nuclease activity, efficient internalization and intracellular trafficking, targeting a specific cell population. Such engineered DNA containers can significantly increase the gene transfer efficiencies.

In general, there three different pathways when cells uptake the nanomaterials: (1) the nanomaterials enter the cell and follows by exocytosis process, (2) the nanomterials enter the cell entry and are transported to the nuclear membrane and (3) the nanomaterials enter the cells and follow by the nuclear translocation process. The endocytosis pathway can be illustrated as the engulfment of the nanomaterials by the cell membrane and the formation of endosome around the internalized nanomaterials. The endosome could fuse with the cell lysosomes, which account for the later degradation of the internalized species in the lysosomes. Thus, to escape from the lysosome to avoid degradation is a very important for development of efficient transfection reagents. There have been several nanomaterials developed so far that are capable of delivering DNA into cells including cationic lipids, cationic polymers, glycolic acids and metallic nanoparticles. In the following sections, we will discuss the current status of these nanomaterials.

7.2.1 The cationic lipids

Several frequently used cationic lipids include (2,3-bis(oleoyl)propyl)-trimethyl) ammonium chloride(DOTMA); 1,2-dimyristyloxypropyl-3-dimethyl-hydroxyethyl ammonium bromide (DMRIE); dioctadecyldimethyl ammonium bromide (DODAB);1,2-diacyl-3-trimethylammonium propane (DOTAP); 3(N-(N',N'-dimethyl-laminoethane)-carbamoyl) cholesterol (DC-Chol).for neutral lipids used such as dioleoylphosphatidyl ethanolamine (DOPE); dioleoylphosphatidyl choline (DOPC); and cholesterol. All these cationic lipids contain primary amine of high densities, which are protonatable at neutral pH. The positively charged cationic lipids allow the formation of stable complexes with plasmid DNA molecules.
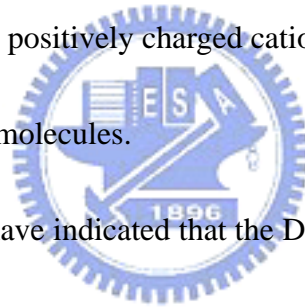
Torchilin and coworkers have indicated that the DNA in the liposome modified with TAT peptide could lead to efficient translocation into the cell cytoplasm with later migration into the perinuclear zone [2]. DNA-liposome complexes using TAT peptide may be used as a non-endocytotic intracellular delivery where the cytotoxicity was lower than that of commonly used cationic lipid based gene delivery. Comparative studies of cytotoxicity of the cationic TAT peptide liposomes and the Lipofectin in NIH / 3T3 cells was performed. The results indicated that at some concentration, TAT peptide Liposomes with 10 mol % of DOTAP were nontoxic for cells after 24 hours of incubation. In contrast, the use of Lipofectins led to 35- 65% cell death depending on the concentration of Lipofectins.

Moreover, the TAT-liposome-plasmid complexes were measured to be about 25% less toxic that the Lipofectin-plasmid lipoplex in the NIH/3T3 cell after four hours of incubation.

7.2.2 The cationic polymer

In addition to the cationic lipids, the cationic polymers are also often used in the transfection studies since it is possible to design a polymer with the desired properties. There are several cationic polymers that have been investigated as the transfection reagents including polyallylamine, peptoids, methacrylamide, and cyclodextrin-containing polymers. These polymers are different in their structures ranging form linear to highly branched molecules and in their complexation with nucleic acid, which could affect their transfection efficiency. Commonly used cationic polymers for gene delivery are polylysine, polyethylenimine (PEI), and polyamidoamine dendrimer (PAMAM). Recently, Kong et al. has utilized FRET technique to examine the cellular uptake of the plasmid DNA containing, non-degradable poly(ethyleneimine) (PEI) polymer on the hydrogel surfaces [3]. It was shown that the levels of gene transfer and expression depended on the stiffness of cell-adhesive hydrogels and the uptake of the pDNA-PEI complexes increased due to the expansion of the cells on the hydrogel surfaces. In another study, Kawano et al. have exploited the possibility of using PEG-modified cationic gold nanoparticles with electroporation for in vivo gene delivery [4]. Since the DNA-gold nanoparticle complexes

have a positive charge, they can bind non-specifically to the plasma proteins to form aggregates during the intravenous injection. To improve the long term stability of the DNA-gold complexes in the blood flow and tissues, proper surface modification on the gold nanoparticles are needed. To his end, it was found that PEG coated poly-cations can provided longer lasting circulation for in vivo gene delivery.

7.2.3 The biodegradable polymer

Another class of transfection reagent is based on the biodegradable polymers, which are expected to be compatible with human bodies, therefore, non-toxic to the cells. One of the recent research targets is the polysters based on latic and glycolic acid (PLGA). PLGA is an FAD approved material that degrades by hydrolysis on implantation in the body. Specifically, PLGA hydrolysis leads to a low pH within the microsphere that can result in DNA degradation. Therefore, the release rate of the drug embedded within the PLGA matrix is governed by the rate of polymer degradation. Recently, it was illustrated by Luby et al. that poly (lactide-co-glycolide) microparticles encapsulated DNA elicited immune responses to plasmid-encoded antigens in mice and humans [5]. PLGA systems, which have been expressly designed to deliver DNA vaccines, may further enhance the immune response. Indeed, microscale delivery vectors have focused primarily on the targeting delivery of DNA vaccines to antigen-presenting cells.

Another class of biodegradable polymer is the poly(lactic-co-glycolic acid) polysters, which varied in their molecular weight and lactic /glycolic ratios and could be incorporated with plasmid DNA into the porous scaffold [3,6]. It was found that the cells grown on a polymer scaffold could be transfected with growth factor encoding plasmid that was released form the biodegradable polymer scaffolds. Jang et al. has shown that the copolymer of lactide and glycolide could be used to fabricate three-dimensional hybrid scaffolds for the tissue engineering [7].Using polycations the DNA complexes implanted within the matrix could accomplish long-time expression in the seed cells.

7.2.4. Metallic nanoparticles

There have been increasing research activities in developing metallic nanoparticles for probing biological system because of the potential applications of nanoparticles in drug and gene delivery [8-13], biosensing [14-16], bioseparation [17, 18]and bioimagin [19, 20]. Among these metallic nanoparticles, gold nanoparticles have been widely studied because of their easy preparation process, chemical stability and possibility for surface modifications [21, 22]. In addition, it was shown that the spherical gold nanoparticles were inherently nontoxic to human cells and could be easily internalized by the cells while the surface modified gold nanoparticles exhibited some degree of toxicity, which depended on the surface charges of the gold nanoparticles [23-26]. Taking the advantage of low cytotoxicity and easy surface

modification process, the spherical gold nanoparticles have been engineered to carry genetic

materials into the cells with very high efficiency [8, 9]. When the oligonucletide modified

gold nanoparticles were used as intracellular gene regulation reagents, it was demonstrated

that the knockdown of gene could be tuned by tailoring the density of DNA on the surfaces of

gold nanoparticles [27]. Despite of these fruitful successes in using spherical gold

nanoparticles for various biological applications, it remains difficult to engineer spherical

gold nanoparticles with multiple functionalities due to their single chemical composition. In

an ideal nanoparticle based biological assay, it is desirable to decorate the surface of

nanoparticles with multiple functionalities such as optical labeling for tracing the particles,

magnetic property for manipulation and chemical or biological functionalities for specific

target recognition [28-30].
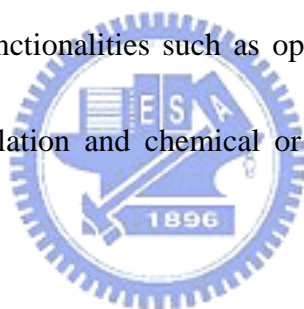
One simple approach to engineer particles with multiple functionalities is to utilize the

nanorods or nanowires produced by template electrodeposition [31]. Since different types of

materials can be deposited into the templates sequentially, it is possible to obtain

multi-segment nanorods or nanowires [32]. Salem and coworkers demonstrated direct

assembly of Au/Pt/Au multisegment nanowires [33] or multi-component magnetic nanowires

[34]. Furthermore, the utilization of nanowires with different segments along the nanowires

provides multiple chemical functionalities by the selective biding of different ligands to

individual segment nanowires. For example, the biotin-terminated thiol was attached to the

gold segment and butane isocyanide was bound to the Pt segment of nanowires.

Recent work by Salem et al. has examined multi-component Au/Ni nanorods for vaccination application [35]. Plasmids encoding ovalbumin was bound to the gold segments of the nanorods through a thiolate linkage. It was found that the delivery of plasmids encoding ovalbumin by both nanorods and gold nanopaticles generated stronger antibody and CD8 T-cell responses than the ovalbumin antigen alone.

7.2.5 Other nanomaterials

In addition to the use of metallic nanoparticles, non-metallic nanomaterials such as carbon nanotubes have also been investigated in the biological system. Kam et al. have reported the studies of the cellular internalization of various proteins adsorbed on acid-oxidized single-walled carbon nanotubes [36] or single- stranded oligonucleotides [37] and more hydrophobic oxidized carbon nanotubes . These proteins could conjugate with carbon nanotubes, which acted as the transporter inside various mammalian cells via the endocytosis pathways [38]. It was found that the nanotubes can get into the cytoplasm of cell and carry out biological functions. Pantarotto et al. have investigated that carbon nanotubes, which were functionalized with a pyrrolidine ring bearing a free amino-terminal oligothylene glycol with a small portion adsorbed to the nitrogen atom [39]. No cytotoxicity was observed in their study and the highest carbon nanotubes concentration for gene delivery experiments

was about 1.2 mg ml^{-1}.The modification carbon nanotubes coated with plasmid DNA were

delivered to cells and it was shown that the gene expression levels was up to 10 times higher

than those achieved with naked DNA alone. From the TEM image, it was shown that the

functionalized multi-walled carbon nanotubes with a diameter of about 20 nm and length of

around 200 nm could cross the cell membrane. The functionalized nanotubes were able to

bind and penetrate into the cells by what seem to be an endosome-independent mechanism.

In another work, Kostarelos et al have demonstrated that the cellular uptake of

ammonium-functionalized cationic nanotubes was independent of functional group and cell

type [40]. They have observed that the neutral charged of acetamido-functionalized carbon

nanotubes or negatively charged of fluorescein isothiocyanate (FITC) with functionalized

carbon nanotubes were congruously taken up by cells. Their results indicated that the cellular

internalization of the functionalized CNT did not depend on the endocytosis. Such conclusion

was inconsistencies with those obtained by Kam's group, which could be attributed to the

shape discrimination in the characteristics of the carbon nanotubes structure studies.
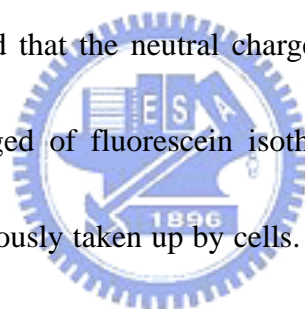
7.3 Experimental procedures for measuring the transfection efficiency of gold nanowires

7.3.1 .Plasmid preparation

A pDsRed-Monomer-golgi (4.9kb) vector encoding the red fluorescent protein

(DsRed-monomer) with golgi location signal was purchased from Clontech (BD Biosciences).

These plasmid DNA molecules were propagated in DH5α host strains and isolated and

purified by using an EndoFree Plasmid Maxi kit (Qiagen GmbH, Hilden, Germany). The

concentration of plasmid DNA molecules was determined by measuring the absorbance at 260

nm.

7.3.2. AgNi segment binding

AgNi nanowires ($\sim 10^8$) suspended in the distilled water was added 200 μl of 0.1 M

AEDP (priecre) for 24 hour. Following 50 ng of plasmid was added AgNi nanowires

suspension solution ($\sim 10^5$), and incubation at 4℃ for 24hour. The nickel segment associated

with ADEP, which is carboxylate end group bind to the nickel portion. The disulphide linkage

acts as cleavable point with the space to promote DNA release within cell. The plasmids are

bound to amines presented on the surface of the nickel segment. After 2 M $CaCl_2$ of 10μL was

added compact the surface immobilized plasmids. After 100 nM fluorescent staining of

YOYO-1 dye was adsorbed on nickel segment nanowires surface. Unbound portion were

removed by washing with PBS solution and cellular incubation for uptake. Multiple cellular

staining was performed as follow: cell membranes were stained red color with a solution of

wheat-germ agglutinin conjugated with tetramethylrhodamine Alexa Fluor 594 WAG dye and

the nuclei were counter stained in blue color with a solution of Hoechst 33342 dye.

7.3.3. Cell culture and transfection

Fibroblast NIH 3T3 and HeLa S3 (BCRC) were cultured in T75 flasks with growth media, which were Dubbeco's modified Eagle's medium (DMEM, Gibco) for fibroblast cells, and Minimum Essential Medium (MEM, Gibco) for HeLa cells, at 37^0C in a 5% CO_2 atmosphere. 10% fetal bovine serum (FBS, PAA Laboratories), and PEN-STREP-AMPHO solution (Biological Industries) were added to both media. In a typical transfection experiment, 3T3 and HeLa cells were seeded in 6-well plates at a density of 1×10^5 cells. To compare the transfection efficiency of the nanowires with other transfection reagents, we have tested two types of commonly used transfection reagents, PolyFect (Qiagen) and calcium phosphate, and bared plasmid DNA molecules were used as controls.
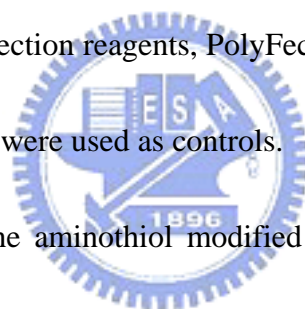
The protocol for using the aminothiol modified nanowires as transfection reagents is described as follows: for 3T3 cells, 50 ng of DNA (pDsRed-Monomer- golgi) were mixed 10 µl of aminothiol modified gold nanowires (10^7/ml) suspended in the sterile water. The nanowire solution was incubated with 89 µl of growth medium without serum for 10 minutes and then 600 µl of growth medium was added into the solution. To conduct transfection experiment, the medium in the cell culture was removed and the cells were washed with PBS solution. After pipetting the nanowire solution into the cell culture, additional 1 ml of fresh medium was added.

Similar protocols for the dendrimer-based commercial agent PolyFect (Qiagen) and calcium

phosphate were used. 50 ng of DNA were dissolved in 89 μl medium without serum and then 10 μl of PolyFect transfection reagent was added to the medium. After 10 minutes of incubation, 600 μl growth medium was added to the transfection mixture. When the calcium phosphate was used as the transfection reagent, 50 ng of DNA were mixed 10 μl of 2M $CaCl_2$ solution with phosphate buffer. The mixture solutions were added with 89 μl of medium without serum and incubated for10 min. The final solution was prepared by adding 600 μl of growth medium. Both PolyFect and calcium phosphate mixture solutions were added to the washed cell culture together with 1 ml fresh growth medium. The naked DNA solution contained 50 ng of DNA and 99 μl of medium without serum. After 10 minutes of incubation, the final naked DNA solution was prepared by adding 600 μl of growth medium. Similar protocols were used for the HeLa cells. The only difference was that the amount of plasmid DNA used in each experiment was increased to 500 ng.

After 24 hours of incubation with the transfection reagents, the cells were washed with PBS solution and 1.5 ml of fresh medium was added to each well. The transfection efficiency was measured by counting the number of cells that exhibited red fluorescence and the total number of cells on an inverted microscope (Olympus IX 71) equipped with a color CCD (Olympus, DP70). To measure the location of the nanowires and the expressed DsRed monomer, a confocal microscope (Leica TCS SP5) was used where the transfection

experiments were conducted on 3 mm glass bottom dishes coated with collagen coating

(Bioptechs,Inc).

7.3.4. Gel electrophoresis

To measure the amount of the plasmid DNA that can be carried by the nanowires, gel

electrophoresis was used. Gels were prepared with 1% (w/v) agarose and ran for 40 min at

50V. The buffer solutions used in this experiment were TBE buffer (90mM Tris-acetate and

2mMEDTA, pH 8.3, Sigma) and the plasmids were stained with 2µl SYBR green

(Invitrogen).

7.4 Results and Discussions

7.4.1. Characterization of nanowires

The anodic aluminum oxide membranes (200 nm) were used as the templates for

electrodeposition. Following the procedure described in the literatures, it is possible to obtain

optical microscope image of multi-segment nanowires in figure 1(A) and (B). One important

issue in developing multifunctional biological probing system is the capability of delivering

external materials such as drugs or DNA through the multifunctional probes. The combined

DIC and fluorescence confocal image of AgNi multisegment nanowires were incubated in

fibroblast cells as seen in Figure 1(C).   To simplify this problem, we have concentrated on

the study of the transfection efficiency using single segment gold nanowires. The detail

fabrication procedures and experimental parameters for gold nanowires are described in the

experimental section. Shown in figure 2 are the SEM image and the size distribution of the 5

μm long gold nanowires. The size of the nanowires were measured to be 4.78 ±0. 7 μm in

figure 2 (B) and the zeta potential measured for the newly synthesized gold nanowires was

about -83±1.7 mV. To bind the negatively charged DNA molecules, the surface of the

nanowires were modified with aminothiol to exhibit positive surface potential, which was

measured to be +11.4±1.4 mV.

7.4.2. Binding efficiency of nanowire

Once the positively charged gold nanowires were prepared, the next step was to bind the

negatively charged plasmid to the nanowires through the electrostatic interaction. To find out

the optimal biding efficiency of the plasmid to the nanowires, we have tested 5 different

concentrations of 5 μm long aminothiol modified gold nanowires (5 x 10^3, 2.5 x 10^4, 5 x 10^4,

2.5 x 10^5, 5 x 10^5 / ml), which were incubated with 50 ng of the DsRed-Monomer-golgi

vector for 24 hours. These solutions were then mixed with XYBR green and loaded in an

agarose gel. The result is shown in figure 3 where the plasmid bands in land 5 and 6 were

missing indicating that at these concentrations all the plasmids were bound to the nanowires.

Therefore, we estimated that the binding efficacy for the plasmid DNA molecules on the 5 μm

long aminothiol modified nanowires were about 1 pg/nanowire. The zeta potential of the

plasmid bonded gold nanowires was measured to be -9.3±0.5mV, which clearly indicated that

DNA bound to gold nanowires to form complex. The DNA gold nanowire complex could

protect the DNA molecules from the attack of the DNA nucleases.

7.4.3. Transfection efficiency of nanowires

To test the transfection efficiency of the aminothiol modified gold nanowires, 5 μm long

nanowires with concentration of 10^5 nanowire/ml was mixed with the 50 ng of

DsRed-Monomer-golgi vector and incubated over night. Two cell lines, NIH 3T3 and HeLa

S3, were used in this experiment. The control experiments were conducted with dendrimer

based commercial transfection agent (PolyFect) and calcium phosphate. The transfection

efficiency for the naked plasmids was also measured. The viability of the cells incubated with

the transfection reagents was checked separately by staining the cell with trypan blue 24 hours

after the transfections. The transfection efficiency was calculated by measuring the ratio of the

number of cell exhibited red fluorescence to the total number of the cells on the surfaces and

normalized to the cell viability. Shown in figure 4 are the combined DIC and fluorescence

images of 3T3 cells 24 hours after transfection using four different transfection reagents. The

viability of the 3T3 cells 24 hours after transfection was measured to be 90%, 65%, 65% and

71% for gold nanowires, PolyFect, calcium phosphate and naked DNA, respectively. It is

clear that aminothiol modified gold nanowires exhibited the highest transfection efficiency

with very low toxicity for 3T3 cells. In one of our previous measurements [41], it was shown

that more than 30% of the gold nanowires could be internalized by the 3T3 cells within 8

hours , which may explain the high transfection efficiency of the micrometer long gold

nanowires.

As for the HeLa cells, the condition changed. Very little amount of cells were transfected

24 hours after incubation with all transfection reagents despite of the fact that more DNA

molecules were used. After a few days, the cells started to exhibited red fluorescence. Shown

in figure 5 are the combined DIC and fluorescence images of the transfected HeLa cells six

days after transfection. The viability of the HeLa cells 24 hours after incubation with the

transfection reagents was measured to be 95%, 87%, 86% and 90% for gold nanowires,

PolyFect, calcium phosphate and naked DNA, respectively. HeLa cells seemed to resist to the

addition of the transfection reagents. Therefore, lower cytotoxicity as well as lower

transfection efficiency was measured for the HeLa cell lines. The transfection efficiencies of

four different reagents for both cell lines are summarized in figure 6. In both cases, the gold

nanowires exhibited the highest transfection efficiency while very little cytotoxicity to both

cells lines was measured. To achieve higher transfection efficiency for other transfection

reagents, DNA loading in the μg region was needed [42]. Therefore, we concluded that the

micrometer long nanowires could effectively deliver plasmid DNA into both 3T3 and HeLa

cells.

Once we know that the micrometer long gold nanowires can effectively deliver DNA into cells, the next question is whether the nanowires can be visualized through optical microscope, therefore, allowing the monitoring of the location of nanowires inside the cells. To trace the location of the nanowires, the plasmid DNA coated gold nanowires were incubated with YOYO-1 dye, which was known to emit strong green fluorescence when bound to the DNA molecules. Shown in figure 7 is the multi stain confocal image of the YOYO-1 labeled plasmid DNA on the gold nanowires. The combined DIC and fluorescence confocal image of the YOYO-1 labeled gold nanowires on HeLa cells. Cellular membrane are stained in red color with Alexa Fluor 594 WAG dye and nuclei are counter stained in blue color with Hoechst 33342 dye. The nanowires inside the HeLa can be clearly seen from the confocal images with sub-micrometer resolution. This was thought to directly indicate that gold nanowire traffic intracellulary, leading to perinuclear accumulation. The Z-stack imaging indicated that the intracellular and perinuclear localization of the gold nanowire with dye signal .By monitor the location of the nanowires inside the cells, it is possible to trace the trajectory of the nanowires, therefore, allowing the studies of the interaction between the nanowires and cells.

7.5 Conclusion

In summary, we have reported the studies of transfection efficiency for the surface functionalized nanowires. It was found that the transfection efficiency of the aminothiol modified gold nanowires was the highest among the tested transfection reagents while almost no cytotoxicity was observed for gold nanowires under our experimental condition. It was also shown that it is possible to trace the nanowires inside the cells with sub-micrometer resolution. Therefore, we concluded the micrometer long multi-segment nanowires could be used for probing living cells with several advantages including easy fabrication and surface modification process, high transfection efficiency with very low cytotoxicity and readily observable by a confocal microscope.

Reference

1. V. Budker, T. Budker, G. F. Zhang, V. Subbotin, A. Loomis and J. A. Wolff, *J. Gene Med*. 2000, **2**, 76.

2. V. P. Torchilin, T. S. Levchenko, R. Rammohan, N. Volodina, B. Papahadjopoulos-Sternberg and G. G. M. D'Souza, *P Natl Acad Sci USA* 2003, **100**, 1972.

3. H. J. Kong, J. D. Liu, K. Riddle, T. Matsumoto, K. Leach and D. J. Mooney, *Nat. Mater*. 2005, **4**, 460.

4. T. Kawano, M. Yamagata, H. Takahashi, Y. Niidome, S. Yamada, Y. Katayama and T. Niidome, *J. Control. Release* 2006, **111**, 382.

5. T. M. Luby, G. Cole, L. Baker, J. S. Kornher, U. Ramstedt and M. L. Hedley, *Clin. Immunol.* 2004, **112**, 45.

6. M. C. Ford, J. P. Bertram, S. R. Hynes, M. Michaud, Q. Li, M. Young, S. S. Segal, J. A. Madri and E. B. Lavik, *P Natl Acad Sci USA* 2006, **103**, 2512.

7. J. H. Jang and L. D. Shea, *J. Control. Release* 2003, **86**, 157.

8. M. Thomas and A. M. Klibanov, *P Natl Acad Sci USA* 2003, **100**, 9138.

9. K. K. Sandhu, C. M. McIntosh, J. M. Simard, S. W. Smith and V. M. Rotello, *Bioconjugate Chem.* 2002, **13**, 3.

10. Y. Zhao, B. Sadtler, M. Lin, G. H. Hockerman and A. Wei, *Chem. Commun.*,2004, 784.

11.   N. Morishita, H. Nakagami, R. Morishita, S. Takeda, F. Mishima, B. Terazono, S. Nishijima, Y. Kaneda and N. Tanaka, *Biochem. Bioph. Res. Co.* 2005, **334**, 1121.

12.   M. M. O. Sullivan, J. J. Green and T. M. Przybycien, *Gene Ther.* 2003, **10**, 1882.

13.   R. Hong, G. Han, J. M. Fernandez, B. J. Kim, N. S. Forbes and V. M. Rotello, *J. Am. Chem. Soc.* 2006, **128**, 1078.

14.   Y. W. C. Cao, R. C. Jin and C. A. Mirkin, *Science* 2002, **297**, 1536.

15.   S. J. Park, T. A. Taton and C. A. Mirkin, *Science* 2002, **295**, 1503.

16.   K. Aslan, M. Wu, J. R. Lakowicz and C. D. Geddes, *J. Am. Chem. Soc.* 2007, **129**, 1524.

17.   J. M. Nam, C. S. Thaxton and C. A. Mirkin, *Science* 2003, **301**, 1884.

18.   P. C. Lin, P. H. Chou, S. H. Chen, H. K. Liao, K. Y. Wang, Y. J. Chen and C. C. Lin, *Small* 2006, **2**, 485.

19.   Q. Y. Hu, L. L. Tay, M. Noestheden and J. P. Pezacki, *J. Am. Chem. Soc.* 2007, **129**, 14.

20.   J. Chen, F. Saeki, B. J. Wiley, H. Cang, M. J. Cobb, Z. Y. Li, L. Au, H. Zhang, M. B. Kimmey, X. D. Li and Y. Xia, *Nano Lett.* 2005, **5**, 473.

21.   A. Verma and V. M. Rotello, *Chem. Commun.* 2005, 303.

22.   G. Han, N. S. Chari, A. Verma, R. Hong, C. T. Martin and V. M. Rotello, *Bioconjugate Chem.* 2005, **16**, 1356.

23. E. E. Connor, J. Mwamuka, A. Gole, C. J. Murphy and M. D. Wyatt, *Small* 2005, **1**, 325.

24. B. D. Chithrani, A. A. Ghazani and W. C. W. Chan, *Nano Lett.* 2006, **6**, 662.

25. C. M. Goodman, C. D. McCusker, T. Yilmaz and V. M. Rotello, *Bioconjugate Chem.* 2004, **15**, 897.

26. H. Takahashi, Y. Niidome, T. Niidome, K. Kaneko, H. Kawasaki and S. Yamada, *Langmuir* 2006, **22**, 2.

27. N. L. Rosi, D. A. Giljohann, C. S. Thaxton, A. K. R. Lytton-Jean, M. S. Han and C. A. Mirkin, *Science* 2006, **312**, 1027.

28. M. Ferrari, *Nat. Rev. Cancer* 2005, **5**, 161.

29. X. H. Gao, Y. Y. Cui, R. M. Levenson, L. W. K. Chung and S. M. Nie, *Nat. Biotechnol.* 2004, **22**, 969.

30. A. G. Tkachenko, H. Xie, D. Coleman, W. Glomm, J. Ryan, M. F. Anderson, S. Franzen and D. L. Feldheim, *J. Am. Chem. Soc.* 2003, **125**, 4700.

31. S. R. Nicewarner-Pena, R. G. Freeman, B. D. Reiss, L. He, D. J. Pena, I. D. Walton, R. Cromer, C. D. Keating and M. J. Natan, *Science* 2001, **294**, 137.

32. L. A. Bauer, D. H. Reich and G. J. Meyer, *Langmuir* 2003, **19**, 7043.

33. A. K. Salem, M. Chen, J. Hayden, K. W. Leong and P. C. Searson, *Nano Lett.* 2004, **4**, 1163.

34.   A. K. Salem, J. Chao, K. W. Leong and P. C. Searson, *Adv. Mater.* 2004, **16**, 268.

35.   A. K. Salem, C. F. Hung, T. W. Kim, T. C. Wu, P. C. Searson and K. W. Leong, *Nanotechnology* 2005, **16**, 484.

36.   N. W. S. Kam, T. C. Jessop, P. A. Wender and H. J. Dai, *J. Am. Chem. Soc.* 2004, **126**, 6850.

37.   N. W. S. Kam, Z. A. Liu and H. J. Dai, *Angew. Chem. Int. Edit.* 2006, **45**, 577.

38.   N. W. S. Kam and H. J. Dai, *J. Am. Chem. Soc.* 2005, **127**, 6021.

39.   D. Pantarotto, R. Singh, D. McCarthy, M. Erhardt, J. P. Briand, M. Prato, K. Kostarelos and A. Bianco, *Angew Chem Int. Edit.* 2004, **43**, 5242.

40.   K. Kostarelos, L. Lacerda, G. Pastorin, W. Wu, S. Wieckowski, J. Luangsivilay, S. Godefroy, D. Pantarotto, J. P. Briand, S. Muller, M. Prato and A. Bianco, *Nature Nanotechnology* 2007, **2**, 108.

41.   L. A. Bauer, N. S. Birenbaum and G. J. Meyer, *J. Mater. Chem.* 2004. **14**, 517.

42.   H. Akita, R. Ito, I. A. Khalil, S. Futaki and H. Harashima, *Mol. Ther.* 2004, **9**, 443.
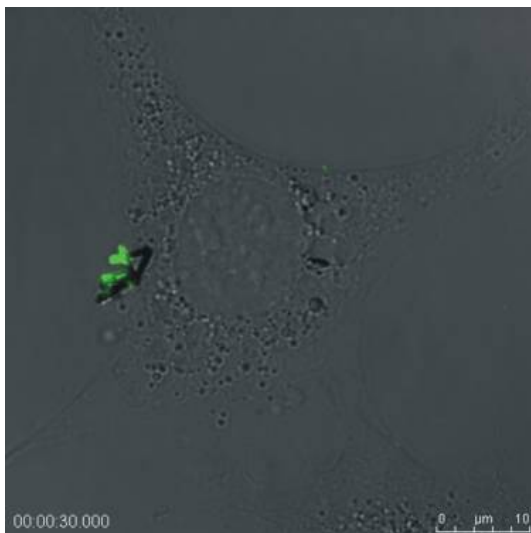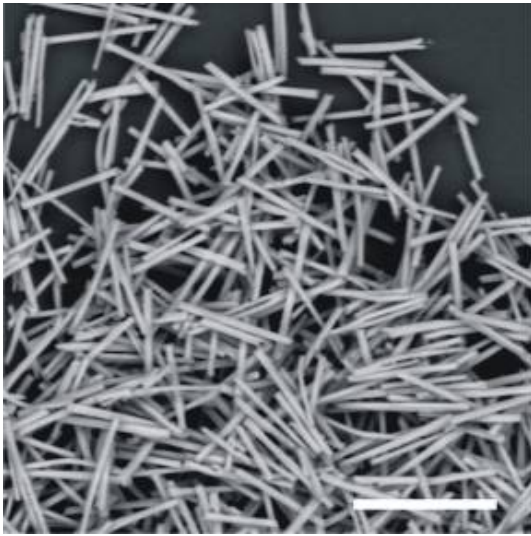
(A)

(B)
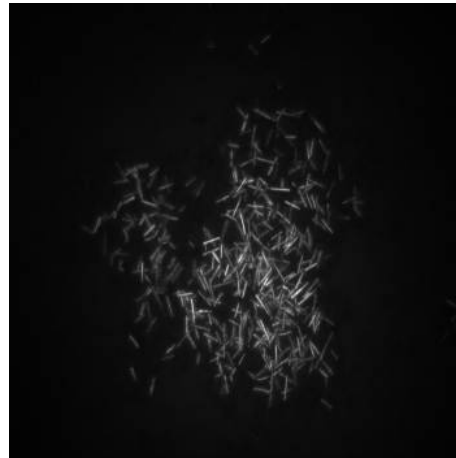
(C)

Figure 1 (A) The optical image of multi-segment Ag-Ni nanowire. (B) The optical image of

multi-segment Ag-Ni nanowires. The light and dark stripes are due to alternating of silver and

nickel metal, having different reflectivity at the observation wavelength. (C).The combined

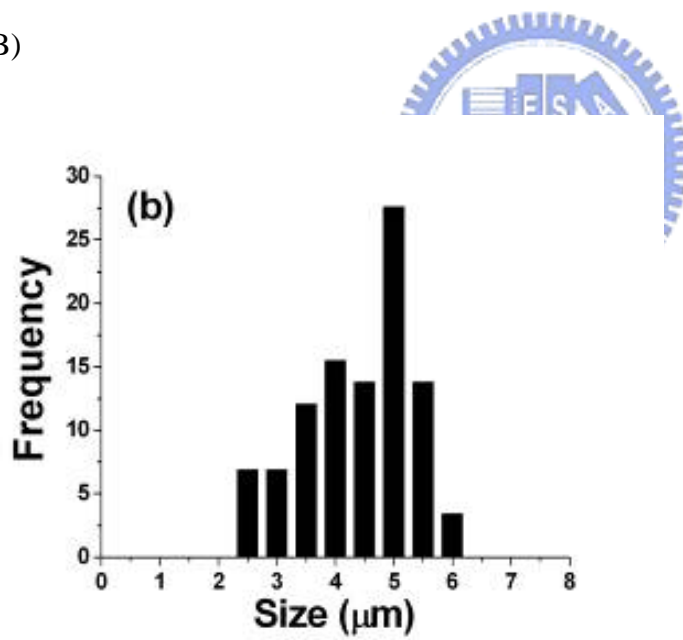DIC and fluorescence confocal images of Ag-Ni nanowires in 3T3 cell.

(A)

(B)

Figure 2.(A) The SEM image of 5 μm long gold nanowires. The bar is 5 μm. (B) Size
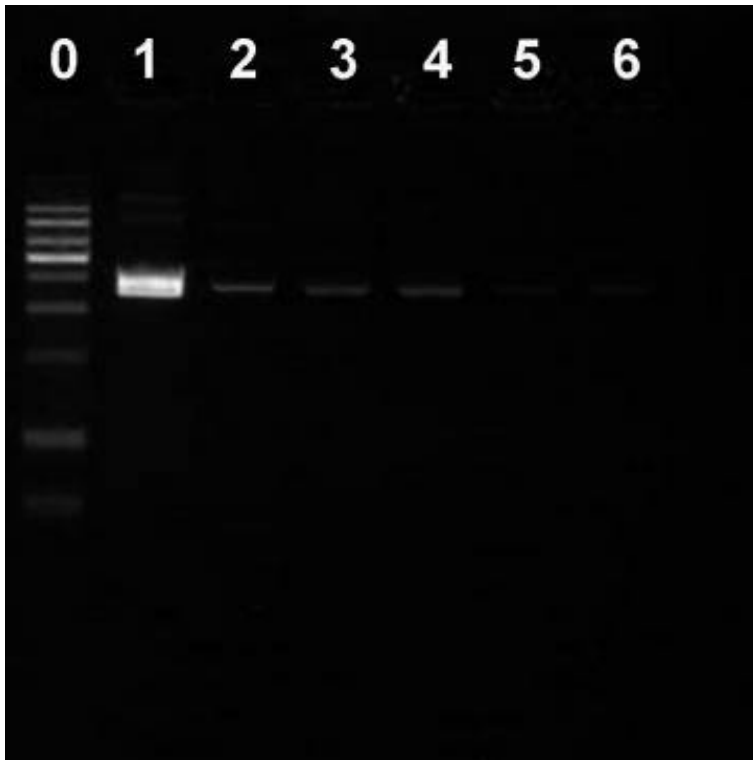
distribution of 5 μm gold nanowires.

Figure 3. Agarose gel electrophoresis of the aminothiol modified gold nanowires and plasmid.

Land 0 is the DNA marker. Land 1 is the 50 ng plasmid DNA without nanowires. Land 2 to 6

are the mixture of 50 ng plasmid DNA with increasing numbers of the gold nanowires (5 $\times$

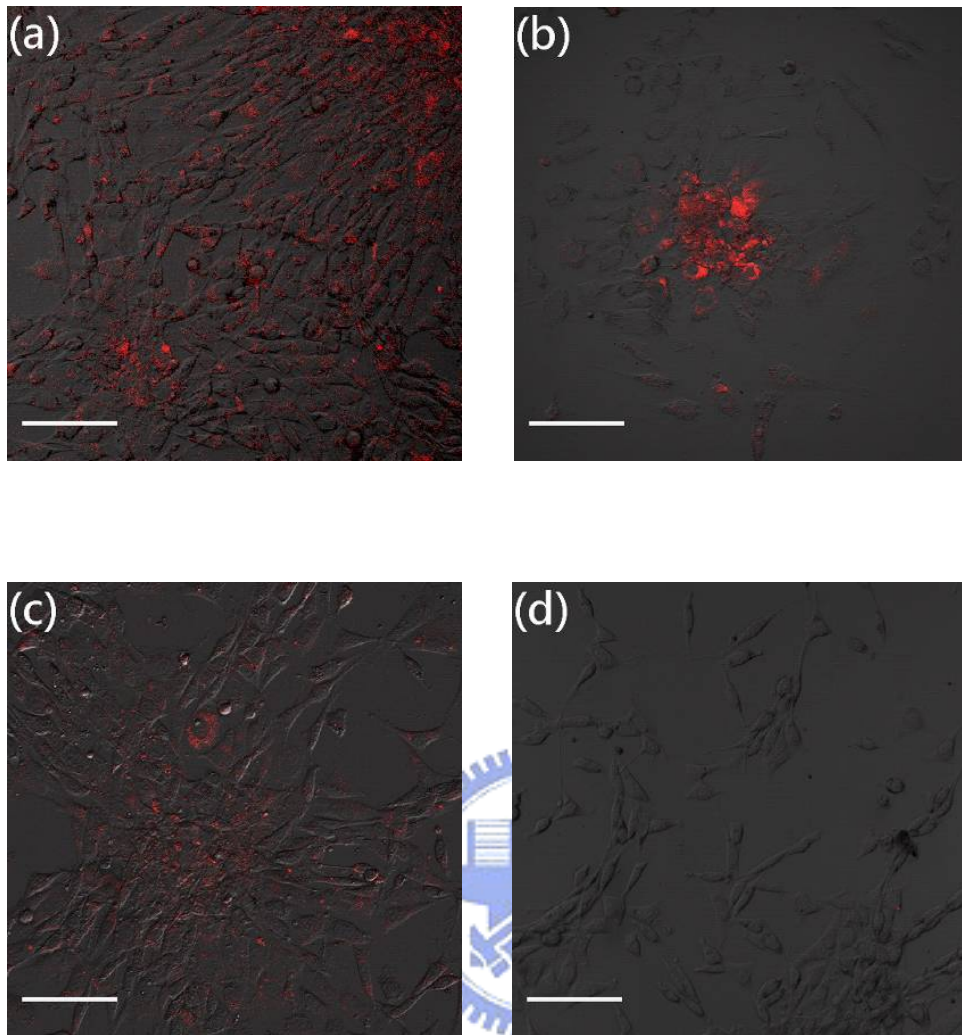10^3 , 2.5 $\times$ 10^4, 5 $\times$ 10^4, 2.5 $\times$ 10^5 ,5 $\times$ 10^5).

Figure 4 The combined DIC and confocal images of 3T3 cells 1 days after using (a) gold

nanowires (b) PolyFect (c) calcium phosphate (d) naked DNA as the transfection reagents.
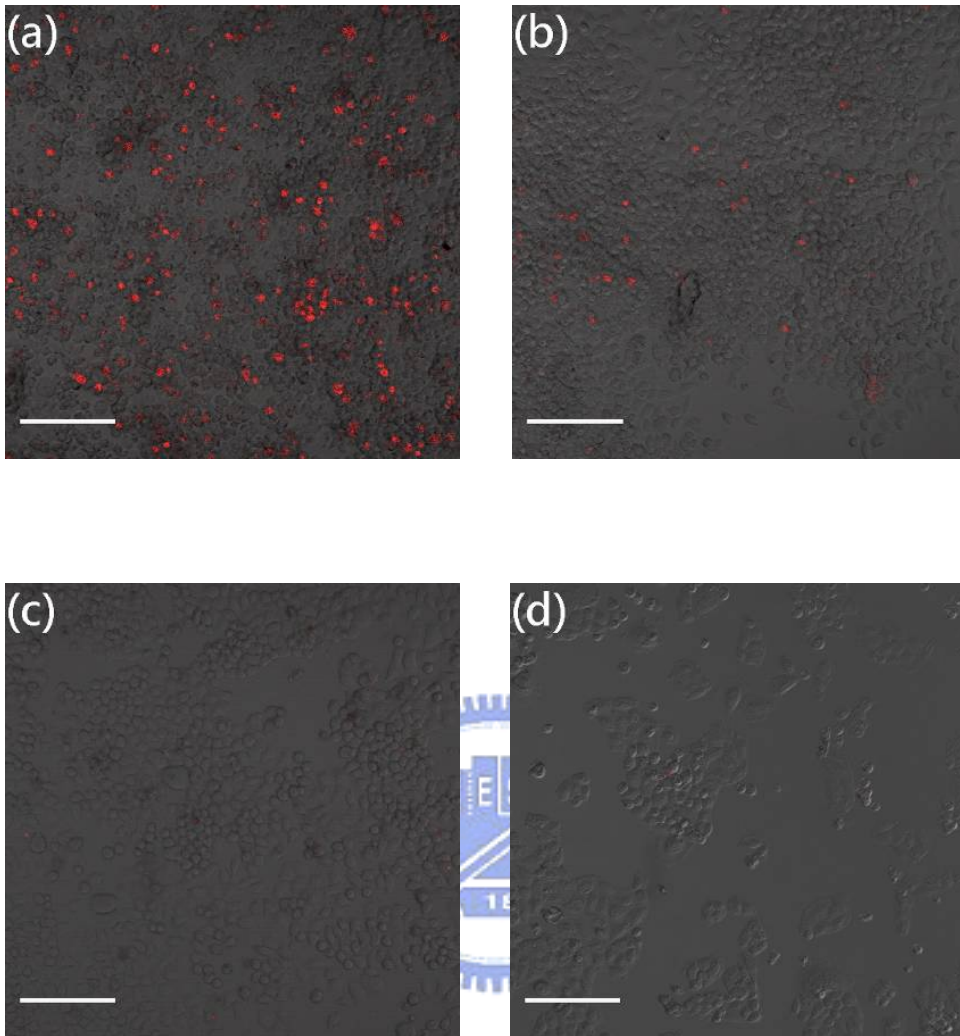
Bar: 100 μm

Figure 5 The combined DIC and confocal images of HeLa cells 6 days after using (a) gold

nanowires (b) PolyFect (c) calcium phosphate (d) naked DNA as the transfection reagents.
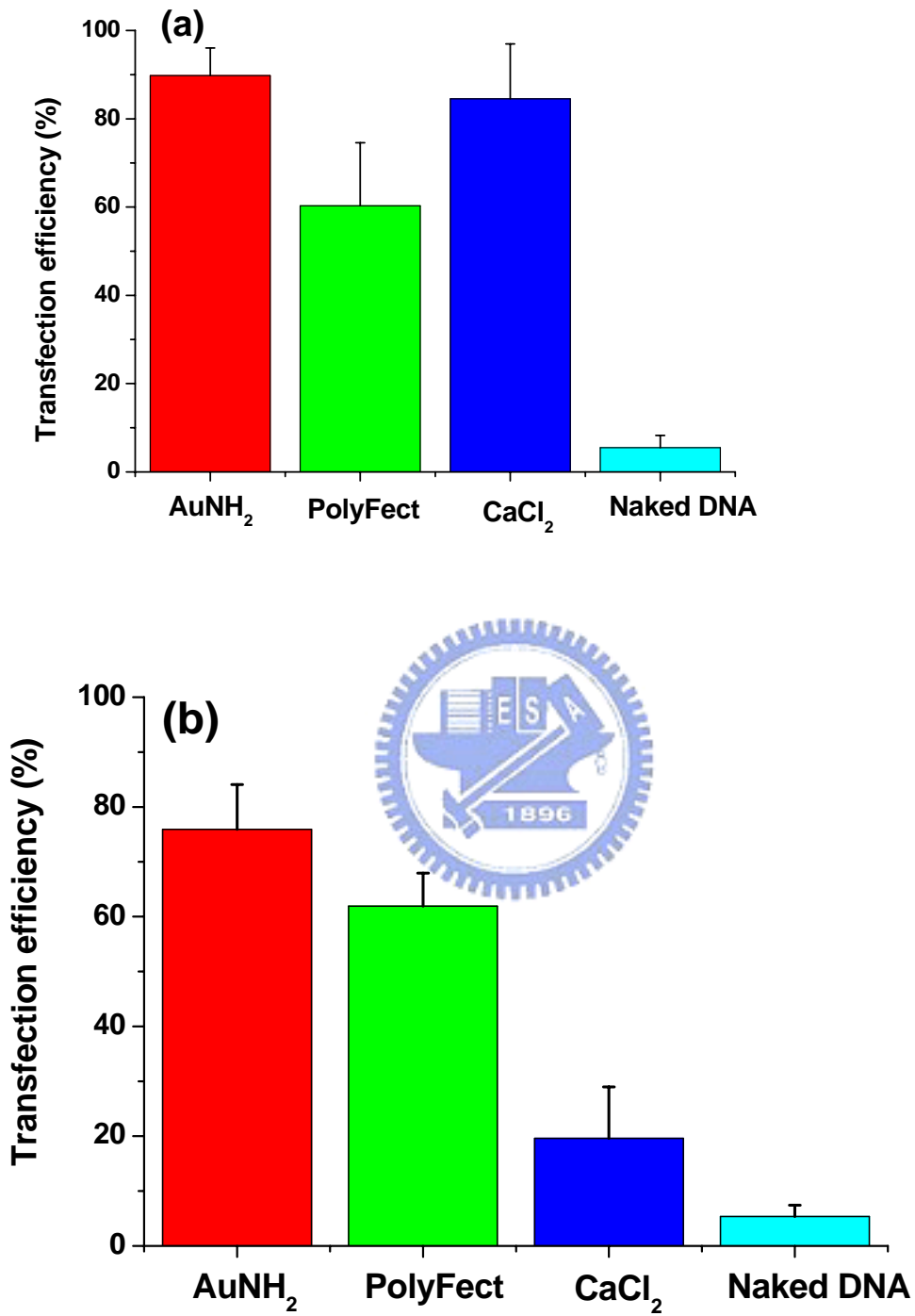
Bar: 100 µm

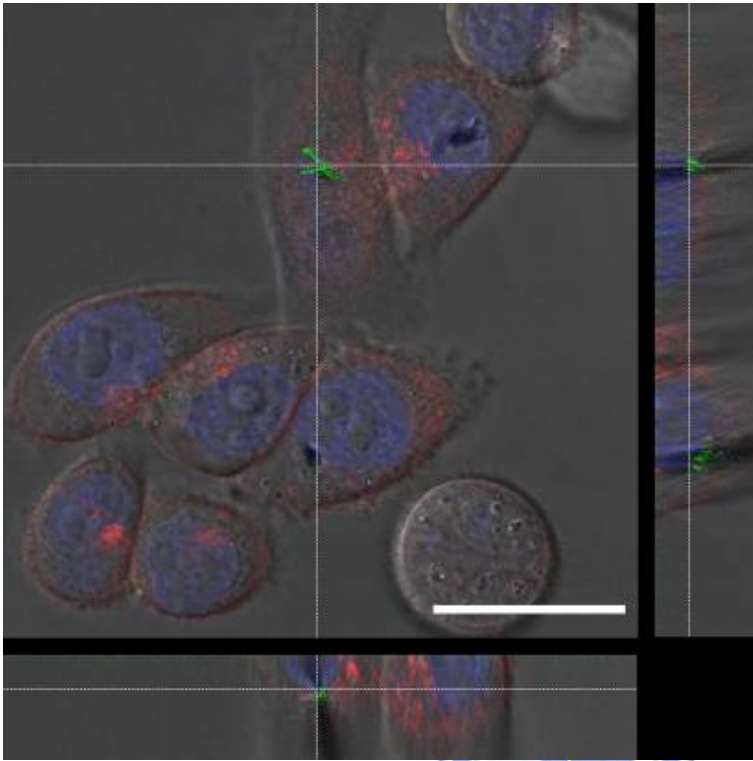Figure 6. The transfection efficiency measured for different transfection reagents in (A) 3T3 cells (B) HeLa cells.

Figure 7.　The stacked laser scanning confocal microscopy images of the aminothiol

functionalized gold nanowires coated with plasmid and labeled with YOYO-1 dye (green) in

HeLa cells.　Bar: 25μm.

Publications

1） Chiung-Wen Kuo, J.Y. Shiu, Kung Hwa Wei and Peilin Chen*, *"Monolithic Integration of Well-Ordered Nanoporous Structures in the Microfluidic Channels for Bioseparation"* J. Chromatorg. A 2007, **1162**, 175-179 (SCI: 3.554)

2） Chiung-Wen Kuo, Jun-Jung Lai, Kung Hwa Wei and Peilin Chen*, *"The Studies of the Surface Modified Gold Nanowires inside the Living Cells"* Adv. Func. Mater. 2007, **18**,3707 (SCI:6.770)

3） Chiung-Wen Kuo, Jun-Jung Lai, Kung Hwa Wei and Peilin Chen*, *"Surface Modified Gold Nanowires for Mammalian Cell Transfection"* Nanotechnology ,2008, **19**, 25103 (SCI:3.037)

4） Chiung-Wen Kuo, Kung Hwa Wei, Chun-Hsun Lin, Jau-Ye Shiu and Peilin Chen*,*"Nanofluidic System for the Studies of Single DNA Molecules"* Electrophoresis, (accepted) (SCI:4.101)

5） Chiung-Wen Kuo, Jau-Ye Shiu, Kung Hwa Wei, and Peilin Chen*, *"Functionalized Silver Nanowires for Live Cell Study"*, Chem. Lett. (accepted) (SCI:1.734)
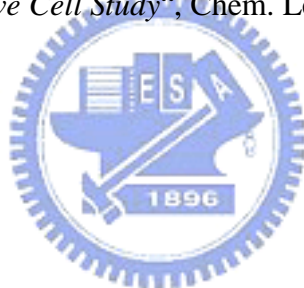
Chiung-Wen Kuo (郭瓊雯)

Research Center for Applied Sciences   Tel: 2-2789-8000 ext 55 (O)
Academia Sinica   Fax: 2-2782-6680 (O)
Nankang, Taipei 115, Taiwan   Email:kuo55@gate.sinica.edu.tw

Education:

1999   M. S. in Chemistry, National Chung Cheng University, Taiwan
1992   B. S. in Chemistry, Chung Yuan Christian University, Taiwan

Research Experiences:

2003-present   Part-time Research Assistant, Research Center for Applied Sciences, Academia Sinica, Taiwan
2001-2003   Research Assistant, Research Center for Applied Sciences, Academia Sinica, Taiwan

Honors and Awards:

2004   MRS Best Poster Award

Capabilities:

- Development of nanofabrication techniques
- Fabrication of orders AAO membranes
- Synthesis of multisegament nanowires
- Surface functionalization of nanoparticles
- Cell culture and toxicity assays
- Confocal, TRIF microscope
- Life cell imaging
- Transfection

Conferences:

2004 MRS Fall meeting, Boston

List of Publications:

1. C.W. Kuo, J.Y. Shiu, K.H. Wei and P. Chen*,   *J. Chromatorg.* A,1162, 175 (2007)
2. C.W. Kuo, J. J. Lai, K. H. Wei and P. Chen*, *Adv. Func. Mater,* 18,3707, (2007)
3. C.W. Kuo, J. J Lai, K. H. Wei and P. Chen*, *Nanotechnology* , 19,25103,(2008)
4. C. W. Kuo, K. H. Wei, C-H Lin, J.Y. Shiu and P. Chen*, *Electrophoresis*, (accepted)
5. C. W. Kuo, J.Y. Shiu, K.H. Wei and P. Chen *, *Chem. Lett.* (accepted)
6. C.W.Kuo, J.Y. Shiu, P. Chen, and G.A. Somorjai, *J. Phys. Chem. B* , 107, 9950(2003)
7. C.W. Kuo, J.Y. Shiu, Y.H. Cho and P. Chen, *Adv. Mater.* 15, 1065(2003)